Molecular analysis of mechanisms leading to CYP2D6 intermediate and ultrarapid metabolizer phenotypes

Von der Fakultät Geo- und Biowissenschaften der Universität Stuttgart
zur Erlangung der Würde eines Doktors der Naturwissenschaften
(Dr. rer.nat.) genehmigte Abhandlung

vorgelegt von
Claudia Toscano
aus Karlsruhe

Hauptberichter: Prof. Dr. D. Wolf
Mitberichter: Prof. Dr. P. Scheurich
Tag der mündlichen Prüfung: 27.03.06

Dr. Margarete Fischer-Bosch Institut
für Klinische Pharmakologie Stuttgart
2006

Hiermit erkläre ich, dass ich die vorliegende Dissertation selbstständig und unter ausschließlilcher Verwendung der angegebenen Hilfsmittel angefertigt habe.

Für Victorio und meine Familie

Danksagung

Herrn Prof. Eichelbaum danke ich für die Möglichkeit die Doktorarbeit am Dr. Margarete Fischer-Bosch Institut für Klinische Pharmakologie anfertigen zu können und für sein stetiges Interesse an deren Fortkommen. Bei Herrn Prof. Wolf und bei Herrn Prof. Scheurich bedanke ich mich für die Begleitung und Begutachtung meiner Dissertation an der Universität Stuttgart.

Mein besonderer Dank gilt meinem Arbeitsgruppenleiter PD Dr. Uli Zanger, als Mentor und Quelle wertvoller Anregungen und Diskussionen, der stets neue Motivation zu schöpfen wusste und maßgeblich zum Erfolg dieser Arbeit beigetragen hat.
Weiterhin möchte ich mich bei PD Dr. Matthias Schwab für die hilfreichen Anstöße und für seine mitreißende Begeisterungsfähigkeit bedanken.

Ein herzlicher Dank geht an meine Kollegin Dr. Kathrin Klein für ihre immense Hilfsbereitschaft und kostbare Tipps.

Bei allen Kollegen des Dr. Margarete Fischer-Bosch Institutes und vor allem bei den Mitgliedern der Arbeitsgruppe Zanger/Schwab möchte ich mich bedanken für die gute und nette Zusammenarbeit. Für die technische Unterstützung im Labor möchte ich mich bei Igor Liebermann und Britta Klumpp besonders bedanken.

Mein besonderer herzlicher Dank für den wissenschaftlichen und moralischen Beistand während meiner Doktorarbeit gilt meinen Freunden und Kollegen Dr. Tanja Saussele und Marco Hofmann.

Schließlich möchte ich mich besonders bei meinen Mann Victorio für seine großartige Zuwendung und unendliches Verständnis und bei meiner Familie für die liebevolle Unterstützung bedanken.

Table of contents

Table of contents I
Abbreviations V
Summary VII
Zusammenfassung X
1 Introduction 1
1.1 Drug metabolism 1
1.2 The Cytochrome P450 enzyme family 2
1.3 Pharmacogenetics 5
1.4 Sparteine/Debrisoquine polymorphism 5
1.5 The *CYP2D* gene locus on chromosome 22 8
1.6 Molecular mechanism of the CYP2D6 polymorphism 9
1.6.1 Alleles with normal enzyme activity 12
1.6.2 Alleles with increased enzyme activity 12
1.6.3 Alleles with decreased enzyme activity 12
1.6.4 Null alleles 13
1.7 Clinical significance of CYP2D6 phenotypes 14
1.8 Objectives 15
2 Material and Methods 17
2.1 Material 17
2.1.1 Chemicals, reagents and enzymes 17
2.1.2 Instruments 19
2.1.3 Buffers and solutions 20
2.1.4 Cell lines and culture media 22
2.1.4.1 Bacterial cell culture 22
2.1.4.2 Eukaryotic cell culture 22
2.1.5 Expression vectors 23
2.1.6 Antibodies and recombinant proteins 24
2.1.7 DNA and liver samples 24

2.1.8 Oligonucleotides 25
2.2 Methods 26
2.2.1 Molecular biological methods 26
2.2.1.1 Transformation of DNA in bacterial cells 26
2.2.1.2 Isolation of plasmid DNA from E.coli with Mini/Midi/Maxi-Prep kit (Qiagen) 27
2.2.1.3 DNA digestion with restriction endonucleases 27
2.2.1.4 Dephosphorylation of DNA 27
2.2.1.5 Ligation of DNA 27
2.2.1.6 Agarose gel electrophoresis 27
2.2.1.7 Isolation of DNA fragments from agarose gel 28
2.2.1.8 Elution of DNA fragments from LMP-agarose gel 28
2.2.1.9 Isolation of total RNA from liver tissue and transfected cells 28
2.2.1.10 Quantitation of DNA and RNA 29
2.2.1.11 Polymerase chain reaction (PCR) 29
2.2.1.12 Site directed mutagenesis 29
2.2.1.13 Sequencing of double stranded DNA 29
2.2.1.14 Construction of plasmids 30
2.2.1.14.1 pCMV expression plasmids containing genomic *2D6 *1, *2, *41, *2J, *2J(1)* and **2J(2)* 30
2.2.1.14.2 Reporter gene vectors pGL3-Tk (-105) ex6/in6 *wt* and **41* 31
2.2.1.14.3 Cloning CYP2D6 splice variant ex5-9 32
2.2.1.15 Genotyping assays 32
2.2.1.15.1 Principle of DHPLC 32
2.2.1.15.2 Genotyping assay for 2988G>A SNP by DHPLC 32
2.2.1.15.3 Genotyping assay for 2988G>A SNP by TaqMan 33
2.2.1.15.4 Genotyping assay for *CYP2D7* del138T by TaqMan 33
2.2.1.15.5 Genotyping for other alleles based on TaqMan assays 34
2.2.1.16 Quantitation of specific mRNAs in human liver 34
2.2.1.16.1 Synthesis of cDNA 34
2.2.1.16.2 Conditions for Real-Time PCR 35
2.2.1.16.3 Analysis of CYP2D6 mRNA in human liver and transfected cells 35
2.2.1.16.4 β-Actin and COUPTFI 35

2.2.1.16.5 HNF4 36
2.2.1.17 RT-PCR and quantitative DHPLC analysis 36
2.2.2 Cell culture 37
2.2.2.1 Cultivation and transient transfection of eukaryotic cell lines 37
2.2.2.2 Cell harvesting and determination of β-Galactosidase activity 37
2.2.2.3 Determination of Firefly Luciferase activity 38
2.2.2.4 mRNA stability assay 38
2.2.3 Protein and enzymatic methods 38
2.2.3.1 Determination of protein content 38
2.2.3.2 SDS-polyacrylamide gel electrophoresis of proteins (SDS-PAGE) 38
2.2.3.3 Immuno blot (Western blot analysis) 39
2.2.3.3.1 Protein detection 39
2.2.3.4 Measurement of propafenone hydroxylation activity 39
2.2.4 Computer programs and statistics 40
3 Results 41
3.1 Study Populations 41
3.2 Analysis of the intermediate metabolizer phenotype 42
3.2.1 Sequencing of the *CYP2D6* gene 43
3.2.2 In vivo population analysis of CYP2D6 activity 45
3.2.2.1 Genotyping 2988G>A SNP by DHPLC and TaqMan 45
3.2.2.2 2988G>A as a new molecular marker for allele **41* 51
3.2.2.3 In vivo genotype-phenotype correlation in other ethnic groups 52
3.2.3 Studies of *CYP2D6* in human liver 53
3.2.3.1 In vitro analysis of *CYP2D6* in livers samples 53
3.2.3.2 RT-PCR and quantitation of CYP2D6 mRNA by DHPLC 55
3.2.4 Elucidation of the causal mutation of the **41* allele by recombinant expression 58
3.2.4.1 Recombinant CYP2D6 expression in different cell lines 58
3.2.4.2 RT-PCR analysis of **41, *2* and **1* constructs 61
3.2.4.3 mRNA stability analysis of *2D6*41, *2* and **1* constructs in Huh7 cells 62
3.2.4.4 Reporter gene assay of exon/intron 6 constructs 65
3.2.4.5 ESE analysis of the sequence surrounding exon/ intron 6 66

3.2.5 Intermediate metabolizer allele *CYP2D6*2J* 67
3.2.5.1 Recombinant CYP2D6 expression in Huh7 cells 67
3.2.5.2 RT-PCR analysis of **2J, *2J(1)* and **2J(2)* constructs 69
3.2.5.3 mRNA Mfold analysis 70
3.2.5.4 ESE analysis of the sequence surrounding exon 6 72
3.3 Analysis of the ultrarapid metabolizer phenotype 72
3.3.1 *CYP2D6* analysis in human liver 72
3.3.1.1 Quantitation of CYP2D6 apoprotein content by Western blot 72
3.3.1.2 CYP2D6 expression in relation to enzyme activity 74
3.3.2 Genotyping *CYP2D7* SNP del138T by TaqMan 75
3.3.3 Relationship between HNF4 and COUPTFI mRNA expression and CYP2D6 protein expression 76
3.3.3.1 Quantitation of HNF4 and COUPTFI mRNA in human liver 76
3.3.3.2 Analysis of HNF4, COUPTFI mRNA and CYP2D6 protein expression 76
4 Discussion 80
4.1 Elucidation of the molecular mechanism of the IM phenotype 80
4.1.1 *CYP2D6*41* allele: sequence and in vivo analysis 80
4.1.2 *CYP2D6*41* allele: Recombinant expression 81
4.1.3 Elucidation of the mechanism behind 2988G>A SNP 83
RNA stability 83
Reporter gene analysis 83
Alternative splicing 84
4.1.4 *CYP2D6*2J* allele 86
Modulation of alternative splicing 87
C*YP2D6*59* allele affecting mRNA stability? 87
4.2 Analysis of the UM phenotype 88
4.2.1 In vivo analysis 88
4.2.2 Expression of the pseudogene *CYP2D7* 89
4.2.3 Transcriptional regulation of *CYP2D6* 90
References 92
Lebenslauf 101
Publikationen 102

Abbreviations

APS	ammonium persulfate
AP	alkaline phosphatase
a.u.	arbitrary units
AUC	area under the curve
bp	base pairs
BSA	bovine serum albumine
°C	degree Celsius
CMV	cytomegalovirus
COUPTF	chicken ovoalbumin upstream-promoter transcription factor
CYP	Cytochrome P450
Da	Dalton
DR1	direct repeat 1
DMSO	dimethylsulfoxide
DTT	dithiothreitol
DHPLC	denaturing high-performance liquid chromatography
dNTP	2´-deoxynucleoside 5´-triphosphates
E.coli	*Escherichia coli*
EDTA	Ethylenediaminetetraacetic acid
EM	extensive metabolizer
ER	endoplasmic reticulum
FAM	6-Carboxyfluorescein
h	hour
HNF	hepatic nuclear factor
H_2O_{mp}	millipore water
IM	intermediate metabolizer
IPTG	isopropyl-β-thio-galactoside
LB	Luria Bertani
M	mol/l

m	minute
mA	milliAmpere
MR	metabolic ratio
MGB	minor groove binder
$NADP^+$	nicotinamide adenine dinucleotide phosphate
PAGE	polyacrylamide gel electrophoresis
PBS	phosphate buffered saline
PCR	polymerase chain reaction
PM	poor metabolizer
RIM	reaction injection mix
RLU	relative light units
rpm	rotation per minute
RT	reverse transcriptase
s	second
SD	standard deviation
SDS	sodium dodecyl sulfate
SNP	single nucleotide polymorphism
TAE	Tris/Acetat/EDTA
TE	Tris/EDTA
TEAA	triethylammonium acetate
TEMED	N,N,N',N'-tetramethylethylenediamine
U	unit
UM	ultrarapid metabolizer
UV	ultraviolet
V	volt
VIC	reporter fluorescent dye
X-Gal	5-bromo-4-chloro-3-indolyl β-D-galactopyranoside

Summary

Genetic polymorphisms in drug metabolizing enzymes and transporters can considerably influence an individual's ability to metabolize and eliminate drugs and other xenobiotics. The consequences are unexpected reactions of patients to drug treatment. Depending on whether the polymorphism causes reduced or increased metabolism rate the consequences of a normal dosage can be adverse reactions or reduced efficacy. CYP2D6 is one of the most important drug metabolizing enzymes in human liver showing high interindividual variability with clinical relevance for drug treatment.

Four distinct phenotypes are commonly observed in Caucasian populations, namely ultrarapid metabolizer (UM), extensive metabolizer (EM), intermediate metabolizer (IM) and poor metabolizer (PM) based on their drug oxidation capacity. The research of the last 25 years showed that interindividual differences are essentially caused by genetic polymorphisms at the *CYP2D* gene locus on chromosome 22. The numerous known allelic variants lead to increased, normal, decreased or absent 2D6 protein and/or function. Today, the presence of null mutations on both chromosomes allows the reliable identification of individuals with PM phenotype for adjustment of drug dosing. In contrast, ultrarapid and intermediate metabolizers, who may also be at increased risk, have a considerably poorer predictivity.

The intermediate metabolizer phenotype comprises 10-15 % of a distinct population subgroup characterized by impaired but detectable residual enzyme activity. Two already known alleles, *2D6*9* and *2D6*10* were shown to be associated with lower in vivo metabolic capacity but they account for not more than 10-20 % of Caucasian IMs. In attempt to elucidate the genetic basis of the IM phenotype in the major fraction, the *CYP2D6*41* allele was identified in our pharmacogenetic group at the IKP Stuttgart, which was found to be the second most frequent *CYP2D6* deficient allele. The **41* allele is genetically closely related to the functionally **2* allele but lacks the -1584C>G mutation in the promoter region. Additionally, the 2988G>A polymorphism in intron 6 was found, but it remained unclear which of both mutations

was causally responsible for impaired function of the **41* allele. Moreover it was unknown whether this were the only sequence differences or whether there were additional unidentified mutations present on the *2D6*41* allele.

In this work it could be clearly demonstrated that the intron 6 polymorphism 2988G>A was causally responsible for markedly decreased expression of the gene product and its function in liver. An association between increased levels of a nonfunctional splice variant lacking exon 6 and the 2988G>A change was initially discovered by RT-PCR analysis of liver RNA of genotyped patients. Quantification by denaturing HPLC revealed up to 7.3-fold increased levels of the splice variant and up to 2.9-fold less functional transcript in carriers of *2D6*41*, in good concordance with concomitant changes in immunoquantified CYP2D6 protein. The entire genomic sequence coding for *2D6*41, 2D6*2* and *2D6*1* alleles lacking the 5' upstream region was then recombinantly expressed in COS-1 (African green monkey kidney cell line) and human Huh7 hepatoma cell lines. The expressed *2D6*41* allele, differing from the **2* allele only by the presence of the intron 6 mutation, resulted in 2- to 5-fold reduced levels of CYP2D6 mRNA, apoprotein, and enzyme activity. These experiments established the causal relationship between the intron 6 SNP 2988G>A and the low expression phenotype associated with allele *2D6*41*. To confirm the suspicion of an involvement in the splicing process further experiments to assess mRNA stability and reporter gene analyses in transiently transfected HepG2 and Huh7 hepatoma cells were performed. However no changes in mRNA turnover or transcription rate attributable to this polymorphism were observed. *In silico* analyses suggested that 2988G>A modifies binding sites for the splicing factors SRp40 and SF2/ASF. Further two individuals with an unexplainable phenotype were analyzed with a similar strategy. Both had genotype *2D6*2/*4* usually associated with normal function. Full genomic sequencing and haplotype analysis confirmed the previously identified silent mutation 2939G>A in exon 6 (former allele variant *2D6*2J*, now termed *2D6*59*), as well as an additional novel 2291G>A change in intron 4. Transient expression in Huh7 hepatoma cells with the respective genomic *CYP2D6* sequence resulted in about three-fold reduced levels of mRNA, immunoreactive 2D6 protein and propafenone hydroxylase activity of constructs carrying either both or only the 2939G>A change. These data demonstrate profound effects of a silent mutation on expression and function of *CYP2D6*. By molecular characterization of these two alleles associated with intermediate metabolizer phenotype this part of the work

contributed to a better prediction of impaired *CYP2D6* function in humans. This can lead to improved predictivity of adverse drug reactions in clinical studies and finally to a safer drug treatment.

Ultrarapid drug metabolism mediated by *CYP2D6* is associated with inheritance of alleles with duplicated or amplified functional *CYP2D6* genes. However, genotyping for duplicated *CYP2D6* alleles only explains a fraction (10-30 %) of the UM phenotype observed in Caucasian populations. Accordingly, the intention of this work was to find an explanation for the phenomenon of "duplication-negative UM" and, if applicable, to improve its predictivity. Genotyping for the presence of the del138T in the *2D7* pseudogene by TaqMan in 287 Caucasian liver samples allowed to test the hypothesis whether this phenotype may be caused by presence of an active *2D7* pseudogene in *2D6* duplication-negative UM samples. The *CYP2D7* pseudogene has a frameshift mutation ins138T in exon 1 which disrupts the open reading frame leading to a nonfunctional gene. However no positive subjects were identified. Another hypothesis was based on a previous work about HNF4 and COUPTFI, positive and negative regulator, respectively, where it was shown that both competed for the same binding site on the *CYP2D6* promoter. Using TaqMan real-time PCR the amount of HNF4 and COUPTFI mRNA was measured in 87 liver samples to test whether an imbalance in the expression of these two transcription factors may cause increased *CYP2D6* expression. However no significant correlations between CYP2D6 expression and COUPTFI and/or HNF4 were found, therefore this hypothesis unlikely explains the duplication-negative UM. In conclusion, although by testing these two plausible hypotheses the duplication-negative UM phenotype could not be clarified, the systematic analysis of nearly 300 liver samples contributed with many valuable data to the further characterization of the CYP2D6 enzyme and its genetic polymorphism.

Zusammenfassung

Genetische Polymorphismen in Arzneimittel metabolisierenden Enzymen und Transportern können die Fähigkeit, Arzneimittel und andere Fremdstoffe zu metabolisieren und auszuscheiden, erheblich beeinflussen. Die Folge sind unerwartete Reaktionen der Patienten auf die Arzneimitteltherapie. So können bei normaler Dosis Nebenwirkungen oder reduzierte Wirkung die Folge sein, je nachdem, ob die Metabolisierungsrate durch den Polymorphismus verlangsamt oder erhöht wird. CYP2D6 stellt eines der wichtigsten am Arzneimittelmetabolismus beteiligten Enzyme der menschlichen Leber dar, das in der Population eine erhebliche interindividuelle Variabilität zeigt, die für die Arzneimitteltherapie klinische Relevanz besitzt. Gemessen an der Arzneimittelstoffwechselkapazität lassen sich vier Phänotypen unterscheiden: ultraschnelle Metabolisierer (UM), normal effiziente Metabolisierer (EM), intermediäre Metabolisierer (IM) sowie langsame Metabolisierer (PM). Die Forschung der vergangenen 25 Jahre hat gezeigt, dass diese interindividuellen Unterschiede im Wesentlichen durch genetische Polymorphismen im *CYP2D* Genlokus auf Chromosom 22 verursacht werden. Zahlreiche allelische Varianten sind bekannt, die zu erhöhter, normaler, erniedrigter oder fehlender CYP2D6 Proteinmenge und/oder enzymatischer Funktion führen. Personen mit PM Phänotyp können heute anhand des Vorliegens von Nullmutationen auf beiden Chromosomen mit großer Zuverlässigkeit identifiziert und ggf. mit einer veränderten Dosis behandelt werden. Im Gegensatz dazu sind die ebenfalls mit einem Risiko behafteten ultraschnellen und intermediären Metabolisierer wesentlich schlechter vorhersagbar.

Der intermediäre Metabolisierer-Phänotyp stellt eine Populationsubgruppe von 10-15 % dar und ist charakterisiert durch eingeschränkte aber noch nachweisbare Restenzymaktivität. Die beiden schon länger bekannten Allele *2D6*9* und *2D6*10* sind mit erniedrigter *in vivo* Metabolisierungskapazität assoziiert, dennoch ließen sich dadurch nicht mehr als 10-20 % der kaukasischen IMs erklären. Im Bestreben die genetische Basis für den IM Phänotyp aufzuklären wurde in der Arbeitsgruppe

Pharmakogenetik am IKP Stuttgart das *CYP2D6*41*-Allel identifiziert, das sich als zweithäufigstes Defektallel des CYP2D6 Gens herausstellte. Genetisch ist das **41* Allel eng mit dem voll funktionsfähigen **2*-Allel verwandt, von dem es sich vor allem durch das Fehlen einer -1584C>G Mutation im Promoter unterscheidet. Eine weitere Mutation 2988G>A war im Intron 6 von **41* gefunden worden. Es war jedoch nicht bekannt, welcher der beiden SNPs kausal für die erniedrigte Expression des Allels **41* verantwortlich war. Es war ebenfalls nicht zuverlässig bekannt, ob dies die einzigen Sequenzunterschiede waren oder ob möglicherweise eine weitere, noch nicht identifizierte Mutation auf dem **41* Allel existierte.

In dieser Arbeit konnte nun zweifelsfrei gezeigt werden, dass der Intronpolymorphismus 2988G>A kausal für eine stark erniedrigte Expression des Genprodukts und damit seiner Funktion in der Leber verantwortlich ist. RT-PCR Analysen mit RNAs aus genotypisierten Leberproben zeigten zunächst, dass der 2988G>A Austausch mit einer Zunahme einer nichtfunktionellen Splice-Variante, der das Exon 6 fehlte, assoziiert war. Eine Quantifizierung mittels denaturierender HPLC offenbarte, dass Träger des *2D6*41* Allels bis zu 7,3-fach mehr Splice-Variante und 2,9-fach weniger Normal-Produkt aufwiesen, was in guter Übereinstimmung war mit der in denselben Leberproben gemessenen CYP2D6 Proteinexpression. Daraufhin wurde die gesamte genomische Sequenz, welche für die *2D6*41, 2D6*2* und *2D6*1* Allele kodiert, jedoch ohne Promotorregion, in COS-1 (Nierenzelllinie der afrikanischen grünen Meerkatze) und humanen Huh7 Hepatoma Zellen rekombinant exprimiert. Das *2D6*41*-Allel, das die Intron 6 Mutation als einzigen Unterschied zum **2* Allel aufwies, exprimierte eine 2- bis 5-fach reduzierte Menge an CYP2D6 mRNA, Apoprotein und Enzymaktivität. Diese Experimente lieferten den unzweifelhaften Nachweis für einen kausalen Zusammenhang zwischen der Intron 6 Mutation 2988G>A und der phänotypisch erniedrigten Expression, die mit dem *2D6*41* Allel assoziiert ist. Weitere Experimente wurden zum Mechanismus der 2988G>A Mutation durchgeführt. In Experimenten zur mRNA-Stabilität und Reportergen-Analysen in transient transfizierten HepG2 und Huh7 Hepatomzellen wurden jedoch keine Hinweise auf veränderte RNA Abbaurate oder Transkriptionsrate gefunden, die auf diesen Polymorphismus zurückzuführen wären. *In silico* Analysen ergaben jedoch Hinweise darauf, dass der 2988G>A Austausch die Bindungsstelle für die Splicing-Faktoren SRp40 und SF2/ASF modifiziert.

Zwei weitere Individuen mit nicht erklärtem Phänotyp wurden mittels ähnlicher Strategie untersucht. Beide waren Träger des **2/*4* Genotyps, eine Allel-Kombination, die i.d.R. mit normaler Funktion assoziiert ist. Sequenz- und Haplotypanalyse bestätigten das Vorhandensein der bereits beschriebenen stillen 2939G>A Mutation in Exon 6 (früher als Variante *2D6*2J,* jetzt als Variante *2D6*59* bezeichnet) sowie einer neuen Mutation (2291G>A) im Intron 4. Transfektionsexperimente in Huh7-Zellen mit den entsprechenden genomischen *CYP2D6* Sequenzen ergaben eine 3-fach reduzierte mRNA und Enzymaktivität sowie ein 3-fach reduziertes CYP2D6 Apoprotein für diejenigen Konstrukte, die beide Mutationen oder die 2939G>A alleine trugen. Diese Daten belegen die tiefgreifende Auswirkung einer stillen Mutation auf die *CYP2D6* Expression und Funktion.
Mit der molekularen Charakterisierung der beiden Allele, die mit dem intermediären Metabolisierer Phänotyp assoziiert sind, trägt dieser Teil der Arbeit zu einer verbesserten Vorhersage der CYP2D6 Enzymaktivität beim Menschen bei. Dies kann in klinischen Studien zu einer verbesserten Vorhersage von unerwünschten Arzneimittelwirkungen und damit letztlich zu einer sichereren Arzneimitteltherapie führen.
Ultraschnelle CYP2D6 Metabolisierer sind oft mit der Vererbung von Allelen assoziiert, die eine funktionelle 2D6 Genduplikation oder –amplifikation tragen. Dennoch findet sich die *2D6* Genduplikation nur bei 10-30 % aller ultraschnellen Metabolisierer innerhalb der kaukasischen Bevölkerung. Deshalb wurde in dieser Arbeit versucht, eine Erklärung für dieses Phänomen zu finden um ggf. eine verbesserte Vorhersage zu erreichen. Die Genotypisierung des SNPs del138T im *CYP2D7* Pseudogen mittels TaqMan in 287 Leberproben diente zur Überprüfung der Hypothese eines aktiven CYP2D7 Pseudogens in CYP2D6 duplikations-negative UM Proben. Das *CYP2D7* Pseudogen besitzt eine Leserastermutation ins138T im Exon 1, die das offene Leseraster zerstört und deshalb nicht-funktionell ist. Es konnte gezeigt werden, dass sich in der untersuchten Probensammlung keine positiven Individuen befanden. Eine weitere Hypothese basierte auf einer vorhergehenden Arbeit, die zeigen konnte, dass HNF4 und COUPTFI, ein positiver und ein negativer Regulator, um die gleiche Bindungstelle im *CYP2D6* Promotor konkurrieren. In 87 Leberproben wurde die HNF4 und COUPTFI mRNA Expression mit TaqMan real-time PCR bestimmt, um ein eventuelles Ungleichgewicht in der Expression dieser zwei Transkriptionsfaktoren zu untersuchen, was wiederum zu einer erhöhten

CYP2D6 Expression führen könnte. Auch in diesem Fall konnte keine signifikante Korrelation zwischen der CYP2D6 Proteinexpression und COUPTFI und HNF4 mRNA beobachtet werden. Demgemäß scheint diese Hypothese keine Erklärung für erhöhte *CYP2D6* Expression bei UMs ohne Duplikationsallel zu sein. Obwohl mit diesen beiden getesteten, plausiblen Hypothesen keine weitere Erklärung für den ultraschnellen Metabolisierer Phänotyp gefunden wurde, trägt die hierbei durchgeführte, systematische Untersuchung von nahezu 300 Leberproben mit vielen wertvollen Daten zur weiteren Charakterisierung des Enzyms CYP2D6 und seines genetischen Polymorphismus bei.

1 Introduction

1.1 Drug metabolism

Every organism takes up many different foreign compounds (xenobiotics) such as food components, pollutants, chemicals and drugs from the environment. Elimination of these exogenous substances as well as of many endogenous substrates like hormones from the organism often requires first their biotransformation through the enzymes of the drug or xenobiotic metabolizing system. Metabolism usually converts drugs to metabolites that are more water soluble and thus more easily excreted via kidney and bile. Most drugs are converted to pharmacological inactive products whereas some prodrugs are metabolized to therapeutically active compounds. Even toxic metabolites may be formed. A considerable portion of xenobiotics are metabolized by the intestine already after oral intake, however, the mainpart of drug metabolism occurs in liver. Drug metabolism is divided in two phases: to phase I belong functionalization reactions where functional groups are introduced by oxidation, reduction, and hydrolysis. Table 1-1 lists the most important drug metabolizing enzymes in humans. For example, alcohol dehydrogenases are responsible for the NAD-dependent dehydrogenation of primary and secondary alcohols to aldehyde and ketons; aldehyde dehydrogenases are responsible for the NAD- or NADP-dependent oxidation of alcohols to carboxylic acid; flavin monoamino oxydases are involved in the oxidation of amines and thiols. However, Cytochrome P450 enzymes play the major role in phase I metabolism, as they catalyze the metabolism of more than half of all drugs (Clarke and Jones, 2002). This superfamily of enzymes will be discussed in more detail in section 1.2. Conjugation reactions are typical for phase II enzymes, linking the functional groups created by phase I to watersoluble groups provided by the cells intermediary metabolism. UDP-glucoronosyltransferases (UGT) catalyze the conjugation with activated glucuronic acid. Typical substrates are bilirubin, steroid hormones, bile acid, biogenous amines, lipophilic vitamins, pollutants and drugs. Glutathione S-transferases (GST) catalyze the conjugation of endogenous and exogenous substrates with glutathione. Other

phase II enzymes are N-acetyl transferases (NAT), which catalyze acetylation reactions by using acetyl coenzyme A. Best known in humans is NAT2, which acetylates aromatic amines (e.g. isoniazid, a drug used in tubercolosis treatment) for being the first example for an enzyme showing genetically determined differences (Table 1-1).

Table 1-1 Common human drug metabolizing enzymes

Phase I enzymes	**Gene number[1]**	**Localisation**
Aldehyde dehydrogenase	≥ 12	ER, mitochondria, cytosol
Alcohol dehydrogenase	≥ 12	cytosol
Flavin monoamino oxydases (FMO)	≥ 5	ER
Cytochrom P450 monooxygenases	≥ 20	ER
Epoxidhydrolases	≥ 2	ER and cytosol
Esterases	≥ 5	ER and cytosol
Phase II enzymes		
UDP-glucoronosyltransferases (UGT)	> 17	ER (lum)
Glutathion-S-transferases (GST)	> 20	ER, cytosol
N-Acetyltransferases (NAT)	2	cytosol
Methyltransferases (MT)	> 5	cytosol
Sulfotransferases (SULT)	> 7	cytosol

ER= endoplasmatic reticulum
[1] estimated number of functional genes in humans, excluding pseudogenes.

1.2 The Cytochrome P450 enzyme family

The most important enzymes involved in drug metabolism belong to the cytochrome P450 family. Their name originated from early observations describing them as a pigment (P) with a spectral absorbance maximum at 450 nm seen in the presence of a reducing agent and carbon monoxide (Klingenberg, 1958). This property distinguishes them from most other hemoproteins, which display an absorption maximum at 420 nm under these conditions. The term cytochrome P450 today refers

to a superfamily of heme proteins present in nearly all organisms including yeast, bacteria, plants and higher animals. Prokaryotic cytochrome P450s are cytosolic proteins, whereas in eukaryotes these proteins are embedded in the membrane of the endoplasmatic reticulum by an amino-terminal membrane anchor. They are composed of an apoprotein between 480 and 560 amino acids and of a prosthetic heme group, with a heme iron which is coordinated by a conserved cysteine. Substrates for this enzyme system include endogenously synthesized compounds, such as steroids and fatty acids, and exogenous compounds such as drugs, food additives or industrial by-products. Typical reactions catalyzed by cytochrome P450 are hydroxylations, *N-, S-,* or *O*-dealkylations, *N-, S*-oxidations, deaminations, dehalogenations, desulfatations, epoxidations and peroxidations. The general stochiometric reactions catalyzed by cytochrome P450 is as follows:

$$NADPH + H^+ + O_2 + SH \longrightarrow NADP^+ + H_2O + SOH$$

The reaction is referred to as a monooxygenation and the enzyme as a monooxygenase because only one of the two oxygen atoms is incorporated into the substrate (S). The introduction of functional groups then facilitates conjugation reactions by phase II enzymes. The reduction equivalents provided by NADPH are transferred to the CYP enzyme by the membrane bound lipoprotein enzyme NADPH-cytochrome P450 reductive or in some cases by the small heme protein cytochrome b_5 (15 kDa) (Figure 1-1).

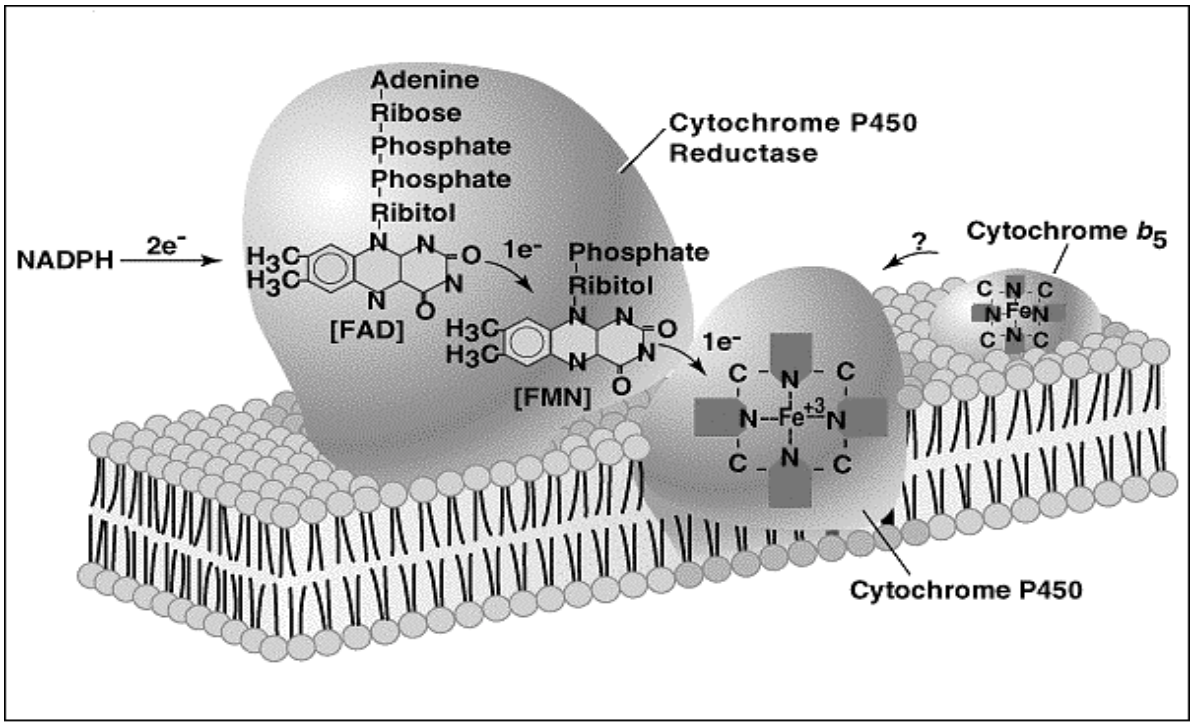

Figure 1-1 Components of the endoplasmatic reticulum (microsomal) cytochrome P450 monooxigenase system. Electron transfer from NADPH+H+ to cytochrome P450 is catalyzed by cytochrome P450 reductase, whereas cytochrome P450 catalyzes the cleavage of oxygen and the oxidation of the substrate. Both the reductase and the cytochrome P450 are embedded into the microsomal membrane via their hydrophobic N-terminal anchor sequence.

In humans, the cytochrome P450 gene super family comprises 57 functional genes and 58 pseudogenes (www.drnelson.utmem.edu/cytochrome P450 html). Based on their sequence homology all members of cytochrome P450 enzymes are classified in families and subfamilies. P450 sequences that display greater than 40 % amino acid identity are placed into the same family, and sequences that are more than 55 % identical are placed into the same subfamily (Nelson et al., 1996). An interesting feature of these enzymes are their broad and overlapping substrate specifities; a single P450 protein can metabolize numerous structurally diverse chemicals or one chemical can be metabolized by several P450s, providing the organism's capacity to metabolize and detoxify countless substances taken up from the diet and environment. The numerous members of the families CYP1, CYP2 and CYP3 represent the most important enzymes of xenobiotic phase I metabolism. To the relevant drug metabolizing isoenzymes belong the isozymes CYP1A2, CYP2A6, CYP2B6, the 2C subfamily including CYP2C8, CYP2C9, and CYP2C19, CYP2D6 and CYP2E1, as well as the CYP3A subfamily with the relevant members CYP3A4 and CYP3A5.

1.3 Pharmacogenetics

Pharmacogenetics is concerned with understanding the relationship between genetic variation and an individual's response to medicinal products. Interindividual differences in response to a xenobiotic compound were probably described first by Pythagoras in 510 BC when he noted that some, but not all, individuals develop haemolytic anemia in response to fava bean ingestion. In a report by Gorrod and Oxon in 1902, a genetic component was suggested to be involved in biochemical processes where the cause of inter-individual differences in adverse drug reactions was due to enzyme deficiencies. Thirty years later in 1932, Snyder described the first population based study to identify ethnic differences in a pharmacogenetic trait, namely the phenylthiocarbamate non-taster phenotype. In 1957, Motulsky and in 1959 Vogel released the term "pharmacogenetics" originally defined as "clinically important hereditary variation in response to drugs" (Vogel, 1959) and the discipline was established by Kalow's monograph "Pharmacogenetics" in 1962 (Gorrod A.E. and Oxon M.D., 1902; Snyder, 1932; MOTULSKY, 1957; Kalow, 1962). The term genetic polymorphism defines monogenic traits that exist in the normal population in at least two phenotypes, neither of which occurs with a frequency lower than 1 % (Snyder, 1932; Vogel and MOTULSKY, 1986; Meyer, 1991). Pharmacogenetics attempts to identify genetic variations leading to unexpected drug effects, to clarify the underlying molecular mechanism, to evaluate the clinical relevance and to develop appropriate phenotyping and genotyping tests.

1.4 Sparteine/Debrisoquine polymorphism

In the mid-seventies of the last century the first example of a genetically based enzyme defect among the cytochrome P450 system was discovered. During a pharmacokinetic study on debrisoquine, a sympatholytic antihypertensive drug, Smith and colleagues observed that a few volunteers suffered from unexpected adverse reactions even by administering subtherapeutic doses (Smith, 1986). Then it was found to be due to impaired 4-hydroxylation of debrisoquine. At the same time, a group of physicians in Bonn independently observed increased side effects associated with decreased oxidative metabolism of sparteine, an oxytocic and antiarrhythmic alkaloid (Eichelbaum et al., 1979; Smith, 1986) due to impaired oxidation of sparteine to 2,3- and 5,6-dehydrosparteine (Mahgoub et al., 1977;

Eichelbaum et al., 1979; Eichelbaum et al., 1986). These initial observations were followed both for debrisoquine and sparteine by population studies by determination of the urinary metabolic ratio (MR). The MR is defined as the ratio of the amounts of unchanged drug and drug metabolite that appear in the urine within a certain time.

$$MR = \frac{\text{Amount of sparteine}}{\text{Amount of 2.3 - and 5.6 dehydrosparteine metabolite}}$$

First analyses with sparteine and debrisoquine showed that the distribution of this parameter was nearly bimodal and allowed the definition of an antimode as threshold between two important phenotypes, termed as extensive metabolizer and poor metabolizer (EM and PM) of debrisoquine (antimode MR=12.6) and sparteine (antimode MR=20) respectively (Figure 1-2). Family studies established that in both cases poor metabolizers are homozygous for a recessive gene whereas extensive metabolizers are either homozygous or heterozygous for the dominant gene (Evans et al., 1980; Steiner et al., 1985). So it was shown that the metabolic defect is under a monogenic control and inherited as an autosomal recessive trait. Later on, it was demonstrated that the involved drug metabolizing enzyme was the cytochrome P450 2D6 (Gonzalez et al., 1988).

In addition to sparteine and debrisoquine many other therapeutically important drugs were identified which underlie the metabolism by the same enzyme. Most of the drugs are structurally heterogeneous and belong to different treatment groups. Therefore, this polymorphism has far-reaching pharmacological and clinical significance (Table 1-2).

Table 1-2 Clinical drugs of different therapeutic classes known to be metabolized by CYP2D6

CYP2D6 substrate	Therapeutic class
Alprenonol	beta-blocking agent
Amitriptyline	antidepressant
Bufuralol	beta-blocking agent
Chlorpromazine	neuroleptic
Citaloprame	antidepressant
Clomipramine	antidepressant
Codeine	analgetic
Debrisoquine	antihypertensive

CYP2D6 substrate	Therapeutic class
Desipramine	antidepressant
Dextrometorphan	antitussiv
Encainide	antiarrhythmic
Flecainide	antiarrhythmic
Fluoxetine	antidepressant
Haloperidol	neuroleptic
Imipramine	antidepressant
MDMA (methylenedioxymethamphetamine)	recreational drug amphetamines
Metoprolol	beta-blocking agent
Nortriptyline	antidepressant
Paroxetine	antidepressant
Perphenazine	neuroleptic
Perhexiline	calcium antagonist
Propafenone	antiarrhythmic
Risperidone	neuroleptic
Sparteine	antiarrhythmic
Tamoxifene	anticancer agent
Thioridazine	neuroleptic
Timolol	beta-blocking agent
Vinblastine	anticancer agent

Most of the CYP2D6 metabolized substrates are cardiovascular or psychologically active agents (Table 1-2). The consequence is that PMs possess a higher risk to suffer from adverse drug reactions, particularly when the administered drugs exhibit a narrow therapeutic window (Eichelbaum et al., 1986; Brosen and Gram, 1989; Cholerton et al., 1992). On the other hand, some substrates of CYP2D6 are so called pro-drugs, which need a previous metabolic activation unless they became intrinsic active agents. As an example, the conversion from codeine to active analgetic morphine occurs primary through CYP2D6 catalyzed *O*-demethylation. Indeed it was shown that this drug is ineffective in poor metabolizers (Chen et al., 1988; Chen et al., 1991).

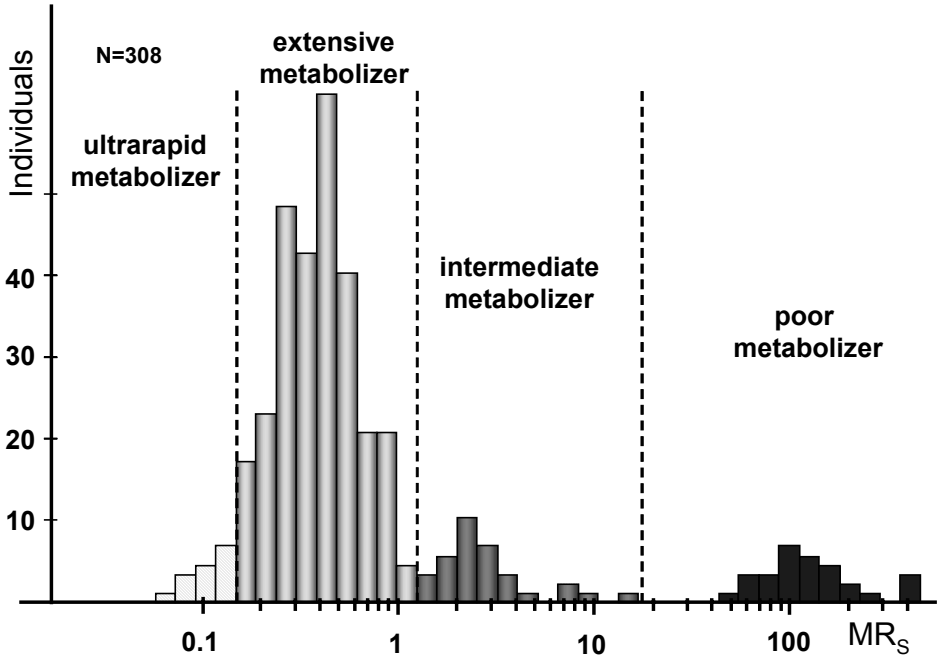

Figure 1-2 Phenotype distribution in a European population. The sparteine MR ranges for four phenotypes are indicated by perpendicular line: ultrarapid metabolizers (UM): MR<0.15; extensive metabolizers (EM): 0.15≤MR≤1.2; intermediate metabolizers (IM): 1.2<MR<20; and poor metabolizers (PM) MR≥20.

Among Caucasians this phenotype, caused by lack of functional CYP2D6 enzyme, occurs with a frequency of 5-10 %. The extensive metabolizer phenotype is the result of presence of two functional alleles or the combination of one functional allele and one nonfunctional allele. The MR distribution for sparteine (MR_S) shows an extensive deviation from a normal distribution and often separates into two groups comprising the major 'normal' extensive metabolizer group (75-85 %) and a subgroup of approximately 10-15 % of the population termed intermediate metabolizers (Bock et al., 1994). Moreover, an additional subgroup at the opposite extreme is represented by ultrarapid metabolizers (UM) which sometimes carry more than two functional gene copies resulting in extremely high drug oxidation capacity (Johansson et al., 1993; Ingelman-Sundberg, 1999) (Figure 1-2).

1.5 The CYP2D gene locus on chromosome 22

The human *CYP2D* locus consists of three highly homologous genes, *CYP2D8P, CYP2D7* and *CYP2D6*, which are located in this orientation (5' to 3') within a contiguous region of about 45 kb (Kimura et al., 1989) (Figure 1-3). Like other members of the *CYP2* gene family, *CYP2D* genes consist of nine exons and eight

introns, *CYP2D6* spanning 4378 bp. *CYP2D8* and *CYP2D7* share 92 % and 97 % homology to *CYP2D6*, respectively, and are probably the result of a gene duplication (Heim and Meyer, 1992). *CYP2D8* and *CYP2D7* were classified as pseudogenes by Kimura et al, 1989, who were not able to detect specific mRNA by Northern blot in human liver. *CYP2D8* is a true pseudogene with multiple deletions and insertions and no open reading frame. The *CYP2D7* coding sequence contains only a single inactivating mutation, an insertion T138 in the first exon, causing a shift of the reading frame and premature translation termination (Kimura et al., 1989). Based on *Xba* I restriction fragment length polymorphisms the CYP2D gene cluster is defined by different haplotypes (13 kb, 29 kb und 44 kb) which differ in the number of pseudogenes and functional *CYP2D6* gene.

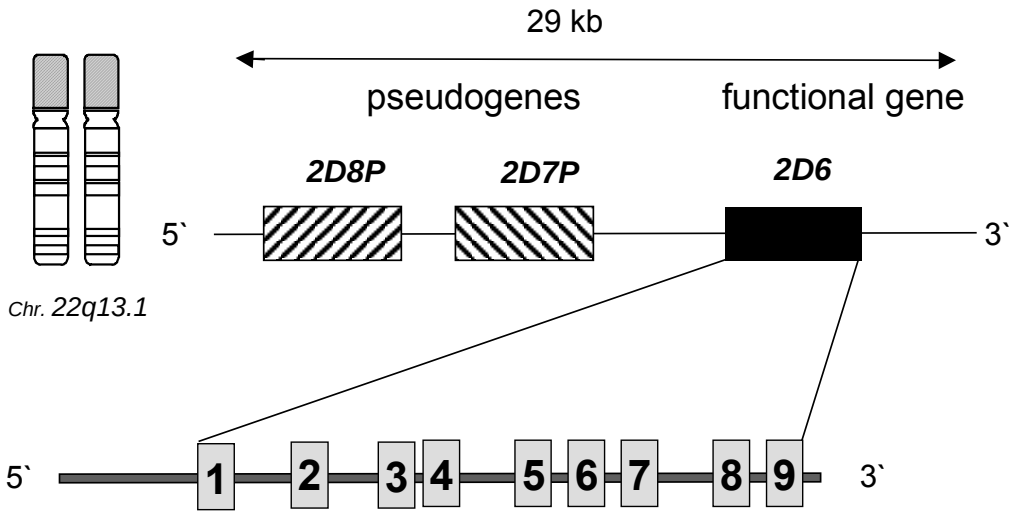

Figure 1-3 *CYP2D* gene cluster. Localisation of the *CYP2D* gene cluster on the long arm of chromosome 22(q13.1) and the position of the pseudogenes *CYP2D8 and CYP2D7* and the functional *CYP2D6* in the CYP2D gene cluster. In the lower part, exons (numbered boxes) and introns (thick lines) are shown.

1.6 Molecular mechanism of the CYP2D6 polymorphism

The *CYP2D6* genetic polymorphism is caused by the presence of multiple alleles. A systematic nomenclature was introduced in 1996 (Daly et al., 1996a). Alleles that share “key mutations”, i.e., a sequence variation with major functional effect or leading to an amino acid change, are designated by the same allele number whereas further allelic variants (with the same key mutation but with different additional sequence variation) are distinguished by letters (Ingelman-Sundberg et al., 2000;

Zanger et al., 2004). The CYP allele nomenclature homepage at http://www.imm.ki.se/CYPalleles/ currently lists 58 alleles with a total number of currently 89 distinct variants. Figure 1-4 shows molecular details of those alleles and their protein products for which reliable phenotype information is currently available.

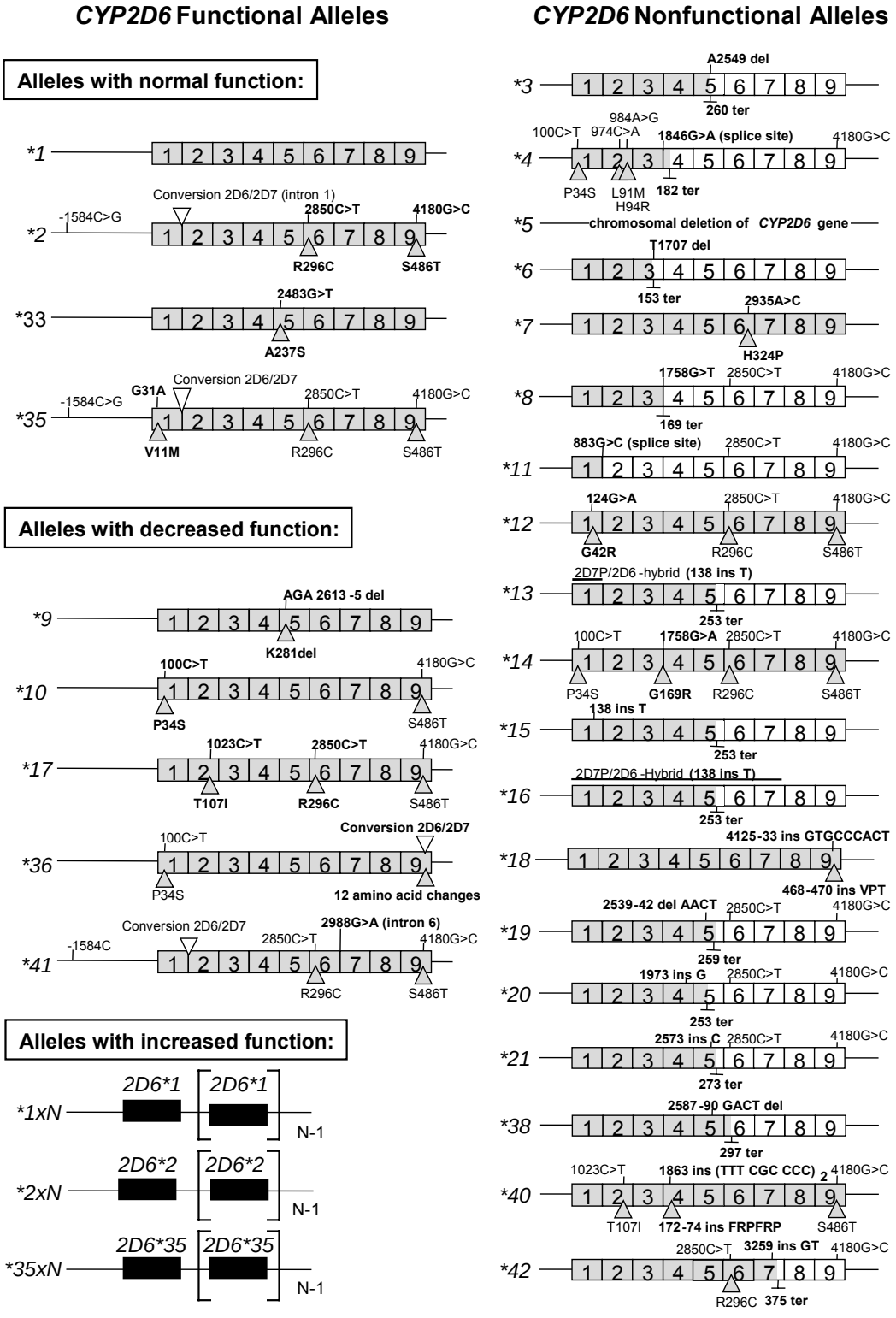

Figure 1-4 Structure of functional and non-functional *CYP2D6* alleles. Only alleles with available phenotypic information are shown. The 9 exons are indicated by numbered boxes with DNA polymorphisms indicated on top (*del* deletions, *ins* insertion). Predicted amino acid changes and translation termination (*ter*) are indicated below. Open reading frames are indicated by *shaded boxes*. Adapted from Zanger et al., 2004

1.6.1 Alleles with normal enzyme activity

The wild type allele **1* has per definition a normal enzyme activity (Kimura et al., 1989). The *CYP2D6*2* allele carries an extended intronic part of the *CYP2D7* gene which originated presumably from a gene conversion, and two mutations, 2850C>T and 4180G>C, leading to amino acid changes R296C and S486T, respectively. Up to date, only minor phenotypic consequences of these two nonsynonymous SNPs have been described. Recombinant 2D6.2[R296C, S486T] appeared to have somewhat lower activity as 2D6.1 (Zanger et al., 2001; Yu et al., 2002) but studies in human liver tissues revealed higher expression of 2D6.2 versus 2D6.1 at the protein level (Zanger et al., 2001). Nevertheless, *2D6*1* and *2D6*2* alleles had very similar activities in vivo (Zanger et al., 2004). In Caucasians the *2D6*2* allele has a frequency of about 20-30 % (Sachse et al., 1997; Griese et al., 1998; Zanger et al., 2001). Allele *CYP2D6*35,* a variant form of the **2* allele, carries the additional 31G>A mutation leading to Val11Met change and having functional activity and expression level comparable to wild type (Griese et al., 1998; Allorge et al., 2001).

1.6.2 Alleles with increased enzyme activity

Individuals with extremely high hydroxylation capacity were found to have multiple copies of apparently functional *CYP2D6* as a result of unequal crossover events and other mechanisms (Johansson et al., 1993; Bertilsson et al., 1993; Lundqvist et al., 1999). The 2D6xN (N including **1, *2, *35, *41)* alleles were shown to occur with frequencies of 1 to 2 % in northern European populations (Dahl et al., 1995; Sachse et al., 1997; Griese et al., 1998; Bathum et al., 1998), whereas much higher frequencies were observed in Ethiopians (Aklillu et al., 1996) and in Saudi Arabians (McLellan et al., 1997) and an intermediate frequency was found in Spanish populations (Agundez et al., 1995).

1.6.3 Alleles with decreased enzyme activity

Some variants were shown *in vivo* or *in vitro* to code for protein products that are either expressed at lower levels or that have a significantly lower than normal enzyme activity. *CYP2D6*9* has a 2613-15delAGA in exon 5 which results in the lack of codon 281 and low amount of an enzymatically functional variant CYP2D6 protein.

The **9* allele has a frequency of about 1 to 2 % in Caucasians (Tyndale et al., 1991; Broly and Meyer, 1993).

*CYP2D6*10* has a C100T mutation in exon 1 leading to Pro34Ser which is the functionally dominant mutation. Proline 34 is part of a proline-rich region that is highly conserved among microsomal P450s and may function as a hinge between the hydrophobic membrane anchor and the globular heme-binding portion of the enzyme (Yamazaki et al., 1993). The consequences of this mutation are decreased P450 levels but residual enzymatic activity (Zanger et al., 2001; Yu et al., 2002). In Caucasians the *2D6*10* allele has a frequency of about 2 % and accounts for 10 to 20 % of individuals with IM phenotype (Sachse et al., 1997; Griese et al., 1998). In Oriental populations the frequency of *2D6*10* exceeds 50 % and is responsible for a shift in the median metabolic ratio of debrisoquine/ sparteine to higher values compared to Caucasians (Yokota et al., 1993; Armstrong et al., 1993; Wang et al., 1993).

The *CYP2D6*41* allele is a slow form of the functional **2* allele initially identified by the pharmacogenetic group at IKP and shown to be distinct from *2 the latter by the absence of the *2-associated promoter polymorphism -1584C>G (Raimundo, 2001). In the course of further investigations, an intron 6 mutation 2988G>A was suggested to be also linked to the **41* allele (Raimundo, 2001). However, the relationship between the two polymorphisms and their impact on the function of CYP2D6 gene expression or function remained unknown. The molecular mechanism leading to decreased enzyme activity will be discussed in this work. The frequency of **41* in the Caucasian population is approximately 8 % and the **41* allele in combination with a null allele allows to identify more than 50 % of all IM in Caucasians (Raimundo, 2001).

1.6.4 Null alleles

Null alleles do not encode a functional protein product and in the case of *CYP2D6* there is no detectable residual enzymatic activity. Only null alleles cause the PM phenotype if present in homozygous or compound heterozygous compositions. Different mechanisms were found to lead to the total loss of function:

Several alleles have single base pair mutations or small insertions/ deletions that interrupt the reading frame or that interfere with correct splicing leading ultimately to

prematurely terminated protein products (*2D6*3* and *2D6*4*; Kagimoto et al., 1990; *2D6*6*, *8, *11, *15, *19, *20, *38, *40, *42, *44*).

Only a few alleles code for full-length but non-functional proteins (*2D6*7*; Evert et al., 1997; *2D6*12, *14, *18*). At least three alleles are the result of larger chromosomal deletions resulting in deletion of the entire *CYP2D6* gene (*2D6*5*; Gaedigk et al., 1991) or in *CYP2D6/2D7* hybrid genes with interrupted open reading frame (*2D6*13* and *2D6*16;* Daly et al., 1996b).

*2D6*4* is the most frequent null allele in Caucasians which occurs with an allele frequency of about 20-25 % and is responsible for 70 to 90 % of all PMs. The 1846G>A key mutation causes a shift of the consensus acceptor splice site of the third intron by one base, thereby resulting in a spliced mRNA with one additional base that has an altered reading frame and premature stop codon.

1.7 Clinical significance of CYP2D6 phenotypes

The incidence of adverse drug reactions during drug treatment still represents a serious problem. A meta-analysis of prospective studies determined that the incidence of adverse drug reactions represents between the fourth and sixth leading cause of death in hospitalised patients in USA (Lazarou et al., 1998). On the other hand for some drugs only 50-75 % of the patients respond to the treatment. One third of all adverse drug reactions depend on drug interactions, which play a considerable role in polypharmacy (Spear, 2001). Besides the influence of age, gender and diseases, also genetic factors, which can account for 20-95 % of the variability within drug distribution and efficacy, play a decisive role in their effectiveness and toxicity (Evans and McLeod, 2003). For the highly polymorphic CYP2D6, the poor metabolizer phenotype can be identified with >99 % certainty as carriers of two null alleles, whereas it has remained much more difficult to predict the metabolic capacity of extensive metabolizers (i.e. individuals carrying one or more functional gene copies).

About 10-15 % of European Caucasians form a distinct subgroup with impaired drug oxidation capacity intermediate between normally efficient and poor metabolizers and are thus termed intermediate metabolizers (IM). Reduced drug oxidation capacity among Caucasian IMs is not simply the result of heterozygosity for a *CYP2D6* null allele, but involves alleles with impaired function, including the more rare alleles **9* and **10*, and the more frequent **41*. The clinical importance of the IM phenotype

should be emphasized as several studies indicate that drug pharmacokinetics in IMs can be more similar to the PM than to the normal EM situation. For example, in a study with nortriptyline, no difference in the AUC and C_{max} was found between five PM and five IM subjects (Dalen et al., 1998). In a study on long-term metoprolol treatment, Rau et al. found similar plasma concentrations in patients with IM and PM phenotype (Rau et al., 2002). Perhexiline metabolism was also found to be markedly different between individuals with normal EM and IM genotype (Barclay et al., 2003).
The ultrarapid metabolizer (UM) phenotype represents the other extreme functional phenotype of the EM distribution. Identification of subjects with ultrarapid metabolic capacity is of potential clinical value. When patients do not respond to generally recommended doses and lower than expected plasma concentrations in relation to dose are measured, it is important to be able to distinguish between high metabolic capacity and non-compliance. UMs sometimes carry more than two functional gene copies resulting in extremely high drug oxidation capacity and require abnormally high drug doses to attain therapeutic plasma levels. The frequency of CYP2D6 duplication/amplification alleles differs between European populations showing a typical North-South divide. However, increased *CYP2D6* gene copy number as a consequence of duplication of alleles predicts a fraction of not more than about 20 % of all ultrarapid metabolizer phenotypes in Caucasians (Johansson et al., 1993; Dahl et al., 1995; Ingelman-Sundberg, 1999). In an attempt to uncover further polymorphisms associated with unusually low MR, Lovlie et al. (2001) selected duplication-negative UM subjects and examined the CYP2D6 promoter region. However, the two variants that appeared to be over-represented among UM individuals could not be clearly associated with the UM phenotype.

1.8 Objectives

The primary objective of this thesis is the molecular analysis of mechanisms leading to CYP2D6 *intermediate* and *ultrarapid* metabolizer phenotypes. With respect to the *intermediate metabolizer*, the specific aims are:

- to identify the causative mutation(s) leading to the impaired function phenotype associated with the *CYP2D6*41* allele;
- to analyze molecular mechanism(s) that lead to impaired function of **41;*
- to use this information for comprehensive genotype-phenotype analysis and to improve *CYP2D6* genotyping;

- to investigate cases of discrepant genotype-phenotype relationship.

With respect to the *ultrarapid metabolizer*, the specific aims are:

- to carry out a extended correlation analysis for the *CYP2D6* gene-duplication alleles and functional phenotype;
- to develop and to test hypotheses to explain the basis of *ultrarapid metabolizer* who are not carriers of such duplication alleles.

To achieve these goals, the following resources and tools are available at the Institute:

- DNA collections from individuals of German and Ghanaian origin who have been phenotyped *in vivo* with sparteine (i.e. metabolic ratio available) and previously genotyped for a large number of *CYP2D6* alleles;
- a collection of well characterized human liver samples from patients not phenotyped *in vivo*. These samples are suitable to study CYP2D6 expression on the mRNA, protein and enzyme activity level and to relate these data to certain SNPs and alleles;

CYP2D6 wild-type cDNA and recombinant systems suitable for expression of functional cytochromes P450 to investigate the impact of individual SNPs on the mRNA, protein and activity level.

2 Material and Methods

2.1 Material

2.1.1 Chemicals, reagents and enzymes

Acetonitrile	Roth, Karlsruhe
Acrylamide/Bis (30:0.8)	Bio-Rad, München
Actinomycin D	Sigma, Deisenhofen
Adenosine triphosphate	Roche, Mannheim
Agarose	Invitrogen, Karlsruhe
Alkaline phosphatase, shrimp	Roche, Mannheim
Ammoniumpersulfate	Merck, Darmstadt
Ampicillin	Sigma, Deisenhofen
Bacto agar	Becton Dickinson, Heidelberg
Bacto yeast	Becton Dickinson, Heidelberg
Bacto trypton	Becton Dickinson, Heidelberg
BIO-RAD Protein Assay	Bio-Rad, München
Bromphenolblue	Aldrich, Deisenhofen
BSA (bovine serum albumin)	Sigma, Deisenhofen
Coenzyme A	Sigma, Deisenhofen
Dimethylformamide (DMF)	Roth, Karlsruhe
Dimethylsulfoxide (DMSO)	Sigma, Deisenhofen
Dithiothreitol (DTT)	Sigma, Deisenhofen
DNA standard (1kb Plus)	Gibco, BRL GmbH, Karlsruhe
Emerald^{TM} Enhancer	Tropix, Applied Biosystems, Forster City, CA, USA
Ethidiumbromide	Sigma, Deisenhofen
Ethylendiamintetraacetic acid (EDTA)	Sigma, Deisenhofen
Ficoll 400	Serva, Heidelberg

Galacton^{R}	Tropix, Applied Biosystems, Forster City, CA, USA
Glycine	Serva, Heidelberg
Glucose 6-phosphate	Roche, Mannheim
HCl	Merck, Darmstadt
IPTG	Roth, Karlruhe
Klenow enzyme	Roche, Mannheim
Lipofectamine 2000^{TM}	Invitrogen, Karlsruhe
Long Ranger Gel Solution	Cambrex, Rockland, USA
Low Melt Agarose	Roth, Karlsruhe
Luciferin	Applichem, Darmstadt
Magnesium chloride	Merck, Darmstadt
Milk powder, low fat	Fluka, Deisenhofen
β-Mercaptoethanol	Sigma, Deisenhofen
$NADP^{+}$	Fluka, Deisenhofen
NaCl, sodium chloride	Merck, Darmstadt
Opti-MEM®	Gibco, BRL, Karlsruhe
Passive Lysis Buffer (5 x)	Promega, Madison, WI, USA
Penicillin-Streptomycin	Merck, Darmstadt
Ponceau S-solution	Sigma, Deisenhofen
Propafenone-HCl	Knoll AG, Ludwigshafen
Rainbow ^{TM} coloured protein molecular weight markers	Amersham, Buckinghamshire, UK
Restriction endonucleases	NEB, Frankfurt
SDS (sodiumdodecylsulfate)	Sigma, Deisenhofen
Sodium hydroxide	Merck, Darmstadt
Sodium phosphate	Merck, Darmstadt
SuperSignal Dura Chemoluminescent Substrate	Pierce, Rockford, USA
T4-DNA Ligase	Roche, Mannheim
Taq DNA Polymerase	Qiagen, Hilden
TEMED	Gibco, BRL GmbH, Karlsruhe
Triethylammonium acetate (TEAA)	Transgenomic Inc., Omaha, NE
Tris-Base	Roth, Karlruhe
Trypsin-EDTA-solution	Gibco, BRL GmbH, Karlsruhe
Tween-20	Merck, Darmstadt

UDPGA (Uridine 5'-diphosphoglucuronic acid)	Sigma, Deisenhofen
Urea	Promega, Madison, WI, USA
X-Gal	Roth, Karlruhe

2.1.2 Instruments

ABI Prism 7500	Applied Biosystem
Agarose gel electrophoresis	
Perfect Blue Gel System S (7 x 8 cm)	PeqLab, Erlangen
Easy Cast model B2 (12 x 13 cm)	Owl, Portsmouth, USA
AutoLumat Plus	Berthold Technologies, Bad Wildbad
Centrifuges:	
Biofuge 13	Heraeus, Hanau
Centrifuge 5417 C	Eppendorf, Hamburg
Sorvall® Superspeed RC2-B	Thermo Electron, Hanau
DNA Sep® Column System	Transgenomic Inc., Omaha, NE
Fastblot B43	Biometra, Göttingen
Fast Prep FP120 Homogeniser	Q-Biogene, Heidelberg
HPLC system (HP 1100)	Agilent Technologies, Waldbronn
HPLC-Reprosil-Pur 120-ODS3 column (50x23 mm I.D., 5 µM)	Trentec Analysentechnik, Gerlingen
Ion trap mass spectrometer	HCT plus, Bruker Daltronics, Bremen
LI-COR 400 DNA Sequencer	LI-COR, Lincoln, Nebraska
Luminescent Image Analyzer LAS-1000	Fuji Photo Film, Düsseldorf
Novaspec II Visible Spectrophotometer	Amersham, Buckinghamshire, UK
PTC200 thermal cycler	MJ Research Inc., Waterdown, MA
UV-Visible Spectroscopy System 8453	Agilent, Waldbronn
WAVE™ DNA Fragment Analysis System (DHPLC)	Transgenomic Inc., Omaha, NE

2.1.3 Buffers and solutions

TAE (50 x)	Glacial acetic acid	57.1	ml
	EDTA (0.5 M, pH 8)	100	ml
	H_20_{mp}	ad 1000	ml
TE 10.01	Tris-HCl (pH 8)	10	mM
	EDTA (pH 8)	1	mM
DNA loading buffer (5 x)	Ficoll (20 %)	874	µl
	Bromphenolblue (0.5 %)	87.4	µl
	EDTA (0.5 M, pH 8)	38	µl
APS 10 %	Ammoniumpersulfate	1	g
	H_20_{mp}	ad 10	ml
Laemmli sample buffer (5 x)	Tris-HCl pH 6.8	60	mM
	Glycerin	24	%
	SDS	2	%
	Bromphenolblue	1	%
	β-Mercaptoethanol	14.4	mM
Electrophoresis buffer (10 x)	Tris-Base	150	g
(SDS-PAGE)	Glycine	720	g
	SDS	50	g
	H_20_{mp}	ad 5000	ml
Blotting Buffer	Tris-Base	14.6	g
	SDS 10 %	18.5	ml
	H_20_{mp}	4000	ml
	Methanol	ad 5000	ml
TBS (10 x)	Tris-Base	150	g
	NaCl	400	g
	KCl	10	g
	H_20_{mp}	ad 5000	ml
Stacking Gel	Acrylamide/Bis (30:0.8)	1.35	ml
(SDS-PAGE)	Tris-HCl 0.5 M (pH 6.8)	2.5	ml
	SDS 10 %	100	µl
	APS 10 %	100	µl
	TEMED	10	µl
	H_20_{mp}	ad 10	ml

Resolving Gel (10 %)	Acrylamide/Bis (30:0.8)	10 ml
(SDS-PAGE)	Tris-HCl 1.5 M (pH 8.8)	7.5 ml
	SDS 10 %	300 µl
	APS 10 %	300 µl
	TEMED	30 µl
	H_20mp	ad 30 ml
Sequencing gel:	Urea	21 g
	Long Ranger Solution	6 ml
	TBE 10 x	5 ml
	DMSO	500 µl
	TEMED	50 µl
	H_20mp	ad 50 ml
after filtration	APS 10 %	400 µl
TBE (10 x) long run	Tris	162 g
	Boric acid	27.5 g
	EDTA	9.3 g
	H_20mp	ad 1000 ml
β-Galactosidase Assay buffer	Na_2HPO_4 (pH 8)	100 mM
	$MgCl_2$	1 mM
	Galacton^R	1.25 µg/ml
β-Galactosidase Stop solution	NaOH	0.2 M
	Emerald^{TM} Enhancer	2.5 %
RIM+ buffer	Luciferin	50 µM
	ATP	2 mM
	$MgCl_2$	10 mM
	Coenzyme A	27 µM
	DTT	30 mM
	Glycylglycine (pH 7.8)	25 mM
Antibiotics and other		
	Stock solution	Final concentration
Ampicillin	100 mg/ml (in 50 % EtOH)	100 µg/ml

Penicillin	105 U/ml	100 U/ml
Streptomycin	10 g/ml	10 mg/ml
IPTG	50 mg/ml (in 50 % EtOH)	50 µg/ml
X-Gal	40 mg/ml (in DMF)	40 µg/ml

2.1.4 Cell lines and culture media

2.1.4.1 Bacterial cell culture

E.coli strains:

XL-1 Blue	Stratagene, La Jolla, California
JM 109	Promega, Madison, WI, USA
TOP10F'	Invitrogen, Karlsruhe

LB-("Luria-Bertani") medium	Tryptone	10 g
(+ Agar)	Yeast extract	5 g
	NaCl	5 g
	H20mp	ad 1 l
	(Agar	15 g)
SOC	Trypton	20 g
	Yeast extract	5 g
	NaCl	0.58 g
	KCl	0.18 g
	$MgCl_2$	2 g
	Glucose	4 g
	H_20mp	ad 1 l

2.1.4.2 Eukaryotic cell culture

Cell lines:

COS-1: African green monkey kidney epithelial cell line, kindly provided by Prof. Dr. Urs Meyer, Division Pharmacology/Neurobiology Biozentrum, University of Basel

Huh7: human hepatoma cell line, kindly provided by Epidauros AG, Bernried

IHH: immortalized human hepatocytes, kindly provided by Prof. Dr. Jan Hengstler, Zentrum für Toxikologie, Leipzig

DMEM (Dulbecco's modified Eagle medium)	Gibco, Carlsbad, California
MEM (Minimum essential medium)	Gibco, Carlsbad, California
L-Glutamine	Gibco, Carlsbad, California
Fetal bovine serum	Biochrom, Berlin

2.1.5 Expression vectors

Table 2-1 Expression vectors used in this study

Vector	Properties	Origin/Reference
pGEM®-T Easy	T7 and SP6 RNA polymerase promoter MCS within the α-peptide coding region of the β-galactosidase enzyme, direct cloning of PCR products	Promega, Madison,WI, USA
pCR4-TOPO	T7 and T3 RNA polymerase promoter direct cloning of PCR products	Invitrogen (Karlsruhe)
pCMV4	mammalian expression plasmid driven by CMV promoter	U. Zanger, IKP Stuttgart
pGL3-Tk(-105)	reporter gene vector driven by 105 bp of the tymidine kinase promoter	O. Burk, (Geick et al., 2001)
pCMVβ	β-Galactosidase expression vector	BD Biosciences Clontech, Palo Alto, USA
pBS SK+2D6	pBluescript SK+ vector containing the *CYP2D6* wild type cDNA	Evert et al., 1997
79-TOPO	pCR4-vector containing a splice variant of *CYP2D6* cDNA between exon 5-9, lacking exon 6	see this study
2D6pCMV	expression plasmid driven by CMV promoter containing the *CYP2D6 wild type* cDNA (M374V)	Evert et al., 1997
pCLA 24	expression plasmid driven by CMV promoter containing the *CYP2D6* wild type genomic sequence	see this study
pCLA 53	expression plasmid driven by CMV promoter containing the *CYP2D6 *2* genomic sequence	see this study

Vector	Properties	Origin/Reference
pCLA 46	expression plasmid driven by CMV promoter containing the *CYP2D6 *41* genomic sequence	see this study
pCLA 41	expression plasmid driven by CMV promoter containing the *CYP2D6 *2J* genomic sequence	see this study
pCLA 52	expression plasmid driven by CMV promoter containing the CYP2D6 **2J* genomic sequence lacking 2291G>A SNP, **2J (1)*	see this study
pCLA 45	expression plasmid driven by CMV promoter containing the CYP2D6 *2J genomic sequence lacking 2939G>A SNP, **2J (2)*	see this study
pCLA 56	pGL3-Tk(-105) vector containing 250 bp of the *wild type* sequence surrounding exon / intron 6	see this study
pCLA 57	pGL3-Tk(-105) vector containing 250 bp of the **41* sequence surrounding exon / intron 6	see this study

2.1.6 Antibodies and recombinant proteins

mouse anti-hu CYP2D6 monoclonal antibody (mAb114)	(Zanger et al., 1988)
Goat anti-mouse IgG peroxidase-conjugate (Calbiochem)	EMD Biosciences, San Diego, CA
Recombinant lymphoblastoid CYP2D6 protein	Gentest, Frankfurt
Recombinant CYP2D6 (db1)	(Zanger et al., 1988)

2.1.7 DNA and liver samples

Since 1999, a large collection of human liver tissues (n>300) and corresponding blood samples has been established at the Dr. Margarete Fischer-Bosch Institute of Clinical Pharmacology, Stuttgart. The liver samples were obtained from non-tumorous tissue from inividuals of Caucasian origin undergoing liver surgery for various reasons at the Humboldt University Berlin Charité, Departement of General, Visceral and Transplantation Surgery (Wolbold et al., 2003). The preparation of genomic DNA from corresponding blood samples and of liver microsomes had been

described earlier (Lang et al., 2001). The study has been carried out in accordance with the declaration of Helsinki and approved by ethics committee of the medical Faculties of the Charité, Humboldt University Berlin, and written informed consent was obtained from each patient.

2.1.8 Oligonucleotides

Table 2-2 Oligonucleotides used in this study

Name	Loc.	Sequence (5'-3')	Purpose
2D6gen_F_*Bgl*II 3874 r	ex 1 in 4	GGAAGATCTATGGGGCTAGAAGCACTGG AATCTCTGACGTGGATAGGAG	Cloning CYP2D6 fragment α
2D6 5' ex 3 2D6gen_R_*Xba*I	ex 2 ex 9	CCTTCATGGCCACGCGC TTAATCTAGACTAGCGGGGCACAGCACA	Cloning CYP2D6 fragment β
2D6_ex6_Bgl/ F 2D6_in6_Bgl//R	ex 6 in 6	AGATCTCTGCTCAGGCCAAGGGGAAC AGATCTTCAAGCCTGTGCTTGGAGCC	Ex6/In6 cloning
2667r_neu Cyp2d6rev3	ex 5 ex 9	ACTGAGGCCTTCCTGGCAGAGAT TCACCAGGAAAGCAAAGA	RT- PCR in human liver
dpyd06-F dpyd06-R	ex 6 ex 6	GAGGATGTAAGCTAGTTTC CCATTTGTGTGCGTGAAGTTC	Normalization
2D6 ex4/5 F 2D6 ex7/8 R	ex 4/5 ex 7/8	TTCTGCGCGAGGTGCTGAATGC GTGATGAGTGTCGTTCCCTTAGGGATG	RT- PCR in transfected Huh7 cells
2D6 In6 AD-F 2D6 In6 AD-R CYP2D6 in6-G probe CYP2D6 in6-A probe	in 6 in 6 in 6 in 6	GGGTGTCCCAGCAAAGTTCAT GCCTCCTGCTCATGATCCTACAT VIC-TACCCTTCCTCCCTC-MGB FAM-TACCCTTTCTCCCTCG-MGB	Genotyping 2988G>A by TaqMan
2D6 N_Qf 2D6 Q_ rev Ex 7 probe	ex 6 ex 7 ex 7	CTCCTGCTCATGATCCTACATCC CGGGATGTCATATGGGTCACACC VIC-TGATTCATGAGGTGCAG-MGB	Quantitation of CYP2D6 normal product
2D6 SV2_Qf 2D6 Q_ rev Ex 7 probe	ex5/7 ex 7 ex 7	GCAGAGATGGAGAAGGCCGT CGGGATGTCATATGGGTCACACC VIC-TGATTCATGAGGTGCAG-MGB	Quantitation of CYP2D6 splice variant
2D7 fw3 2D7 rev probe 2D7 ins138 probe 2D7 del138	ex 1 in 1 ex 1 ex 1	GACCTGATGCACCGGCA GTTTGCTGGTGGTGGGGC VIC-TGCAGCAAGGTTG-MGB 6-FAM-TGCAGCAGGTTG-MGB	Genotyping CYP2D7 del 138T

Name	Loc.	Sequence (5'-3')	Purpose
2D6-F10 2D6-4647 rev	in 5 in 6	CTGTCCCGAGTATGCTCTCG GGTGTCCCAGCAAAGTTCATG	Genotyping 2988G>A by DHPLC
2D6 5' ex 3 2D6 h	ex 2 in 7	CCTTCATGGCCACGCGC GGCTATCACCAGGTGCTGGTGCT	Fragment B: *CYP2D6* preamplification
2D7 ins138T for 2D7 rev	ex 1 in 1	TGGACCTGATGCACCGGCACCAACGCGG GCTGGGCAACCTTGCTGCATGTGGACTT CCAG ATGTTTGCTGGTGGTGGGGCATCCTCAG GACCGAAGCAGTATGGTGTGTTCTGGAA GTCC	ATS positive ctrl
2D7 del138T for 2D7 rev	ex 1 in 1	TGGACCTGATGCACCGGCACCAACGCGG GCTGGGCAACCTGCTGCATGTGGACTTC CAG ATGTTTGCTGGTGGTGGGGCATCCTCAG GACCGAAGCAGTATGGTGTGTTCTGGAA GTCC	ATS negative ctrl
2D7 mut Ex7 for 2D7 mut Ex7 rev	ex 7 ex 7	TTTGGGGACATCATCCCCCTGAGTGTGA CCCATATGACATCCCATG CATGGGATGTCATATGGGTCACACTCAG GGGGATGTCCCCAAA	In vitro mutagenesis

2.2 Methods

2.2.1 Molecular biological methods

2.2.1.1 Transformation of DNA in bacterial cells

1 µl DNA or 5µl ligation reaction were gently mixed with a 50 µl aliquot of commercial available chemically competent *E.coli* cells. The mixture was incubated on ice for 30 min, and then transferred for 40 s in a water bath at 42°C. 250 µl SOC medium were added and the cells were incubated at 37°C with shaking (220 rpm) for 1 h to allow expression of the antibiotic-resistance gene. At least two different dilutions were spread on LB agar plates (+ amp) containing IPTG and X-Gal for blue-white screening, if necessary, and were incubated 16 h at 37 °C.

2.2.1.2 Isolation of plasmid DNA from *E.coli* with Mini/Midi/Maxi-Prep kit (Qiagen)

Highly pure plasmid DNA was obtained by means of Qiaprep kit (Qiagen, Hilden). This procedure is based on alkaline lysis of bacterial cells, followed by purification of the DNA by ion-exchange chromatography.

After harvesting the cells from an overnight culture by centrifugation, the plasmid isolation was carried out according to the manufacturer's instructions. Depending on the DNA amount, either QIAprep Spin Mini, QIAGEN Midi or QIAGEN Maxi Purification kit (Qiagen) were used.

2.2.1.3 DNA digestion with restriction endonucleases

DNA digestions were carried out according to the manufacturer's instructions. Normally 0.1-1 µg DNA was restricted by 1-5 U of endonuclease. Specific enzyme buffers provided with the enzymes were used to achieve the best results. Double digestions were performed consecutively if the enzymes optimal temperatures were not compatible. Restriction digestions were performed in 15-60 µl scale. Incubation times and temperatures were dependent on the enzyme used and varied between 2 and 16 hours at 37 °C. After incubation the digested DNA was analyzed by agarose gel electrophoresis.

2.2.1.4 Dephosphorylation of DNA

Shrimp alkaline phosphatase was added to the digestion mixture and incubated 1 h at 37 °C. The reaction was stopped by adding 3-12 µl DNA loading buffer and subsequent gel electrophoresis was performed.

2.2.1.5 Ligation of DNA

A 3-5 fold molar excess of foreign DNA fragment was mixed with the plasmid after digestion.1 µl Ligase buffer (10 x), 1 µl T4-DNA-Ligase and H_2O_{mp} up to 10 µl were added to the mixture, which was incubated 16 h at 4 °C.

2.2.1.6 Agarose gel electrophoresis

Agarose powder was added to 1 x TAE buffer containing 0.5 µg/ml ethidiumbromide to a final concentration of 1 %. The slurry was heated in a microwave oven until agarose was dissolved. The agarose solution was cooled to 60 °C and poured into the mold and the comb previously properly positioned. After the gel was completely

set, it was transferred into the electrophoresis tank and covered with 1 x TAE (+ 0.5 µg/ml ethidiumbromide) buffer. DNA samples were mixed with 5 x DNA loading buffer and loaded into the slots of the gel. As a size standard the 1 kb-Plus ladder was used. Electrophoresis was performed at 10 V per cm and finally the gel was examined by ultraviolet light (302 nm) and documented using video copy processor (Mitsubishi, Ratingen, Germany).

2.2.1.7 Isolation of DNA fragments from agarose gel

After PCR or digestion and agarose gel electrophoresis, the DNA fragments were isolated from the agarose by means of gel extraction. The band corresponding to the desired DNA fragment was cut using a scalpel, and the agarose piece was treated as described in the QIAquick Gel Extraction Kit (Qiagen).

2.2.1.8 Elution of DNA fragments from LMP-agarose gel

Low-melting-point (LMP) agarose gel was heated, cooled at 60 °C and poured into the gel tray at a 0.8 % final concentration. After gel solidification samples were loaded and the run was performed in 1 x TAE buffer at 6 V/cm. Gel and buffer contained 0.5 µl/ml ethidiumbromide. After identification of the band corresponding to the desired DNA fragment by UV-light, the fragment was cut using a scalpel (volume ca. 100 µl). After adding 50 µl NaCl (5 M) and filled up with TE10.01 to 500 µl, the agarose piece was melted for 10 min at 65 °C. 500 µl Phenol (saturated with 0.5 M NaCl, prewarmed at 37 °C) was added, mixed and incubated for 10 min at 37 °C. After centrifugation (20 min, 14,000 rpm, 4 °C) a phase separation occurred and 2-3 volume of 100 % ethanol was added to 300-400 µl of the supernatant. DNA precipitation was performed for 30 min at –80 °C. After centrifugation (15 min 14,000 rpm) the pellet was washed with 70 % and 100 % ethanol, air dried and dissolved in 10 µl TE10.01 buffer. The concentration of the eluted fragment was estimated by analyzing 1 µl of the eluted fragment in an agarose gel.

2.2.1.9 Isolation of total RNA from liver tissue and transfected cells

Total RNA was prepared from liver tissue using either the RNeasy Midi kit (Qiagen) or Trizol reagent (Invitrogen) with subsequent RNA clean-up using the RNeasy Mini kit (Qiagen) with an on-column DNase I treatment. Total RNA was prepared from transfected cells using the Agilent Total RNA Isolation Mini kit (Agilent, Palo Alto, CA). Preparation was performed according to the manufacturer’s instructions.

2.2.1.10 Quantitation of DNA and RNA

Quantitation of DNA and RNA concentration was based on the spectrophotometric measurement of the absorption in the ultraviolet range. The spectrum was analyzed between 230 and 320 nm with the UV-Visible Spectroscopy System 8453. The absorption at 260 nm allowed the calculation of the nucleic acid concentration in the sample. An OD of 1 corresponds to approximately 50 µg/ml of double stranded DNA and 40 µg/ml for single stranded RNA. The ratio between the values at 260 nm and 280 nm (OD_{260}/OD_{280}) provided an estimate of the purity of nucleic acid. Pure DNA and RNA preparations had OD_{260}/OD_{280} values between 1.8 and 2.0.

2.2.1.11 Polymerase chain reaction (PCR)

PCR reactions were carried out with the Expand High Fidelity PCR System (Roche Diagnostics GmbH, Mannheim) or Taq-DNA-Polymerase (Qiagen) in a total volume of 50 µl. Amplifications were carried out with 1 x reaction buffer (containing 15 mM magnesium chloride), 10-200 ng template DNA (cDNA, genomic DNA or plasmid DNA), 200 µM dNTPs, 15-30 pmol of each primer and 0.85 U of Expand DNA polymerase mixture or 5 U of *Taq* DNA polymerase. Standard conditions were 2 min of denaturation at 94 °C, 30 cycles at 94 °C for 30 s, at 60 °C for 30 s and at 72 °C for 2 min, followed by a last extension step of 7 min at 72 °C. Conditions were optimized depending on target size and T_m of the primers. The PCR product was analyzed by agarose gel electrophoresis.

2.2.1.12 Site directed mutagenesis

In vitro site directed mutagenesis was carried out with QuickChange Site-Directed Mutagenesis Kit (Stratagene, La Jolla, CA) according to the manufacturer's instructions.

2.2.1.13 Sequencing of double stranded DNA

For sequencing PCR products or plasmids, the "Thermo Sequenase Fluorescent Labelled Primer Sequencing Kit with 7-Deaza-dGTP" (Amersham, Buckinghamshire, UK) was used. The 5' fluorescent IRD800 labelled sequencing primers were purchased from MWG. For each sequencing reaction, a mix consisting of 10 µl purified PCR product or plasmid, 1 µl DMSO, 2 µl labelled primer (1 pmol/µl) and 13 µl H_2O_{mp} was prepared. 4.5 µl of this mix was added to 1.5 µl of the A, C, T and G reagent. Cycle conditions were as follows: After 2 min of denaturation at 95 °C the

reaction was allowed to proceed for 30 cycles at 95 °C for 15 sec, at 57 °C for 30 sec and at 70 °C for 15 s followed by a cool-down step at 25 °C. After cycling the reaction was stopped by adding 6 µl formamide loading dye to each reaction of which 1 µl was loaded onto a 5 % polyacrylamid sequencing gel. Electrophoresis and detection of the sequencing products was performed in a LI-COR 4000 DNA sequencer with 1 x TBE long run buffer.

2.2.1.14 Construction of plasmids

*2.2.1.14.1 pCMV expression plasmids containing genomic 2D6 *1, *2, *41, *2J, *2J(1) and *2J(2)*

To amplify genomic CYP2D6 between ATG transcriptional start site and the TAG translational stop codon, two overlapping fragments were prepared from previously sequenced DNA samples: fragments α (2264 bp), primers 2D6gen_F_*Bgl*II and 2255r (Table 2-2) and fragment β (2660 bp), primers 1568f and 2D6gen_R_*Xba*I (underlined: *Bgl*II and *Xba*I restriction sites, respectively, Table 2-2). Primers 2255r and 1568f contain mismatches to ensure selective amplification of *CYP2D6*. PCR fragments α and β were ligated with pGEM-T Easy vector and transformed to *E.coli* JM109. In the resulting plasmids containing 2D6 fragment α and β, the absence of PCR generated mutations was confirmed by sequencing. The fragment α and fragment β, together spanning the entire human genomic *CYP2D6* from +1 (ATG) to 4217 (stop) (Figure 2-1), with an overlap of 687 bp were digested with *Bgl*II/*BssH*II and *BssH*II/ *Xba*I, respectively, whereas the mammalian expression vector pCMV4 was digested with *Bgl*II and *Xba*I. After restriction digestion, agarose gel analysis and isolation from LMP-agarose gel a 3-fragment ligation was performed resulting in plasmids pCLA 24-53. Plasmids **2J(1)* and **2J(2)* were constructed through fragment exchange using appropriate restriction sites.

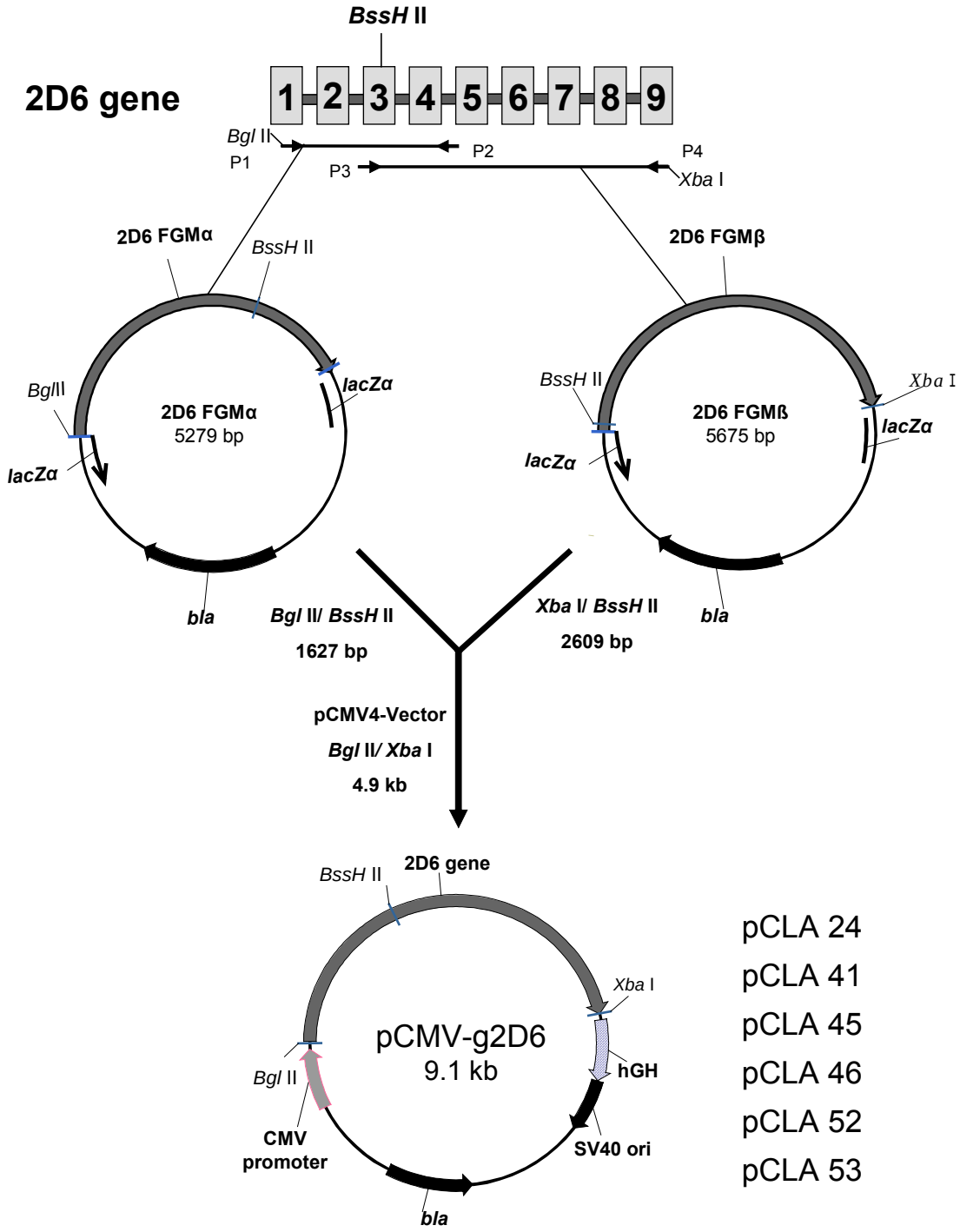

Figure 2-1 Construction of mammalian expression plasmids for transfection assays

*2.2.1.14.2 Reporter gene vectors pGL3-Tk (-105) ex6/in6 wt and *41*

For preparation of the 2D6 exon/intron 6 reporter gene plasmid a region of 250 bp surrounding the 2850C>T and 2988G>A SNPs was amplified from plasmids encompassing the entire *CYP2D6* genomic sequence using primers 2D6_ex6_*Bgl*II F and 2D6_in6_*Bgl*II R (Table 2-2). PCR products were purified by agarose gel electrophoresis and ligated with pCR-4 TOPO. After sequencing analysis confirmed proper amplification, the PCR fragments were digested with *Bgl*II and then subcloned

into the reporter gene vector pGL3-Tk (-105) containing 105 bp of the tymidine kinase promoter.

2.2.1.14.3 Cloning CYP2D6 splice variant ex5-9

79-TOPO, the CYD2D6 plasmid containing a splice variant between exon 5-9, lacking exon 6, was constructed by amplifying a previously genotyped DNA sample using primers 2667r_neu and Cyp2d6rev3 (Table 2-2). The 501 bp PCR fragment was purified by agarose gel electrophoresis and ligated with pCR-4 TOPO. Sequencing analysis confirmed that the insert lacked exon 6.

2.2.1.15 Genotyping assays

2.2.1.15.1 Principle of DHPLC

DHPLC (denaturing high-performance liquid chromatography) identifies mutations based on detection of heteroduplex formation between different alleles in PCR-amplified DNA. The duplexes are analyzed by ion-pair reversed-phase HPLC (IP-RP-HPLC). The mobile phase is composed of water, acetonitrile and the ion-pairing agent triethylammonium acetate (TEAA), the stationary phase consists of a poly(styrene-divinylbenzene) copolymer which binds the DNA. A linear gradient of acetonitrile allows separation of fragments based on the presence of heteroduplexes. Under partially denaturing temperatures, the heteroduplexes elute from the column earlier than homoduplexes because of their reduced melting temperature. As the fragments elute, they are UV-detectable at 260 nm.

2.2.1.15.2 Genotyping assay for 2988G>A SNP by DHPLC

To identify carriers of the 2988G>A SNP in a Caucasian population, a DHPLC genotyping assay was developed. Because the design of primer for this mutation did not allow to discriminate between *CYP2D6* and *CYP2D7* it was necessary to perform a *CYP2D6* specific preamplification step. For this purpose fragment B was amplified using primer 1568f and 3397r (Table 2-2) and the Qiagen Taq DNA Polymerase Kit (Qiagen GmbH, Hilden, Germany). 5µl of the 1:10 diluted fragment B was used as template for the amplification of a 252 bp PCR product using primers 2D6_F10 and 2D6-4647 r (Table 2-2). Following cycling conditions were used: after 5 min of denaturation at 94 °C, the reaction was allowed to proceed for 30 cycles at 94 °C for 2 min, at 58 °C for 30 s and at 72 °C for 30 s, followed by a last extension step of 7 min at 72 °C.

For denaturing HPLC analysis, the WAVE™ DNA Fragment Analysis System was used. 10 µl PCR products were denatured at 95 °C for 5 min, cooled down at 65 °C at -1°C/min, and then applied to a preheated reverse phase column. Elution was achieved with a linear acetonitrile gradient (flow rate 0.9 ml/min) consisting of buffer A (0.1 M TEAA) and buffer B (0.1 M TEAA, 25 % acetonitrile) from 53 % to 62 % buffer B with a separation time of 4.5 min and at an oven temperature of 63 °C. Heteroduplex formation was detected from the melting temperature in comparison to wild type and mutant controls, which were confirmed by sequencing. All PCR fragments were reanalyzed by adding equal amounts of wild type PCR product before denaturing to detect homozygous mutants.

2.2.1.15.3 Genotyping assay for 2988G>A SNP by TaqMan

For high throughput performance with very short “readout times” a new genotyping assay based on TaqMan real-time PCR was developed. The primer and probe sequences were designed using the Primer Express software, version 1.5 (Applied Biosystems, Forster City, CA, USA) in conjunction with manual adjustment. To obtain probes with optimal melting temperatures the complementary strand was used for designing probes. The primers 2D6 In6 AD-F/R (Table 2-2) generate a 115 bp PCR product. The CYP2D6 intron6-G/A probes were conjugated to a nonfluorescent quencher and a MGB group at the 3’ end. Real time PCR was performed using the ABI Prism 7700 sequence detection system and the results were analyzed by use of the Sequence Detection System (SDS) Software Version 1.7 (Applied Biosystems). Each TaqMan run comprised four DNA samples homozygous for allele 1 (AL1), four samples homozygous for allele 2 (AL2) and four reactions in which no DNA template or allelic reference was included (no template control, NTC).

2.2.1.15.4 Genotyping assay for CYP2D7 del138T by TaqMan

For genotyping SNP del138T of the *CYP2D7* pseudogene the primer and probe sequences were designed using the Primer Express software, version 1.5 (Applied Biosystems) in conjunction with manual adjustment. To obtain probes with optimal melting temperatures the complementary strand was used for designing probes. The primers 2D7 fw3/rev (Table 2-2) generate a 181 bp PCR product. The CYP2D7 ins/ del 138T probes [(FAM) or VIC, Table 2-2] were conjugated to a nonfluorescent quencher and an MGB group at the 3’ end. Because no control samples having the 138 T insertion or deletion in *CYP2D7* were available it was necessary to create an

artificial template system (ATS). For this purpose two oligonucleotides of 60 bp, containing primer and probe sequence, overlapping 10 bp were allowed to hybridize and to be filled up by Klenow enzyme. 2D7 del138T for/2D7 rev oligonucleotides were used for the positive control and 2D7 ins138T for/2D7 rev for negative control (Table 2-2). For artificial template synthesis 5 µl of each oligonucleotide were added to 55 µl RNAse free water, 35 µl dNTPs (400 µM) and 10 µl of 10 x Klenow buffer to a total volume of 100 µl. The mixtures were heated at 95 °C for 1 min and were allowed to cool down to room temperature. After addition of 1 µl Klenow fragment enzyme, samples were incubated at 25 °C for 15 min. 2 µl 0.5 M EDTA were added and the reactions were inactivated at 70 °C for 10 min. Finally the artificial templates were diluted with 900 µl TE10.01 buffer. 5 µl of the 1:10,000 diluted ATS were used as template for amplification. Real time PCR was performed using the ABI Prism 7700 sequence detection system and the results were analyzed by use of the Sequence Detection System (SDS) Software Version 1.7 (Applied Biosystems).

2.2.1.15.5 Genotyping for other alleles based on TaqMan assays

Genotyping for alleles **3, *4, *6, *7, *8, *10,*17* was performed using predeveloped TaqMan assays (Applied Biosystems, California, USA). Genotyping del AGA2613-15 (**9*) was performed as described in the diploma thesis of J. Blievernicht (Blievernicht, 2004). The presence of gene duplications and gene deletions (**5*) was determined by a gene copy number assay based on TaqMan quantitative PCR (Schaeffeler et al., 2003). Genotyping for the -1584C>G SNP and **35* was performed as previously described (Griese et al., 1998; Zanger et al., 2001).

2.2.1.16 Quantitation of specific mRNAs in human liver

2.2.1.16.1 Synthesis of cDNA

For cDNA synthesis, the Multiscribe Reverse Transcriptase kit (Applied Biosystems) was used. 1 µg of liver or transfected cells total RNA was adjusted to a volume of 10 µl and the following reagents were added: 5 µl 10 x TaqMan RT buffer, 11 µl $MgCl_2$ (25 mM), 10 µl dNTPs (2.5 mM each), 2.5 µl random hexamers (50 µM), 1 µl RNAse inhibitor and RNAse-free water to a total volume of 50 µl. The random hexamers were allowed to anneal at 25 °C for 10 min. After addition of 1.25 µl MultiScribe Reverse Transcriptase (50 U/µl) samples were incubated at 48 °C for 30 min and inactivated at 95 °C for 5 min.

2.2.1.16.2 Conditions for Real-Time PCR

Quantitative real-time PCR was conducted in an ABI Prism 7500 system using 2 x TaqMan Universal PCR Master mix (Applied Biosystems) in a total volume of 25 µl. The cycling conditions were as follows: After 2 min of incubation at 50 °C and 10 min at 95 °C the reaction was allowed to proceed for 40 cycles at 95 °C for 15 s and at 60 °C for 1 min. Reactions were performed in duplicate and a serial dilution of plasmid standards were analyzed in every run to calculate a calibration curve for relative quantification.

2.2.1.16.3 Analysis of CYP2D6 mRNA in human liver and transfected cells

For quantification of CYP2D6 mRNA normal product, an amplicon of 185 bp spanning exon 6 and 7 was amplified using primers 2D6 N_Qf, 2D6 Q_rev and 2D6 Ex 7 probe at concentrations of 900 nM and 100 nM, respectively, and 40 ng cDNA template. The cycling conditions were as follows: After 2 min of incubation at 50 °C and 10 min at 95 °C the reaction was allowed to proceed for 40 cycles at 92 °C for 15 s and at 62 °C for 1 min. Specificity against *CYP2D7P* was confirmed using a DNA plasmid containing the exon 7 sequence of *CYP2D7P* gene as template. To generate a standard curve, serial dilutions of the pBS SK+2D6 plasmid containing the open reading frame of *CYP2D6* were analyzed over a range from 10^{-6} to 10^{-13} ng.

For quantification of CYP2D6 mRNA splice product, an amplicon of 165 bp spanning exon 5 and 7 (lacking exon 6) was amplified using primers 2D6 SV2_Qf, 2D6 Q_rev and 2D6 Ex 7 probe at concentrations of 300 nM and 100 nM, respectively, and 40 ng cDNA template. Cycling conditions were as described for the *CYP2D6* normal product exept for an annealing temperature of 60 °C. To generate a standard curve, serial dilutions of the 79_TOPO containing the *CYP2D6* splice variant lacking exon 6 were analyzed over a range from 10^{-6} to 10^{-13} ng. β-Actin was used as a housekeeping gene to normalize all *CYP2D6* values and the lowest value was set arbitrarily to 1.

2.2.1.16.4 β-Actin and COUPTFI

For quantification of β-Actin and COUPTFI, TaqMan pre-developed assay reagents were used (probe dye: VIC-MGB and FAM-MGB, respectively) with 800 pg and 40 ng cDNA template, respectively. To generate a standard curve, serial 10-fold dilutions of pooled human liver cDNAs were analyzed over a range from 40 to 0.004 ng.

2.2.1.16.5 HNF4

HNF4 was determined using a quantitative TaqMan assay developed at the Institute (Wolbold and Burk et al., manuscript in preparation).

2.2.1.17 RT-PCR and quantitative DHPLC analysis

Under non-denaturing conditions DHPLC allows to separate and analyze DNA amplicons generated by PCR based on their size.

Total RNA from liver tissue was prepared using the RNAeasy Midi kit (Qiagen GmbH, Hilden, Germany) with an on-column DNase I treatment. Reverse transcription was carried out as described under 2.2.1.16.1. A 643-bp PCR fragment spanning the region from *CYP2D6* exon 5 to 9 was amplified by the use of primers, 2667r_neu and CYP2D6rev3, the latter containing mismatches to ensure selective amplification of *CYP2D6.* For quantification of the 2D6 PCR products, a normalization procedure was applied by adding a constant amount of an unrelated 350 bp DNA fragment to each sample. For this purpose exon 6 of the dihydropyrimidine dehydrogenase (DPYD) was amplified using primer pair dpyd06-F and dpyd06-R (Table 2-2). All amplifications were carried out with the Qiagen Taq DNA Polymerase Kit in a total volume of 50 µl on a PTC-200 thermal cycler. Aliquots of each PCR product were subjected to electrophoresis in a 1.5 % agarose gel stained with ethidium bromide to ensure proper amplification.

Total RNA from transfected cells was prepared using the Agilent Total RNA Isolation Mini Kit (Agilent, Palo Alto, CA). For RT-PCR analysis of CYP2D6 transcripts in transfected cells the primer pair 2D6 ex4/5 F and 2D6 ex7/8 R (Table 2-2) was designed in order to prevent the coamplification of residual plasmid DNA. *CYP2D6*1* functional transcript is predicted to result in a 538 bp PCR fragment using this primer pair.

For denaturing HPLC analysis, the WAVE DNA Fragment Analysis System was used. PCR reactions were applied to a preheated reverse phase column (DNA Sep Cartridge, Transgenomic, Cheshire, United Kingdom) under non-denaturing conditions. Elution was achieved with a linear acetonitrile gradient (flow rate, 0.9 ml/min) consisting of buffer A (0.1 M triethylammonium acetate) and buffer B (0.1 M triethylammonium acetate, 25 % acetonitrile) from 56 % to 66 % buffer B with a separation time of 13.2 min and at an oven temperature of 50°C. Results were analyzed by the use of WAVEMAKER Software Version 4.0.

2.2.2 Cell culture

2.2.2.1 Cultivation and transient transfection of eukaryotic cell lines

COS-1 cells were cultured in DMEM medium supplemented with 10 % fetal bovine serum, 1 % Penicillin/ Streptomycin and 1 % L-Glutamine. Huh7 and IHH cells were cultured in MEM medium enriched with 10 % fetal bovine serum, 1 % Penicillin/ Streptomycin and 1 % L-Glutamine. All cells were cultured in 75 cm^2 polystyrene cell culture flasks (Corning, New York) and maintained in an incubator at 37 °C in 5 % CO_2 atmosphere. When cells reached confluence they were detached using 0.025 % trypsin-EDTA solution and seeded in new culture flasks. Stocks were kept in FCS containing 10 % DMSO and frozen in liquid nitrogen.

The day before transfection COS-1 (4 x 10^5 cells per well), Huh7 (5 x 10^5 cells per well) and IHH (1 x 10^6 cells per well) cells were seeded in 6-well plates (Nunc GmbH, Wiesbaden) and 2 ml medium. Transient transfections were performed using Lipofectamine 2000 according to the manufacturer's instructions. One hour before transfection culture medium was replaced by antibiotics and serum-free Opti-MEM medium. A mixture of 3 µg of the respective expression plasmid, 900 ng pCMV β (Clontech) and Lipofectamine 2000 was added to each well and incubated at 37 °C. After 5 h the DNA-liposome complex was removed and replaced by pre-warmed culture medium. In some experiments, cells were treated with 5 µg/ml Actinomycin D for different time periods at 17 h post transfection. For reporter gene experiments Huh7 cells were seeded in Multiwell 24-well plates (BD Falcon, Heidelberg) with a density of 1 x 10^5 cells per well and 0.5 ml medium. Transient transfections were carried out in triplicates using Lipofectamine 2000 according to manufacturer's instructions. For normalization 150 ng of β-galactosidase expression plasmid pCMV β were cotransfected with 700 ng of the respective firefly luciferase reporter plasmid. After all transfections medium was changed daily.

2.2.2.2 Cell harvesting and determination of β-Galactosidase activity

48 h after transfection, medium was removed and cells were washed twice with ice-cold PBS. Cells were removed from the bottom of the plates using a cell scraper and resuspended in 250 µl PBS. Cell suspensions were homogenized using Lysing-Matrix D and the Fast-Prep Homogeniser (2 x 10 s, speed 6) at 4 °C.

50 µl of cell suspension were used for the determination of β-galactosidase activity. After centrifugation at 5,000 rpm for 5 min, the cell pellet was resuspended in 50 µl

1 x Passive Lysis buffer. β-Galactosidase activity was assayed in 10 µl cell extract which was incubated with 100 µl β-Gal assay buffer for 30 min. After injection of 300 µl β-Gal stop mix and delay of 7 s, luminescence was measured for 5 s using the AutoLumat Plus Luminometer. Measurements were performed in duplicates.

2.2.2.3 Determination of Firefly Luciferase activity

After incubating the cells with 150 µl per well (24 well) 1 x Passive Lysis Buffer for 20 min, they were harvested and firefly luciferase activity was measured in 20 µl cell extract using the AutoLumat Plus Luminometer. Activity was assayed after injection of 300 µl RIM+ buffer and measuring luminescence immediately for 4 s.

2.2.2.4 mRNA stability assay

Seventeen hours after transfection, actinomycin D (ActD) (5µg/ml) was added to inhibit transcription, and the cells were collected 0, 2, 4 and 8 h after treatment. Control cells were cultured for the same time without ActD treatment. For RNA preparation the Agilent Total RNA Isolation Mini Kit (Agilent) was used. CYP2D6 mRNA normal and splice product was quantitated by TaqMan real-time PCR using primers as described in 2.2.1.16.3.

2.2.3 Protein and enzymatic methods

2.2.3.1 Determination of protein content

Total protein content of cell extracts was determined by the Bradford method using the BIO-RAD assay reagent. After 5 µl of cell homogenate were diluted with 795 µl H_2O, 200 µl of the BIO-RAD (5 x) dye solution were added and immediately mixed. Samples were incubated 10 min at room temperature and absorption of protein-dye complex was measured at 595 nm using Novaspec II Visible Spectrophotometer (Amersham). To generate a standard curve, serial dilutions of the BSA protein over a range from 0.72 to 5.76 µg/ml were analyzed. Measurements were performed in duplicates.

2.2.3.2 SDS-polyacrylamide gel electrophoresis of proteins (SDS-PAGE)

The electrophoretic separation of proteins according to their molecular weight was performed in vertical gel electrophoresis chamber SE 600 (Hoefer, San Francisco, USA). A 10 % resolving gel was prepared and poured between two glass plates and

overlaid gently with water. After the gel had polymerized, the overlay was decanted, the stacking gel poured and a comb was inserted. The samples (10-50 µg/lane) were denatured by heating at 95 °C for 5 min in Laemmli gel-loading buffer. Finally they were loaded up into the slots together with the Rainbow protein marker and standard protein samples. Gel electrophoresis was performed in 1 x SDS running buffer at 35 V over night or at 170 V for 4 h at room temperature.

2.2.3.3 Immuno blot (Western blot analysis)

Proteins separated by SDS-PAGE were blotted onto a nitrocellulose membrane using a horizontal Fastblot (Biometra) chamber at 2.7 mA constant current per cm^2 gel for 15 min. For blotting, the gel was layered between a nitrocellulose membrane and blotting papers (Whatman) soaked with blotting buffer. The transfer of the proteins on the nitrocellulose membrane was documented by staining the membrane with Ponceau-S solution and subsequent washing with water.

2.2.3.3.1 Protein detection

To block unspecific antibody binding sites the nitrocellulose membrane was incubated with 5 % low fat milk in TBST (0.05 % Tween 20 in TBS) for 1 h at room temperature with gentle rocking. Subsequently an incubation with the primary antibody for 2 hours at RT followed. After 4 times washing with TBST buffer for 15 min, the membrane was incubated with horseradish peroxidase conjugated secondary antibody for 1 h at RT. Then the membrane was washed 2 times for 15 min in TBST and finally developed with 10 ml Supersignal Dura (Pierce) solution for 5 min in darkness. Detection of the light produced by chemoluminescence was documented by a high sensitive digital camera (LAS-1000, Fuji) with flat frame correction. Quantitative protein analysis was performed using Software AIDA 2.1 (Raytest, Straubenhard) and the standard protein samples.

2.2.3.4 Measurement of propafenone hydroxylation activity

Propafenone-5-hydroxylation was carried out in 0.1 M sodium phosphate buffer pH 7.4 and an assay volume of 100 µl. Liver microsomes (25 µg) or cell homogenate (50 µg) and propafenone (5 and 250 µM, respectively) were preincubated at 37 °C for 3 min. Enzyme reactions were started by adding 10 µl of 10-fold concentrated NADPH-regenerating system (final concentrations, 5 mM $MgCl_2$, 4 mM glucose-6-phosphate, 0.5 mM $NADP^+$ and 4 U/ml glucose-6-phosphate dehydrogenase) and

terminated with 100 µl acetonitrile after 30 min. For the determination of enzymatic activity in human liver microsomes enzyme reactions were started with NADPH-regenerating system and 10 mM UDPGA. After addition of the internal standard (100 pmol $^{2}[H_7]$-5-hydroxypropafenone) and 80 µl H_2O, the samples were mixed and centrifuged at 16,000 g for 5 min. The supernatant was directly injected into the HPLC-system. The metabolite 5-hydroxypropafenone was separated and detected by HPLC-MS/MS spectrometry using a HPLC system equipped with a Reprosil-Pur 120-ODS3 column (50x23 mM, 5 µM particle size) and an ion trap mass spectrometer. Elution was performed with a gradient of 70 % 12 mM ammonium acetate and 30 % acetonitrile to 20 % / 80 % from 0 to 7.1 min. All incubations were performed in duplicate and in the linear range with respect to microsomal protein and cell homogenate and incubation time. Data were processed using the software Quant Analysis.

2.2.4 Computer programs and statistics

Sequence analyses were performed with the program Vector NTI Suite 7 (Invitrogen, Karlsruhe) and with the NCBI-Homepage (Nucleotide, Blast, Genome).

RNA secondary structure predictions were performed with RNA Mfold (www.bioinfo.rpi.edu/applications/mfold) (Zuker, 2003).

RNA binding factors were predicted with the ESE-finder program (http://rulai.cshl.edu/tools/ESE)(Cartegni et al., 2003).

Statistical analyses were performed with GraphPad Prism (Version 3.03) SigmaStat and SigmaPlot 8.0. Depending on whether the data sets were normally distributed or not the unpaired *t*-test or Mann-Whitney test was used for group comparisons. Normal distribution was tested by Kolmogorov and Smirnov and defined as $p>0.1$. Comparison of multiple data sets was performed by one-way ANOVA followed by Dunnett's multiple comparison test. All tests were performed two-tailed and statistical significance was defined as $p<0.05$. Correlation analysis was performed using the Pearson correlation coefficient when data sets were normally distributed, otherwise the Spearman correlation coefficient was calculated.

3 Results

3.1 Study Populations

Genotype-phenotype relationships in this study were investigated using DNA and tissues previously collected at the institute (Table 3-1). In particular, these include

- a German population of 316 subjects phenotyped with sparteine; this collection consists of three parts:
    - genomic DNA from 195 healthy German volunteers (numbered Tü #) who participated in a study of the influence of tobacco and coffee consumption on cytochrome P450 enzyme activity (Bock et al., 1994);
    - genomic DNA from 38 healthy German volunteers (numbered Ik #) recruited in recent years at the institute and phenotyped with sparteine;
    - DNA from 83 patients (numbered Jo #) undergoing cholecystectomy (Osikowska-Evers et al., 1987);
- a German family consisting of father, mother and four daughters, of whom the parents and three daughters have been characterized by sparteine phenotyping and DNA analysis (Raimundo et al., 2000);
- a West-African population of 73 Ghanaians phenotyped with sparteine (numbered Gh #; (Griese et al., 1999);
- a population of 88 DNA samples from western Australian aborigines; from these individuals DNA but no phenotype information was available (Griese et al., 2001)
- a large human liver bank consisting of 300 liver surgical samples collected during recent years at the institute; from these individuals DNA and liver tissue as well as extensive patient documentation but no *in vivo* sparteine oxidation phenotype information was available (Table 3-1).

Table 3-1 Composition of the investigated study population

Population	N	Characteristics	Ethnicity	Information & samples
collection 1	195	healthy volunteers	Tübingen / Stuttgart	MR_S, DNA
collection 2	38	healthy volunteers	Stuttgart / Tübingen	MR_S, blood sample, DNA
collection 3	83	cholecystectomized patients	Bonn	MR_S, liver biopsy, DNA
German collection 1-3	316	Caucasian	German	of all: MR_S, DNA
family	5	healthy volunteers	German	MR_S, blood sample, DNA
liver bank	300	patients	Berlin	Liver tissue, blood sample, DNA, RNA, clinical documentation
Ghana	73	healthy volunteers	West African	MR_S, blood sample, DNA
Australian aborigines	88	healthy volunteers	Western Australia	blood sample, DNA

3.2 Analysis of the intermediate metabolizer phenotype

The genetic basis of the intermediate metabolizer phenotype was initially analyzed in a family study which established its heritability and showed that this phenotype was associated with a "slow metabolizer" variant of the common functional *2D6*2* allele, which was later renamed *2D6*41* (CYPallele nomenclature homepage at www.imm.ki.se/cypalleles). Interestingly both parents had the same initial **2/*4* genotype but the father was an IM whereas the mother was an EM (Figure 3-1) taken from Raimundo et al., 2000.

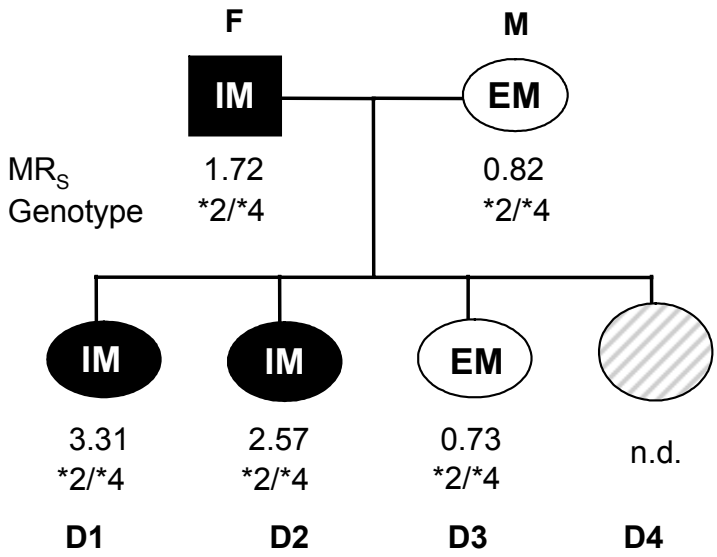

Figure 3-1 CYP2D6 phenotype and genotype analysis in a family. Pedigree of the family analyzed in this study; n.d. not determined (not examined individual). F= father; M= mother; D1-4= daughters.

The initial sequence analysis (Raimundo et al 2000) was restricted to the coding sequences (which were shown to be identical to the *2D6*2* allele) and to about -1.6 kb of 5'-promoter sequence, within which several polymorphisms had been identified. Most notably, the -1584C>G SNP was the only sequence difference between the paternal "slow" form and the maternal "normal" form of the **2* allele. The initial definition of the **41* allele was based only on this difference (Figure 1-4). Nevertheless, subsequent in vitro studies were unable to establish a functional role for -1584C>G in determining CYP2D6 expression. Therefore it seemed useful to further sequence the *CYP2D6* gene throughout all intronic regions in order to either identify further mutation(s) which are linked to the -1584C>G polymorphism, or to exclude the presence of further sequence differences, thus strengthening the case for the -1584C>G polymorphism in determining phenotype.

3.2.1 Sequencing of the *CYP2D6* gene

To completely sequence alleles **41* and **2* throughout all intronic regions, the following samples were chosen for analysis (see Table 3-1):

- the father (sample F: phenotype IM; genotype **41/*4*) and the mother (M: EM, **2/*4*) of the family described previously (Raimundo et al., 2000);
- one DNA sample representing each allele (Tü12: IM, **41/*5* and Tü182: EM, **2/*5*) in combination with the deletion allele **5* (complete gene deletion) to allow unequivocal assignment of sequence differences to each allele;

- additional DNA samples with genotypes **1/*1*, **2/*2*, **4/*4*, and various heterozygous genotypes were partially sequenced for comparison (not shown in Table 3-1).

The *CYP2D6* gene was completely sequenced in these samples throughout all exons and introns and an extended region of upstream sequence, resulting in finally 8.4 kb of uninterrupted sequence. Of a total of 33 observed sequence changes, 19 were confirmatory whereas 14 have not been previously reported. The 19 known SNPs consist of

- six previously described variations within the promoter region including the -1584C>G change linked to **2*
- a cluster of 7 changes in a sequence conversion with *CYP2D7* in intron 1, which is associated with both, **2* and **41* alleles (Johansson et al., 1993; Raimundo et al., 2000);
- two changes (974C>A and 1846G>A) associated with **4* only
- two changes in coding regions found in **2*, **4*, and **41* (1661G>C and 4180G>C)
- one silent mutation in exon 5 (2470T>C; associated with **2C* and **2G* subtypes) found in only one sample
- 2850C>T, which was present in all **2* and **41* alleles.

The 14 previously undescribed differences include five sequence changes (601delC; 1289C>G; 1290G>C; 1330insG; 1439insC) also found in all other sequenced samples, indicating that they may represent sequencing errors in the reference sequence (see legend to Table 3-1). The other nine changes were not detected in seven samples with **1/*1* genotypes but were linked in various ways to alleles **2*, **41*, and/or **4,* thus most likely representing novel SNPs (bold type in Table 3-2). Four of them (310G>T; 746C>G; 843T>G; 3384A>C) were homozygous in all four samples, indicating that they occurred on all three alleles **2, *4* and **41*, whereas two others (3584G>A; 3790C>T) were apparently linked to **2* and **41* only. Finally, the 2988G>A change in intron 6 was the only sequence variation that appeared to be specifically linked to **41* as it was present in both IM samples F and Tü12 but absent from M and Tü182 as well as from other sequenced samples lacking a **41* allele (data not shown).

3.2.2 In vivo population analysis of CYP2D6 activity

3.2.2.1 Genotyping 2988G>A SNP by DHPLC and TaqMan

To determine the correlation between the 2988G>A mutation and the sparteine oxidation phenotype in the population a genotyping assay for the 2988G>A polymorphism was established by denaturing HPLC. The assay was designed to retrieve additional information about the status of the 2850C>T mutation in exon 6 in our German study. Five different specific chromatographic profile pairs (for pure and wild type or mixed DNA fragments) were observed and confirmed by sequencing to represent different haplotypes at the exon/intron 6 region (Figure 3-2).

Table 3-2 Complete sequence analysis of *CYP2D6*2* and *CYP2D6*41* in four subjects F, Tü12, M, Tü182

Reference Sequence Context[a](position in M33388)	SNP[b]	Location	F(IM) *41/*4[d]	Tü12(IM) *41/*5[d]	M (EM) *2/*4[d]	Tü182(EM) *2/*5[d]	Allelic Assignment
AGAACC**C**GGTCTC (36)	-1584C>G	Promoter	C	C	GC	G	*2
AAAATA**C**AAAAAG (194)	-1426C>T	Promoter	CT	C	CT	C	*4
AAAAAG**A**ATTAGG (385)	-1235A>G	Promoter	G	G	G	G	*2, *4, *41
GAGGAC**G**ACCCTC (620)	-1000G>A	Promoter	GA	G	GA	G	*4
GTGTGC**C**CTAAGT (880)	-740C>T	Promoter	TC	T	TC	T	*2, *41
TTCTGC**G**TGTGTA (942)	-678G>A	Promoter	AG	A	AG	A	*2, *41
GCTGAGG**C**T**C**CCC**T**ACCA**GA**AGCAAACATGG**A**[c]	GCCTGAA>C AGCCCG[c]	Intron 1	wt/mut	mut	wt/mut	mut	*2, *41
GGGGAC**G**TCCTGG (1929)	**310G>T**	**Intron 1**	**T**	**T**	**T**	**T**	***2, *4, *41**
CACTGC**C**TCACCG (2220)	del C601	Intron 1	del C	del C	del C	del C	General
GCCCCA**C**GATCAG (2365)	**746C>G**	**Intron 1**	**G**	**G**	**G**	**G**	***2, *4, *41**
CTGGGG**T**GATCCT (2462)	**843T>G**	**Intron 1**	**G**	**G**	**G**	**G**	***2, *4, *41**
GAGGCG**C**TGGTGA (2593)	974C>A	Exon 2	CA	C	CA	C	*4
GGTGAG**C**GTGGCG (2908)	1289C>G	Intron 2	G	G	G	G	general
GTGAGC**G**TGGCGC (2909)	1290G>C	Intron 2	C	C	C	C	general
TGGGGG_CGGGGA (2949)	ins G1330	Intron 2	ins G	ins G	ins G	Ins G	general
AAAGCC_TGCCCC (3058)	ins C1439	Intron 2	ins C	ins C	ins C	Ins C	general
CTCCGT**G**TCCACC (3280)	1661G>C	Exon 3	C	C	C	C	*2, *4, *41
CCCCCA**G**GACGCC (3465)	1846G>A	Intron3/Exon4	GA	G	GA	G	*4
ATTTGC**A**TAGATG (3716)	**2097A>G**	**Intron 4**	**AG**	**A**	**AG**	**A**	***4**
CCTGCA**T**ATCCCA (4089)	2470T>C	Exon 5	T	C	T	T	(*41, *2)
AACCTG**C**GCATAG (4469)	2850C>T	Exon 6	TC	T	TC	T	*2, *41
AGGGAG**G**AAGGGT (4607)	**2988G>A**	**Intron 6**	**AG**	**A**	**G**	**G**	***41**
ACCAGC**A**CCTGGT (5003)	**3384A>C**	**Intron 7**	**C**	**C**	**C**	**C**	***2, *4, *41**
GACCCA**A**CGCCTG (5201)	**3582A>G**	**Intron 7**	**A**	**A**	**AG**	**A**	**(*4)**
CCCAAC**G**CCTGCA (5203)	**3584G>A**	**Intron 7**	**AG**	**A**	**AG**	**A**	***2, *41**
GCATCT**C**CTGCCC (5409)	**3790C>T**	**Intron 7**	**CT**	**T**	**CT**	**T**	***2, *41**
TGGTGA**G**CCCATC (5799)	4180G>C	Exon 9	C	C	C	C	*2, *4, *41

[a]Sequence and SNP position (in brackets) from Kimura et al., 1989 (GenBank acc. no M33388), the affected nucleotide is shown in bold type; [b]position according to CYPallele nomenclature homepage: http://www.imm.ki.se/CYPalleles/ [c]conversion sequence with *CYP2D7* (Johansson et al., 1993); [d]genotypes at the indicated positions are hemizygous for A2 and B2 due to the *2D6*5* deletion; novel sequence changes are in bold type except for those found in all sequences (designated as "general"); [e]assignments inferred from shown and additional data as described in the text.

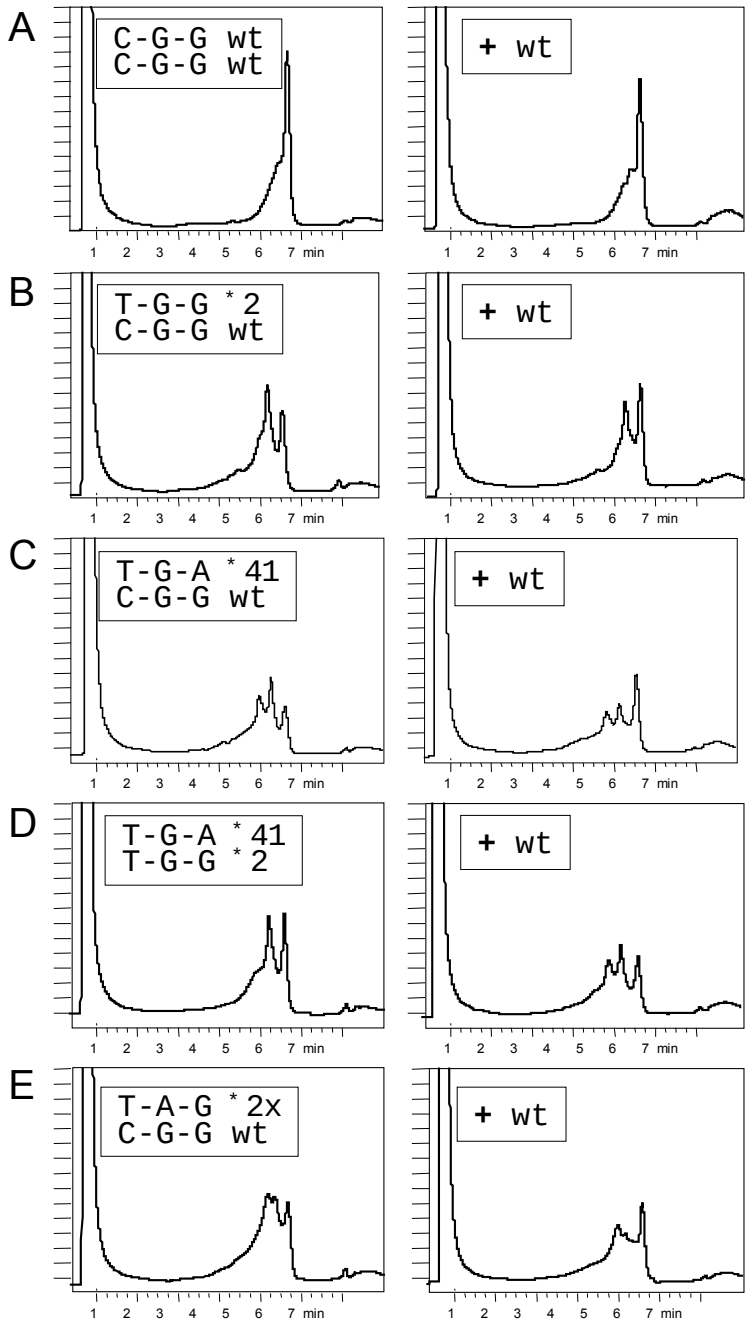

Figure 3-2 Denaturing HPLC profiles of exon/intron 6 region. A 253 bp PCR fragment was prepared from genomic DNA by nested PCR and analyzed by DHPLC either in pure form to detect heterozygous mutations (left) and mixed with equal amounts of wild type (wt) amplicon to detect homozygotes (right). Inserts in left profiles show corresponding haplotypes for 3 polymorphic positions at 2850 bp (C>T), 2939 bp (G>A), and 2988 bp (G>A).

Profile pair A represented wild type alleles homozygous at positions 2850 and 2988 (C/C, G/G); profile B reflected allele **2* in heterozygous condition (C/T, G/G); profile C (C/T, G/A) was found for most **41* heterozygotes, defined as **2*[-1584C]; profile pair D was found in samples carrying a **2* allele in combination with a **41* allele (T/T,

G/A). Two samples (Tü 162, Tü 167) with genotype **2/*4* had the unusual profile E (see below). The 2988G>A change in intron 6 (profile C and D) was present heterozygously in 52 of 308 individuals (16.9 %), corresponding to an allele frequency of 8.4 %. No homozygotes were found, but this distribution was in Hardy-Weinberg equilibrium, as only two homozygotes were to be expected (95 % confidence interval, 0 to 3 individuals).

Because DHPLC is rather time-consuming an additional genotyping assay for the novel intron 6 mutation based on TaqMan Real-Time PCR was developed. In addition to the German population study (see below), the sample collection of 297 liver donor individuals from the liver bank collection was analyzed by both the DHPLC and the TaqMan method. Comparison of the results revealed that the two methods were in 100 % agreement, thus establishing the reliability of the newly developed method.

3.2.1.1 Genotype-phenotype correlation in a Caucasian population

Figure 3-3 shows the distribution of the 308 phenotypes in relation to genotypes, which were all found to be in Hardy-Weinberg equilibrium. For clarity, all null alleles were grouped and termed as **0* and the fully functional alleles **1, *2,* and **35* were sometimes collectively termed **F* if the individual genotypes had similar phenotype distributions.

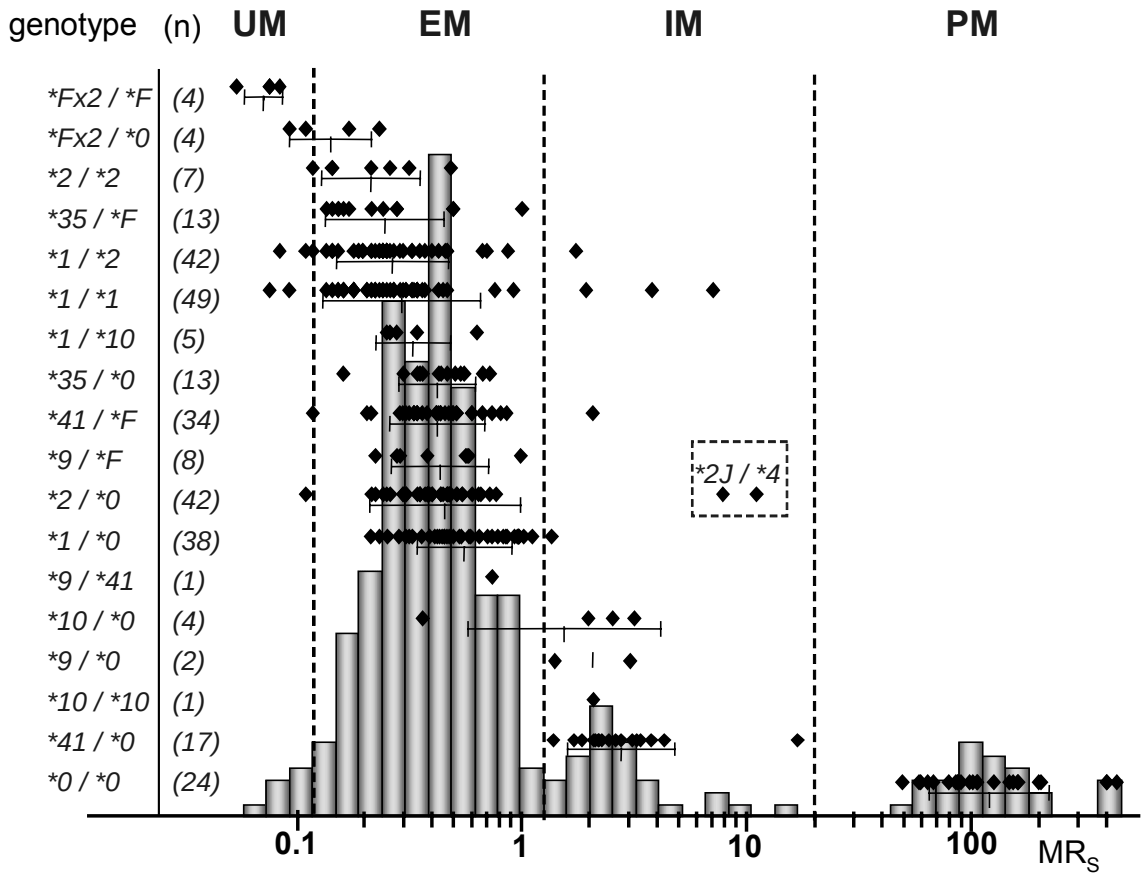

Figure 3-3 CYP2D6 genotype-phenotype correlation in a white population. A population of 308 Germans was phenotyped with sparteine. The x-axis shows the logarithmic metabolic ratio for sparteine (MR_s). Genotypes are shown left with the number of individuals in parentheses. Mean MR_s and SD values are indicated for each genotype below the individual values. The nonfunctional alleles **3, *4, *5, *6, *7* and **8* were collectively termed **0*. For some functional genotypes, alleles **1, *2* and **35* were also grouped and termed **F* (fully functional allele).

As observed with the partial studies published before, all PM individuals (n=24, 7.8 %) could be explained by genotype (**0/*0*).

Within the EM range, the phenotype distributions of the most prominent genotypes were strongly overlapping. There were no significant differences when carriers of two fully functional alleles (genotypes **1/*1, *1/*2,* and **35/*F*) or of one fully functional allele (genotypes **1/*0, *2/*0,* and **35/*0*) were compared. However, the phenotypes of corresponding homozygous and heterozygous genotypes of each allele (i.e. **1/*1* vs. **1/**0 etc) were significantly different. The median MR_s of **1/*1* individuals was 0.30 and it was 1.7-fold lower compared to the median MR_s of 0.53 for **1/*0* carriers ($p<0.001$, Mann-Whitney U-test). The median MR_s of **2/*2* individuals was 0.26 and was 1.88-fold lower than in **2/*0* carriers with a median MR_s of 0.49 ($p<0.05$, Mann-Whitney U-test).

The threshold MR_S for the UM phenotype was conservatively set at 0.15 (Dahl et al., 1995; Griese et al., 1998), leading to the classification of 14 individuals (4.5 %) as ultrarapid metabolizers (UM). Six of these carried a duplicated allele, of which four had a functional gene dose of three (Fig. 3-3). The eight other UMs had the nonpredictive genotypes **1/*2* (n=3), **1/*1* (n=2), **2/*2* (n=1), **2/*41* (n=1), and **2/*4* (n=1).

A total of 31 individuals (10 %) were phenotypic IMs with MR_S between 1.2 and 20. The most frequent genotype among IMs was **41/*0* (n=17, 55 %), which was not found in any non-IM individual (Figure 3-3). Figure 3-4 comprises only genotypes with the related **2, *35* and **41* alleles combined with one non-functional allele. The presence of the 2988G>A change exactly coincided with the transition between the two apparent phenotypic modi. Among the 76 individuals shown in Figure 3-4, there were only two exceptions, namely two IM individuals with **2/*0* genotype (green boxes). DHPLC analysis of these two samples revealed in both cases the unusual profile E (Figure 3-2). Sequencing of the analyzed exon 6-intron 6 amplicon demonstrated two heterozygous positions, the **2*-characteristic 2850C>T (R296C) mutation as well as the additional silent exon 6 change 2939G>A, which was already known and which further specified these alleles as **2J* (www.imm.ki.se/CYPalleles/). Thus, these two exceptions were genetically distinct from all other **2/*0* individuals with EM phenotype. Of the remaining 12 IM individuals six had predictive genotypes, namely **10/*0* (n=3), **9/*0* (n=2), and **10/*10* (n=1), whereas six others were outliers with genotype **1/*1* (n=3), **1/*2* (n=1), **1/*4* (n=1), and **1/*41* (n=1).

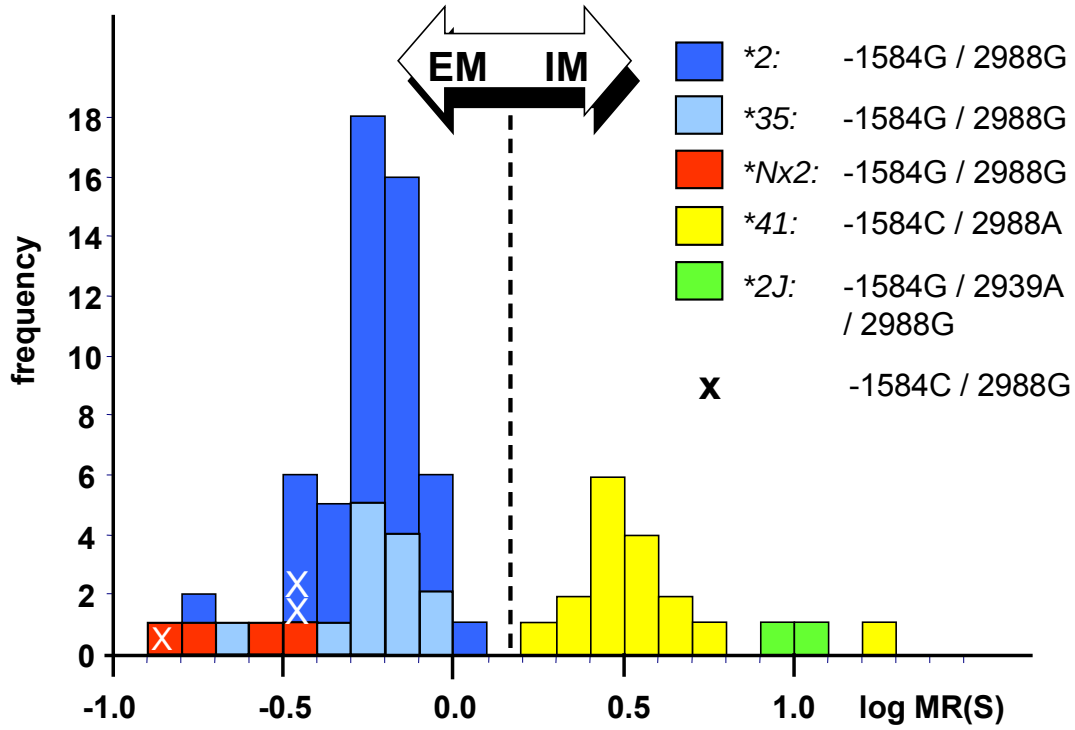

Figure 3-4 Frequency histogram for selected genotypes. Only individuals carrying 1 functional allele of the indicated type together with one nonfunctional allele are shown.

3.2.2.2 2988G>A as a new molecular marker for allele **41*

The high concordance of the novel 2988G>A mutation with the IM phenotype raised the question whether the current definition of **41* (-1584C/2850T) or 2988A was a better predictor of low CYP2D6 activity. In this study six individuals were identified with discrepancies in their genotypes. Namely, 51 of 52 subjects positive for 2988G>A had been assigned -1584C/2850T (i.e. **41*) whereas one sample (Ik 260 in Table 3-3) was considered to be **2* because of -1584G. Conversely, the total number of individuals with a conventionally determined **41* allele was 56, of which five did not carry the 2988G>A change (summarized in Table 3-3). Three of the discordant cases were informative: samples Jo 51 and Jo 53 with previously assigned genotype **4/*41* clearly should be phenotypic IMs, but in fact they were phenotypic EMs. Furthermore, sample Tü 140 is from an UM individual with a proven gene duplication and previously assigned genotype **4/*41x2.* These three cases strongly suggest that presence of 2988G>A in intron 6 is a better predictor of low activity than the previous indirect definition of **41,* namely absence of -1584C>G on a **2* background. It should be further emphasized that 2988G>A was not found to be linked to any other of the investigated alleles, which included **1, *2, *2xN, *4, *6, *7, *8, *9, *10,* and, most notably, **35*. In contrast to 2988G>A, the -1584C>G change was also present in

about 1 % of **1* alleles (2/228), as well as in one PM with genotype **5/*8[-1584G]* and in one further PM with **4[-1584C]/*4[-1584G].*

Table 3-3 Phenotype-genotype comparison for *41 in discrepant cases

Sample	MR_S	-1584C/G	2850C/T	2988G/A	Previous Genotype	Suggested Genotype
Tü 140	**0.12**	**CC**	**CT**	**GG**	***4/*41x2**	***2x2/*4**
Jo 51	**0.54**	**CC**	**TT**	**GG**	***4/*41**	***2/*4**
Jo 53	**0.62**	**CC**	**CT**	**GG**	***4/*41**	***2/*4**
Ik 260	0.35	CG	CT	GA	**1/*2*	**1/*41*
Ik 287	0.55	CG	TT	GG	**2/*41*	**2/*2*
Ik 296	0.26	CG	TT	GG	**2/*41*	**2/*2*

3.2.2.3 In vivo genotype-phenotype correlation in other ethnic groups

Because the linkage between -1584C>G and 2988G>A was reported to be less strong in African populations (Gaedigk et al., 2005b), the relationship between these two SNPs was analyzed in a West African population from Ghana (n=73), all individuals of which had been phenotyped with sparteine (Griese et al., 1999). None of the Ghanaian individuals carried the 2988G>A SNP, although 13 of them would have been assigned at least one **41* allele based on their -1584C/2850T genotype (Table 3-4). Three of the individuals of this Ghanaian population carried informative genotypes (Gh 37: **41/*41*; Gh 47 and Gh 53, **41/*17*), i.e. they would be expected to have significantly higher than average MR_S because they carry two alleles coding for gene products with reduced function. As this was not the case, phenotype-genotype correlation in this population sample was thus in agreement with 2988G>A rather than -1584C>G being responsible for low activity (Table 3-4). Individual Gh 69 was the only one with an IM phenotype (MR_s> 1.2) not correctly explained by genotype. This sample may thus harbour unknown mutation(s) leading to decreased expression and/or function.

The 2988G>A SNP was also analyzed in an Aboriginal population from Western Australia (n=88). Here the 2988G>A change was found heterozygously in only two individuals, representing a low allele frequency of 1.1 %. These data further emphasize a rather localized occurrence of the 2988G>A among European Caucasian populations.

Table 3-4 Genotype-phenotype correlations in a Ghanaian population

Individual #	MR_s	-1584	2850	2988	(-1584/2850)-based genotype	2988-based genotype
Gh 26	0.90	CC	CT	GG	**41/*1*	**1/*2*
Gh 31	0.50	CC	CT	GG	**41/*1*	**1/*2*
Gh 32	0.30	CC	CT	GG	**41/*1*	**1/*2*
Gh 35	0.50	CC	CT	GG	**41/*1*	**1/*2*
Gh 37	**0.50**	**CC**	**TT**	**GG**	****41/*41***	****2/*2***
Gh 46	0.40	CC	CT	GG	**41/*1*	**1/*2*
Gh 47	**0.70**	**CC**	**TT**	**GG**	****41/*17***	****2/*17***
Gh 53	**0.50**	**CC**	**TT**	**GG**	****41/*17***	****2/*17***
Gh 69	2.80	CC	CT	GG	**41/*1*	**1/*2*
Gh 86	0.30	CC	CT	GG	**41/*1*	**1/*2*
Gh 95	0.40	CC	CT	GG	**41/*1*	**1/*2*
Gh 100	0.30	CC	CT	GG	**41/*1*	**1/*2*
Gh 108	0.50	CC	CT	GG	**41/*1*	**1/*2*

3.2.3 Studies of CYP2D6 in human liver

CYP2D6 has been studied in human liver samples before and a good correlation between in vivo MR of sparteine, 2D6 apoprotein and bufuralol 5-hydroxylation activity has been observed (Zanger et al., 2001). Because these were small biopsy samples, they were not available anymore to study the 2988G>A polymorphism. However, a larger collection of human liver tissues (n=300) has meanwhile been established that could be used for further analysis. Because these liver donors have not been phenotyped with sparteine in vivo, only in vitro investigations could be done with these samples.

3.2.3.1 In vitro analysis of CYP2D6 in livers samples

To establish the quality and usefulness of the liver tissues for CYP2D6 investigations, a large number of them was characterized by analyzing CYP2D6 in the microsomal fractions. Quantification of CYP2D6 apoprotein using western blotting with a specific

monoclonal antibody (n=286) and propafenone 5-hydroxylation activity (n=125), as shown in Figure 3-5 were well correlated and showed the expected degree of variability, confirming the new liver bank as valuable and reliable tool for 2D6 related analysis.

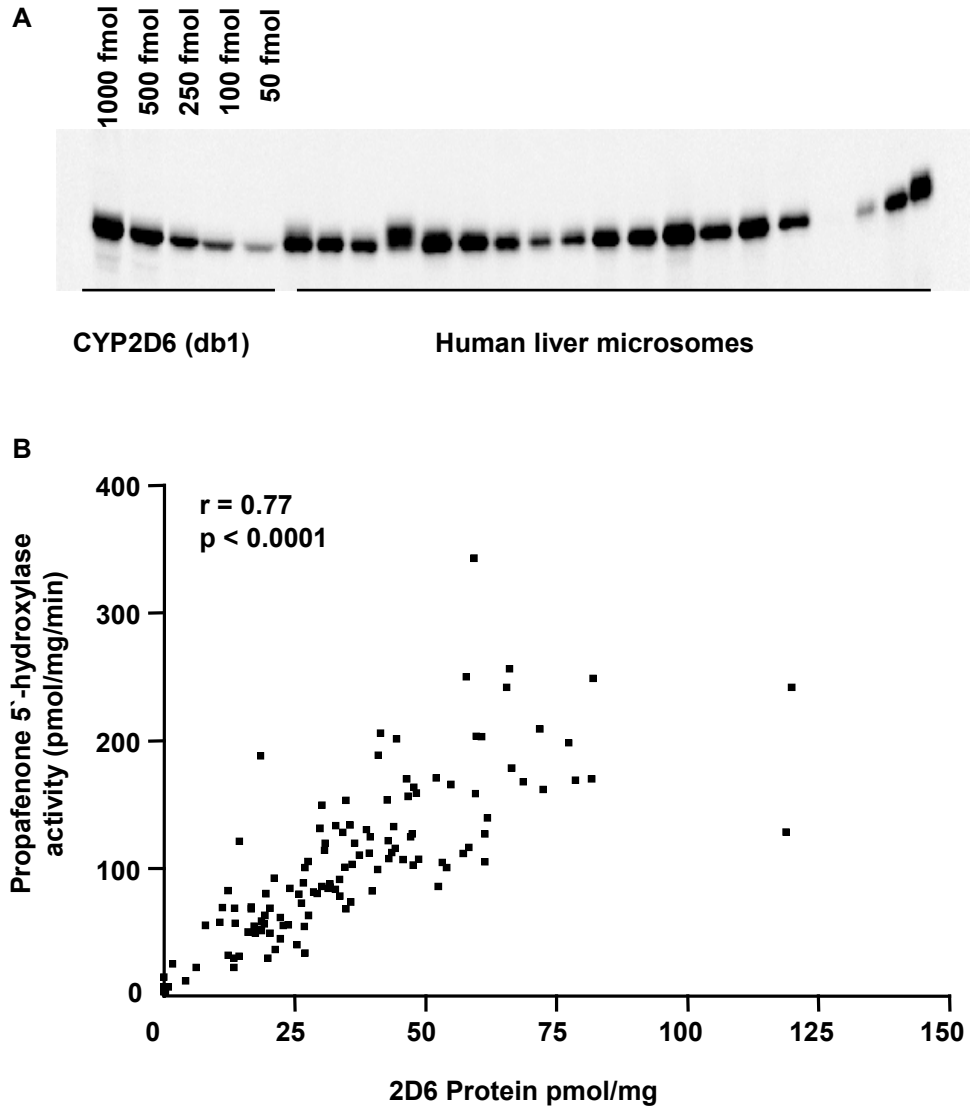

Figure 3-5 Analysis of CYP2D6 protein expression and propafenone hydroxylase activity in human liver microsomes. A, Immunoblot analysis of CYP2D6 in 19 human liver microsome samples (10 µg/lane). CYP2D6 was detected using a monoclonal antibody. Purified CYP2D6 protein (db1) was used as calibration standard. B, Correlation between 2D6 apoprotein expression and propafenone hydroxylation activity in 125 human liver samples; Pearson correlation coefficient is given.

CYP2D6 protein expression analysis was in good agreement with previous data (Zanger et al., 2001) in that carriers of **1/*0* or **2/*0* had on average 2.5-fold higher CYP2D6 protein levels than **41/*0* carriers (Figure 3-6). As expected, individuals carrying *null/null* genotypes did not have any detectable CYP2D6 protein because

most of the *null* mutations lead to prematurely terminated protein products (data not shown). The **2* allele appeared to be higher expressed as the **1* allele, but the differences were not statistically significant in most relevant comparisons.

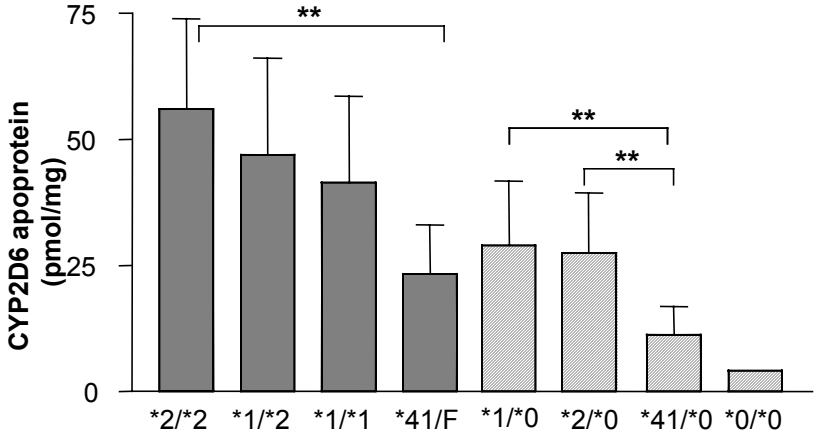

Figure 3-6 Quantitative analysis of CYP2D6 protein in human liver. Quantitation of microsomal 2D6 protein by immunoblotting of microsomes prepared from 76 liver samples. Results are shown in relation to genotype. Results represent means with SD error bars; statistical significance: * $p < 0.05$, ** $p < 0.01$ (unpaired *t*-test).

3.2.3.2 RT-PCR and quantitation of CYP2D6 mRNA by DHPLC

The results presented in chapter 3.2.2 from in vivo phenotyped individuals strongly suggested the 2988G>A mutation to be involved in the functional phenotype of the gene product. Because this mutation was located in an intron, it was previously hypothesized that it could have an influence on splicing events around the region of exon/intron 6. Using an RT-PCR strategy to amplify CYP2D6 transcripts from exon 5 to exon 9 an unexpected 500 bp product could be identified in carriers of the 2988G>A mutation (Raimundo, 2001). Sequence analysis revealed that the additional smaller fragment corresponded to a previously described splice variant, originally termed "c", which lacks the entire exon 6. Because this induces a shift of the reading frame, a stop codon occurs at position 291 resulting in a nonfunctional protein product (Figure 3-7B) (Huang et al., 1997a; Huang et al., 1997b; Woo et al., 1999).

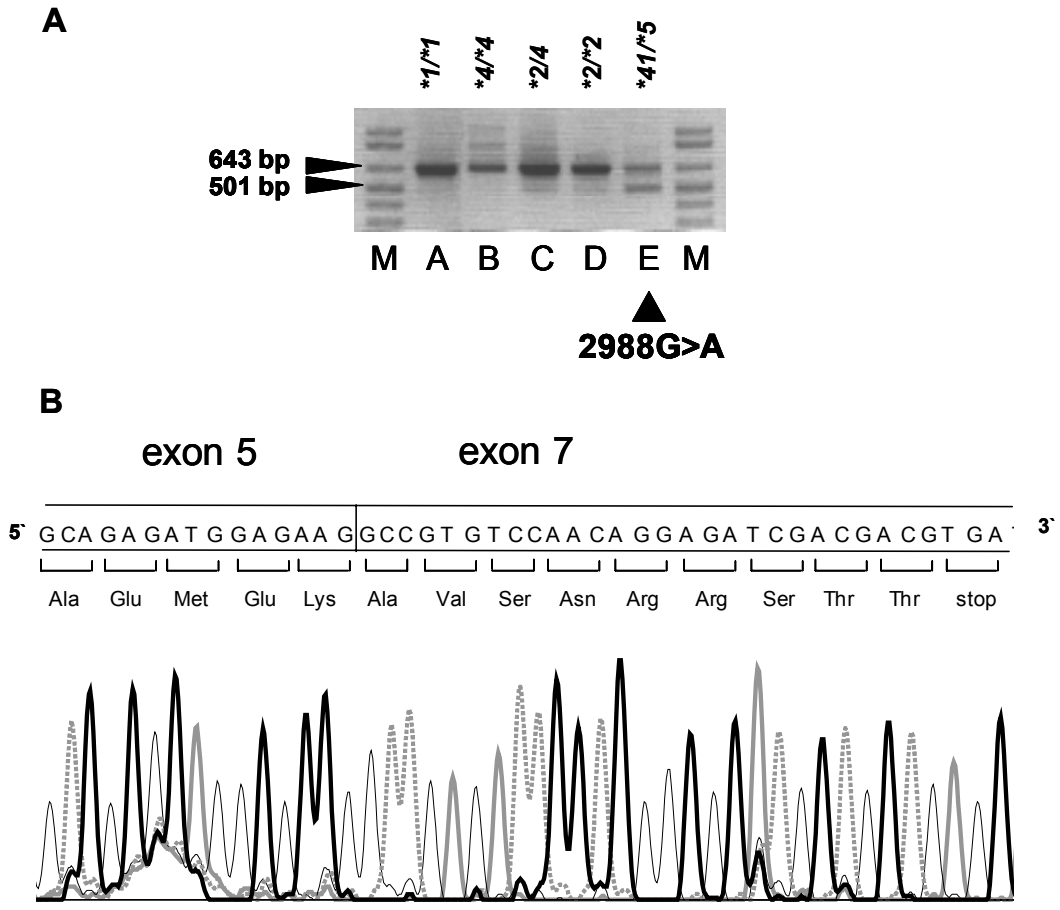

Figure 3-7 Identification of splice variants in human liver. A, RT-PCR products of the CYP2D6 region between exon 5 and exon 9 using RNA of previously genotyped liver samples. Lanes A-E, RT-PCR products obtained from different individuals with the indicated genotype; lane M, 1 kb marker. B, partial sequence analysis of the 501 bp product isolated from a *2D6*41* carrier revealing direct transition from exon 5 to exon 7 (sense strand) and the resulting amino acid sequence.

However, the quantitative relationship between these CYP2D6 transcript products and the CYP2D6 genotype had so far not been investigated nor had the causal relationship between the polymorphisms of the **41* allele and the phenotype been established. Therefore, a semiquantitative method was developed using DHPLC to quantify these two mRNA species in 76 liver samples selected for relevant genotypes (Figure 3-8A). Carriers of **41* in combination with a null allele (**41/null*) had indeed 2-fold and 2.85-fold less of the larger fragment, representing the functional CYP2D6 transcript, in comparison to **1/null* and **2/null*, respectively (Figure 3-8B). Moreover, **41/null* carriers had 7.3 and 2.4-fold more of the splice variant in comparison to **1/null* and **2/null* carriers, respectively (Figure 3-8C).

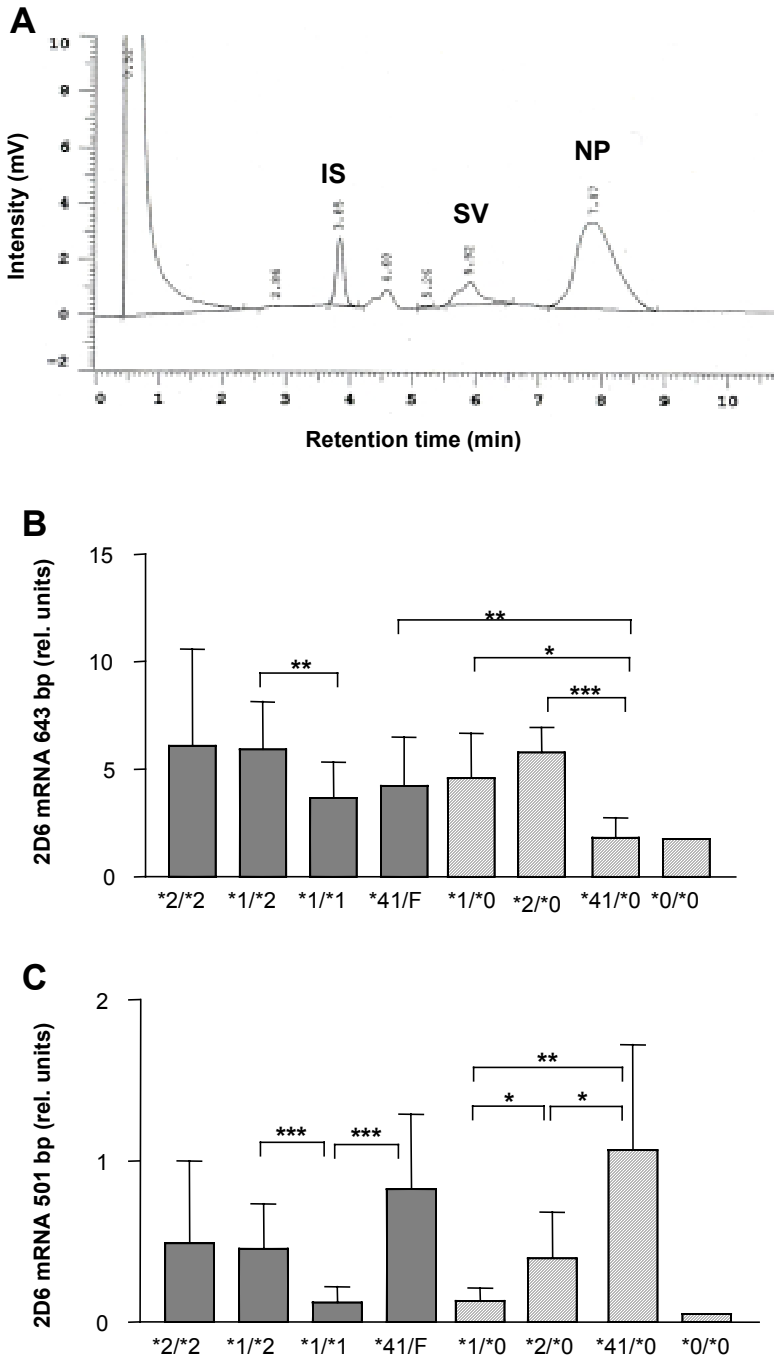

Figure 3-8 Quantitative analysis of CYP2D6 splice products in human liver. A, typical quantitative DHPLC chromatogram, NP, normal product, SV, splice variant, IS, internal standard. B and C, quantitation of RT-PCR amplified transcripts by DHPLC. CYP2D6 mRNA of 76 liver samples selected for genotype were quantified by DHPLC using an internal standardization procedure. Results are shown in relation to genotype. Results represent means with SD error bars; statistical significance: *p < 0.05, **p< 0.01, ***p < 0.001 (unpaired *t*-test).

3.2.4 Elucidation of the causal mutation of the **41* allele by recombinant expression

Taken together these results strongly suggested the involvement of the 2988G>A SNP in determining the phenotypic difference between **2* and **41*, with erroneous splicing as the most likely responsible mechanism. However, the experiments carried out so far still did not establish a causal relationship between the 2988G>A mutation and the low-expression phenotype for *CYP2D6*, nor did they exclude other possibilities for decreased expression of *CYP2D6* in carriers of the **41* allele. In order to gain further insights it was therefore attempted to develop a recombinant expression system to analyze the relevant mutations.

3.2.4.1 Recombinant CYP2D6 expression in different cell lines

To investigate whether the 2988G>A was causally responsible for the low-expressor phenotype of the **41* allele, the genomic sequence of CYP2D6 and variants **2* and **41*, comprising the entire coding region from exon 1 through exon 9 and including all introns (totally 4217 bp) was recombinantly expressed in Huh7 hepatoma, IHH hepatoma and in COS-1 cells. The constructed mammalian expression vectors represented the most common haplotypes of **2* and **41*, i.e. those harbouring the intron 1 conversion sequence as well as the silent exon 3 change 1661G>C in addition to the two nonsynonymous SNPs 2850C>T and 4180G>T (Figure 3-9). Great care was taken to assure that the constructs harboured no artificial mutations and that the only sequence difference in the entire genomic sequence of *2D6*2* and *2D6*41* was the 2988G>A SNP (Table 3-5).

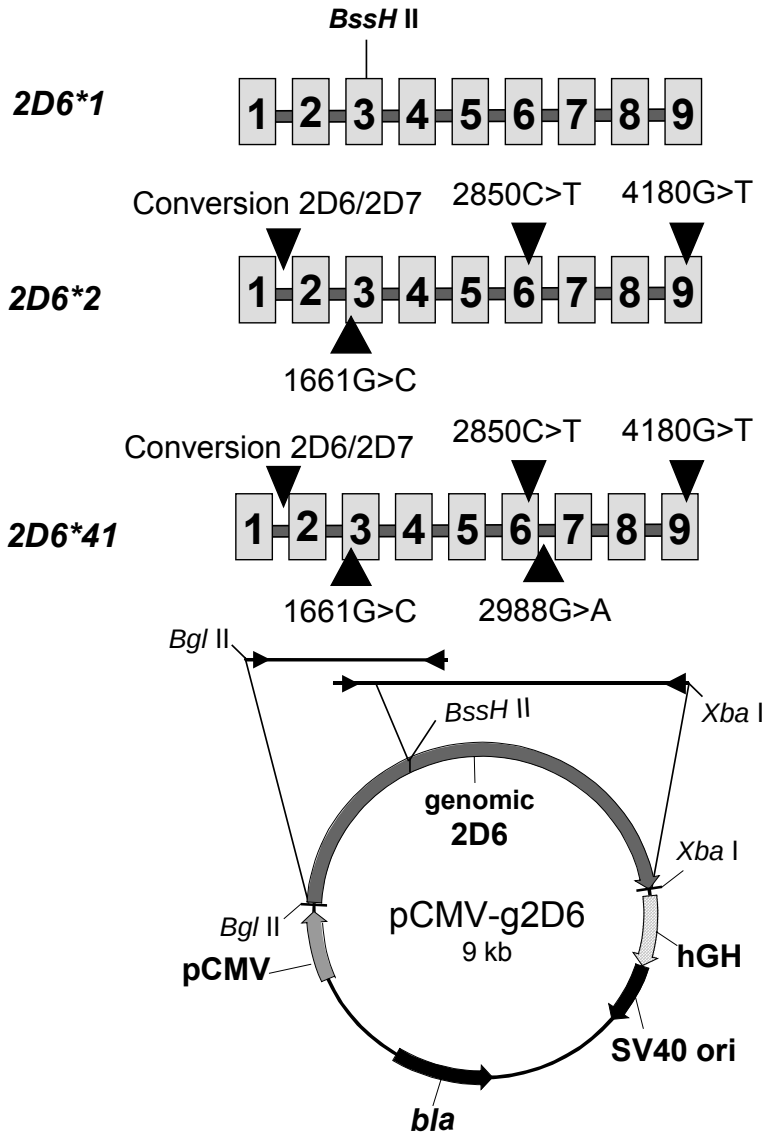

Figure 3-9 Structure of CYP2D6 genomic expression plasmids. pCMV4 expression vectors containing 4217 bp of the *CYP2D6*1, *2* and **41* genomic sequence were constructed as described under *Material and Methods.* The 4.2 kb fragments were amplified from previously sequenced DNA samples. All constructs were confirmed by sequence analysis of the entire insert.

Quantitative immunoblotting and activity measurements using propafenone 5-hydroxylation as a CYP2D6-specific biotransformation of microsomes prepared from transfected cells demonstrated the production of correctly spliced and functionally active P450 holoprotein in both cell lines, as shown by this typical Western blot result (Figure 3-10A). Equal or slightly higher apoprotein amounts for variant 2D6.2 compared to 2D6.1 were observed in good agreement with the liver data. In contrast,

Table 3-5 Complete sequence analysis of recombinant *CYP2D6*1, CYP2D6*2, CYP2D6*41*

Reference Sequence Context[a] (position in M33388)	SNP[b]	Location	*CYP2D6 *1*	*CYP2D6 *2*	*CYP2D6 *41*	*CYP2D6 * 2J*	*CYP2D6 *2J(1)*	*CYP2D6 *2J(2)*
GCTGAGG**C**T**C**CCC**T**AC CA**GA**AGCAAACATGG**A**[c]	GCCTGAA> CAGCCCG[c]	Intron 1	wt	mut	mut	mut	mut	mut
GGGGAC**G**TCCTGG (1929)	**310G>T**	**Intron 1**	**G**	**T**	**T**	**T**	**T**	**T**
CACTGC**C**TCACCG (2220)	del C601	Intron 1	C	del C	del C	del C	del C	del C
GCCCCA**C**GATCAG (2365)	**746C>G**	**Intron 1**	**C**	**G**	**G**	**G**	**G**	**G**
CTGGGG**T**GATCCT (2462)	**843T>G**	**Intron 1**	**T**	**G**	**G**	**G**	**G**	**G**
GGTGAG**C**GTGGCG (2908)	1289C>G	Intron 2	G	G	G	G	G	G
GTGAGC**G**TGGCGC (2909)	1290G>C	Intron 2	C	C	C	C	C	C
TGGGGG_CGGGGA (2949)	ins G1330	Intron 2	ins G	ins G	ins G	ins G	ins G	ins G
AAAGCC_TGCCCC (3058)	ins C1439	Intron 2	ins C	ins C	ins C	ins C	ins C	ins C
CTCCGT**G**TCCACC (3280)	1661G>C	Exon 3	G	C	C	C	C	C
AGAGAG**G**GTGGAG(3910)	**2291G>A**	**Intron 4**	G	G	G	A	G	A
AACCTG**C**GCATAG (4469)	2850C>T	Exon 6	C	T	T	T	T	T
ACATCC**G**GATTGC (4558)	**2939G>A**	**Exon 6**	G	G	G	A	A	G
AGGGAG**G**AAGGGT (4607)	**2988G>A**	**Intron 6**	**G**	**G**	A	G	G	G
ACCAGC**A**CCTGGT (5003)	**3384A>C**	**Intron 7**	**A**	**C**	**C**	**C**	**C**	**C**
CCCAAC**G**CCTGCA (5203)	**3584G>A**	**Intron 7**	**G**	**A**	A	A	A	A
GCATCT**C**CTGCCC (5409)	**3790C>T**	**Intron 7**	**C**	**T**	**T**	**T**	**T**	**T**
TGGTGA**G**CCCATC (5799)	4180G>C	Exon 9	G	C	**C**	**C**	**C**	**C**

[a]Sequence and SNP position (in brackets) from Kimura et al., 1989 (GenBank acc. no M33388), the affected nucleotide is shown in bold type; [b]position according to CYPallele nomenclature homepage: http://www.imm.ki.se/CYPalleles/ [c]conversion sequence with CYP2D7 (Johansson et al., 1993).

variant 2D6.41 expressed at much lower levels (20-35 % of 2D6.2) and concomitantly reduced propafenone 5-hydroxylase activity (Figure 3-10B and C). Similar results were obtained in IHH hepatoma cells although the expression of the 2D6.1 was relatively lower as compared to 2D6.2 and 2D6.41 (data not shown).

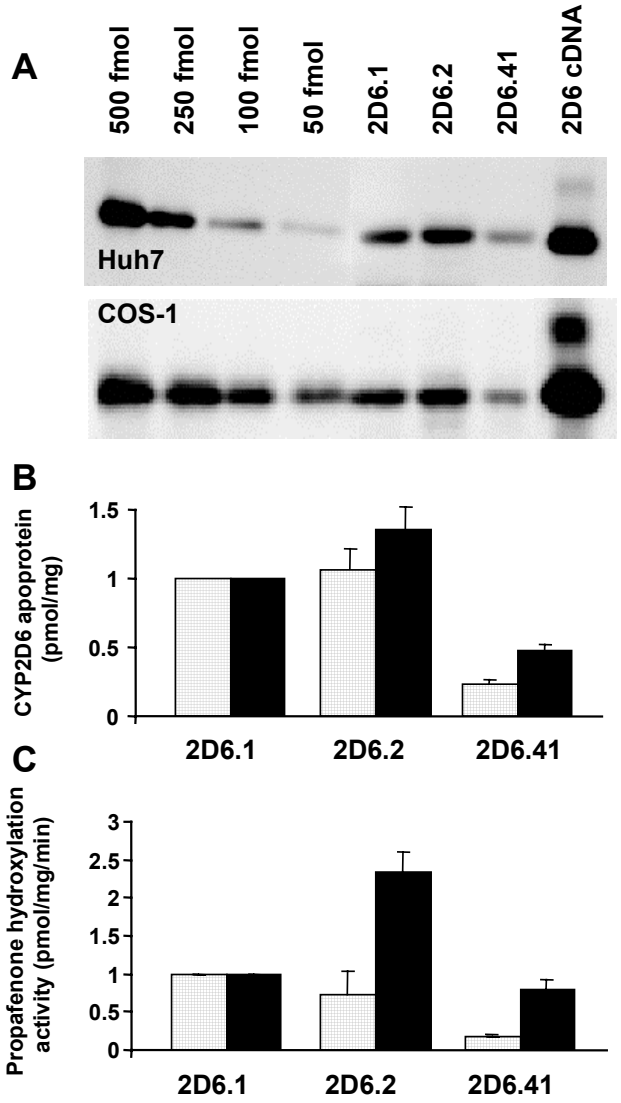

Figure 3-10 Recombinant expression analysis of genomic CYP2D6. A, examples of CYP2D6 immunoblots of transfected Huh7 and COS-1 cells. Recombinant CYP2D6 protein was used as calibration standard (left lanes) and 20-50 µg of transfected cell homogenates, corrected for variable transfection efficiency, were analyzed in each lane. B and C, CYP2D6 protein and propafenone hydroxylation activity, respectively, were determined in transfected Huh7 (full bars) and COS-1 (chequered bars) cell homogenates in relation to CYP2D6.1 set at 1. In all experiments, cells were cotransfected with pCMV-β to correct for variable transfection efficiency by β-galactosidase activity measurement. Results represent the means ± SD of at least three independently performed transfection experiments.

3.2.4.2 RT-PCR analysis of **41, *2* and **1* constructs

A RT-PCR assay to analyze the respective CYP2D6 transcripts in transfected Huh7 and COS-1 cells between exon 5 and 7 was performed. As shown in Figure 3-11, a product pattern similar (exon 5 to 7) to that in human liver (Figure 3-7) was obtained

with the observed fragments identified by sequence analysis as the normally spliced product (NP, 535 bp) and the corresponding splice variant lacking exon 6 (SV, 393 bp). In contrast to human liver, however, only the intensity of the upper band depended on genotype, i.e. the **41* construct resulted in markedly lower levels compared to transfected **2* and **1*, whereas the lower band consistently showed up at invariantly high intensity in all genotypes and in both transfected cell lines. In summary, the base change 2988G>A was thus shown to be sufficient to cause a dramatic change in phenotype of the **2* allele at all levels of gene expression.

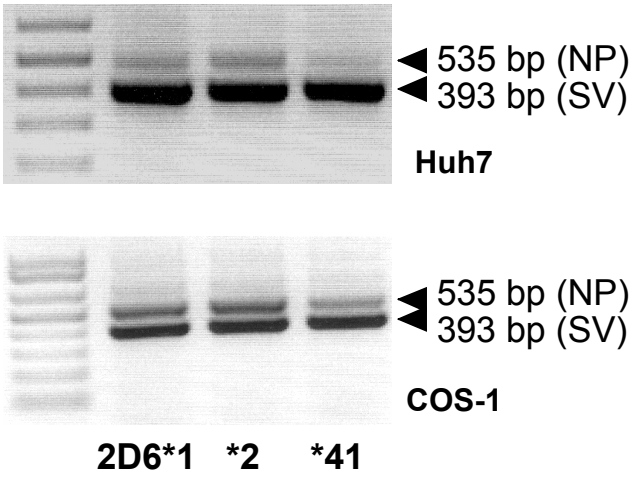

Figure 3-11 RT-PCR analysis of CYP2D6 transcripts in transfected cells. CYP2D6 transcripts were analyzed by agarose electrophoresis of RT-PCR products obtained from Huh7 and COS-1 cells following transfection with the indicated genomic expression plasmids. CYP2D6 was amplified in the region between exons 5 and 7 as described in the Method section. Results representative of several independent experiments are shown.

3.2.4.3 mRNA stability analysis of *2D6*41*, **2* and **1* constructs in Huh7 cells

The above data showed that transfection of human cell lines with the complete CYP2D6 allelic gene variants correctly reflected the allele-associated phenotype at the levels of protein and enzyme activity, whereas at the level of mRNA only the normal, correctly spliced product (NP) behaved similar to human liver. The quantitative analysis of transcripts in liver had suggested an involvement of splicing in determining the phenotype (3.2.3.2). Unfortunately, this could not be confirmed in transfected cells because the splice variant was expressed at high levels and apparently not dependent on genotype. It was therefore not possible to further investigate the splicing mechanism in this recombinant system. However, the system could be used to investigate whether the differences in correct transcript amounts

between **41* (2899G>A), **1* and **2* allele could in part be caused by differences in mRNA stability.

To investigate mRNA stability, Huh7 cells were transfected with the various genomic expression vectors (*CYP2D6*1, *2* and **41*) and transcripts were quantitatively determined following treatment of the cells with actinomycin D (ActD). In the presence of ActD, mRNA decay can be observed as this substance intercalates with double stranded DNA and inhibits mRNA transcription by preventing correct binding of RNA polymerase. Huh7 cells were chosen for these experiments because they are a liver-derived cell line in contrast to COS1 cells which are kidney-derived.

To establish a suitable time-course, transfected Huh7 cells were first harvested and analyzed at different times after transfection. CYP2D6 mRNA expression from the three plasmids was measured by a quantitative real-time PCR method established to distinguish NP and SV transcripts. 18S RNA was used for normalization to account for differences in cDNA synthesis. Figure 3-12 shows an example of a kinetic experiment performed in the absence of ActD, where an exponential increase of mRNA synthesis was observed up to 29 h after transfection.

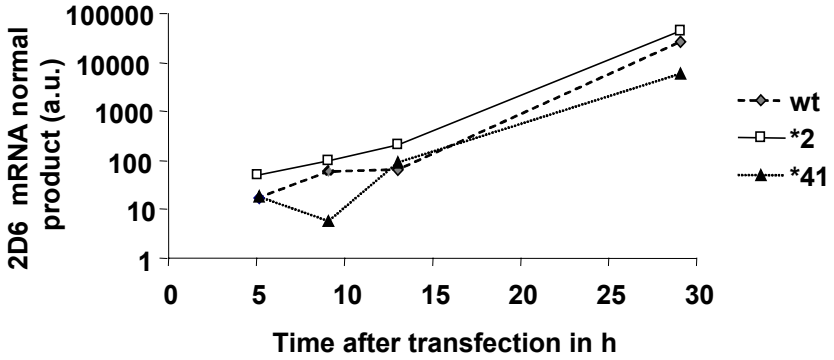

Figure 3-12 CYP2D6 mRNA kinetic experiments. CYP2D6 mRNA transcript normal product of *wt, *2* and **41* constructs was analyzed in Huh7 harvested at timepoint 5, 9, 13 and 29 h by TaqMan real-time PCR. 18S RNA normalized results are shown in logarithmic scale; a.u. arbitrary units.

Based on various experiments, a timepoint 17 h after transfection was chosen for quantitative time-course analysis with different constructs. After transfecting cells with equal plasmid amounts, total RNA was isolated from the collected cells at different times after ActD (5 µg/ml) treatment (0, 4, 8, and 12 h). CYP2D6 mRNA half-lives were determined by plotting the normalized CYP2D6 mRNA results against the exposure time to ActD (Figure 3-13). In these calculations, the amount of CYP2D6 transcript at t_0 was set at 100 %.

CYP2D6 mRNA normal product levels declined after ActD treatment with an estimated half-life of 7.2 h, 7.9 h and 12 h for **1, *2* and **41*, respectively. If differential expression between **41, *1* and **2* was caused by altered mRNA stability and turnover, one would expect to see a considerable decrease of *2D6*41* mRNA normal product half-life after ActD treatment. However, compared to **1* and **2* RNA samples, **41* mRNA normal product had an even increased half-life. Therefore, altered mRNA turnover does not seem to account for differential expression of *CYP2D6*1, *2* and **41.*

Although expression of the splice variant in transfected cells was untypical compared to human liver (see above), the splice variant was also analyzed using a specific primer/probe set for the TaqMan method. Interestingly, the half-lives measured for **1, *2* and **41* were 3.6 h, 3.2 h and 8 h, respectively, indicating a lower general stability of the variant splice product which could probably be due to nonsense-mediated decay, because the erroneous splicing of this transcript leads to a shift of the reading frame and finally to a premature stop codon.

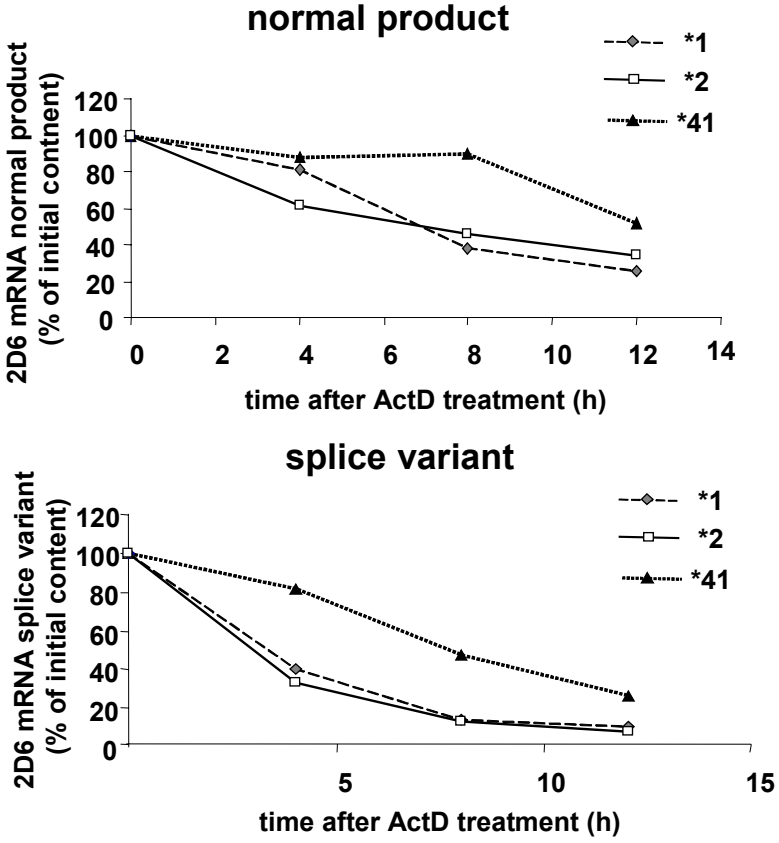

Figure 3-13 Time course of CYP2D6 mRNA levels after actinomycin D treatment. Huh7 cells were transfected with 3 µg plasmid DNA/well *(*1,*2* and **41*), 17 h post transfection, cells were treated with 5 µg/ml ActD for different time periods as indicated and total RNA was isolated. CYP2D6 normal and splice product mRNA levels in 1 µg total RNA were measured by TaqMan real-time PCR. t_0 was set 100%.

3.2.4.4 Reporter gene assay of exon/intron 6 constructs

One alternative plausible hypothesis was that the intronically located SNP may change the functionality of a *cis*-acting element which modulates transcription rate (DeLong and Smith, 2005). To test this hypothesis, Huh7 cells were transfected with two reporter gene constructs (pCla 56 and pCla 57) that contain the firefly luciferase gene driven by the tymidine kinase promoter (Geick et al., 2001) fused to a 250 bp fragment (enh) containing both the 2850C>T and the 2988G>A SNPs or the wild type. However, this fragment did not significantly change promoter activity and no differences were seen between the allelic variants (Figure 3-14).

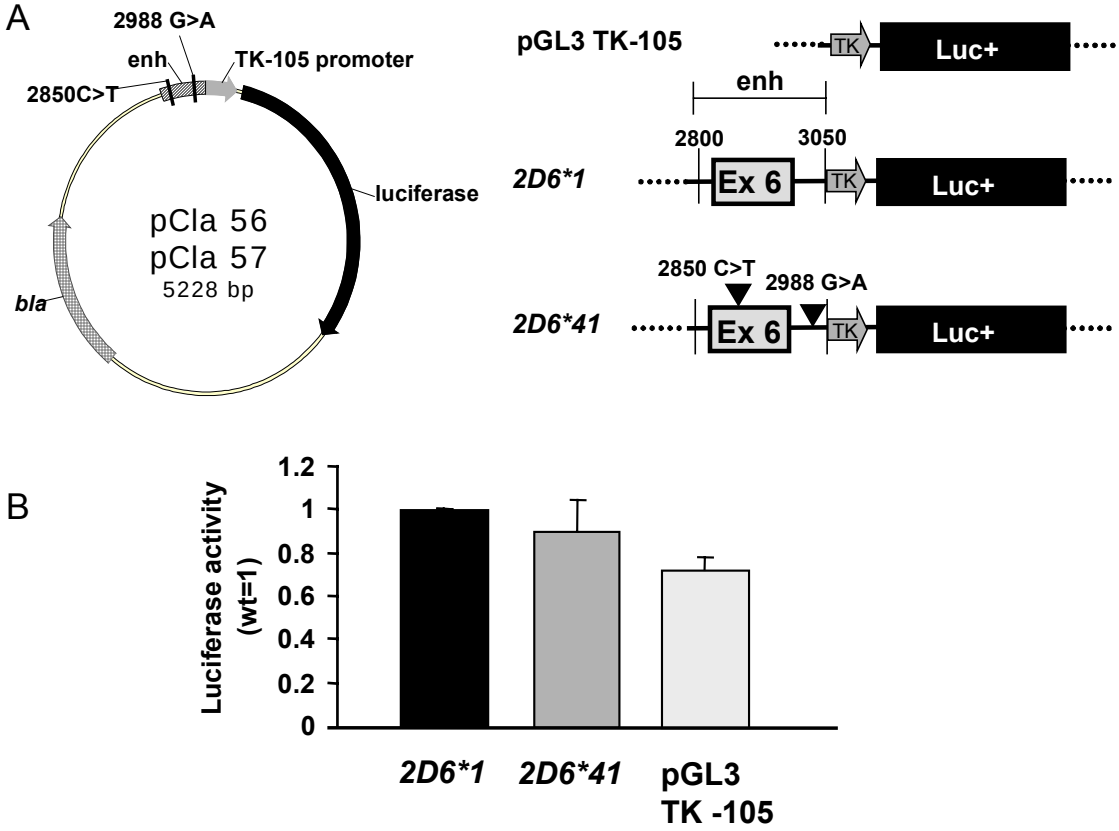

Figure 3-14 Transcriptional activity of CYP2D6 enhancer (enh) element. A, firefly luciferase reporter gene plasmids carrying 250 bp of the wild type and **41* exon/intron 6 region were constructed as described in 'Material and Methods'. B, Huh7 cells were cotransfected with the mentioned plasmids and β-galactosidase control plasmid. β-Galactosidase normalized firefly luciferase activity is shown in relation to the wild type construct which was set at 1; TK: tymidine kinase promoter.

Although these results did not formally exclude an involvement of the exon/intron 6 region in regulating CYP2D6 transcription rate, it seemed unlikely that such a mechanism could quantitatively account for the observed phenotype.

3.2.4.5 ESE analysis of the sequence surrounding exon/ intron 6

Taken together the experimental results strongly point at erroneous splicing as the sole mechanism leading to decreased functional mRNA transcript of allele **41*, because no indication could be found for either decreased mRNA stability or for an involvement in regulating transcription rate of the polymorphic region around the 2988G>A mutation. To analyze the potential impact of the 2850C>T and 2988G>A SNPs on consensus *cis*-elements involved in splicing and on the binding of auxiliary splice factors to these sequences, the ESE-finder program (http://rulai.cshl.edu/tools/ESE) was used. For the analysis sequences comprising the SNPs 2850C>T and 2988G>A and 10 nt upstream and downstream of these positions were included. The presence of 2850C>T decreased the score for SRp55 binding from 3.16 to 1.61 (threshold 2.67) and slightly increased the score for SC35 binding from 2.01 to 2.66 (threshold 2.38). The 2988G>A SNP resulted in even more dramatic changes by decreasing the score for SF2/ASF binding from 3.71 to 1.13 (threshold 1.95) and concomitantly increasing the binding score for SRp40 from 0.27 to 2.88 (threshold 2.67). Thus, in comparison to *2D6*1*, the **2* and **41* alleles had significantly changed scores for ESE consensus sequences, which are predicted to result in altered binding of SRp55 and SF2/ASF proteins (Figure 3-15).

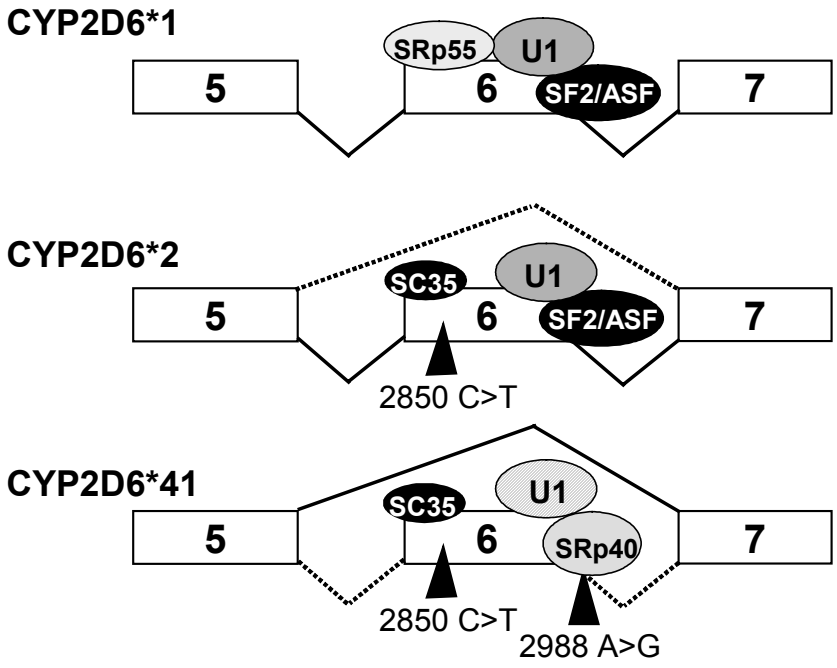

Figure 3-15 In silico analysis of splicing factor binding sites. The sequence (20 nt) surrounding CYP2D6 pre-mRNA at 2850 bp and at 2988 bp was analyzed for putative exonic splicing enhancer motifs using the ESE-finder program as described in Material and Methods. Predicted binding sites are shown schematically for the indicated CYP2D6 alleles. ESE, exonic splicing enhancer; SR, serine-

arginine rich protein; SRp55, SRp40, SC35 and SF2/ASF, SR proteins; U1, small ribonucleoprotein particle (snRNP).

3.2.5 Intermediate metabolizer allele *CYP2D6*2J*

In the course of the German genotype-phenotype correlation study two individuals with a genotype-phenotype discrepancy, having intermediate metabolizer phenotype and *2D6*2/*4* genotype, were identified (see boxed individuals in Figure 3-3). Complete genomic sequence analysis of these two samples throughout all exons and introns had confirmed the presence of the *2D7*-conversion sequence in intron 1, the silent mutation 1661G>C in exon 3, the two nonsynonymous *2D6*2* mutations in exons 6 and 9, as well as a silent mutation 2939G>A in exon 6 and one novel mutation 2291G>A in intron 4 (Figure 3-16, Table 3-5). The 2291G>A and 2939G>A mutations were the only ones specifically associated with the two index cases. It had also been shown that these two mutations occurred together on the **2* allele. (Raimundo, 2001). The 2939G>A SNP was observed before and defines the sub-allele *CYP2D6*2J* (Marez et al., 1997, CYP allele nomenclature homepage: http://www.imm.ki.se/CYPalleles).

3.2.5.1 Recombinant CYP2D6 expression in Huh7 cells

To determine the mutation responsible for impaired function, the same strategy was used as for the **41* allele, the genomic sequence of *CYP2D6*2J* and variants **2J(1)* and **2J(2)*, comprising the entire coding region from exon 1 through exon 9 and including all introns (totally 4217 bp) was recombinantly expressed in Huh7 hepatoma cells. Variant **2J(1)* contained the silent mutation in exon 6 (2939G>A) in the absence of intron 4 mutation 2291G>A whereas **2J(2)* had the inverse constellation (Figure 3-16).

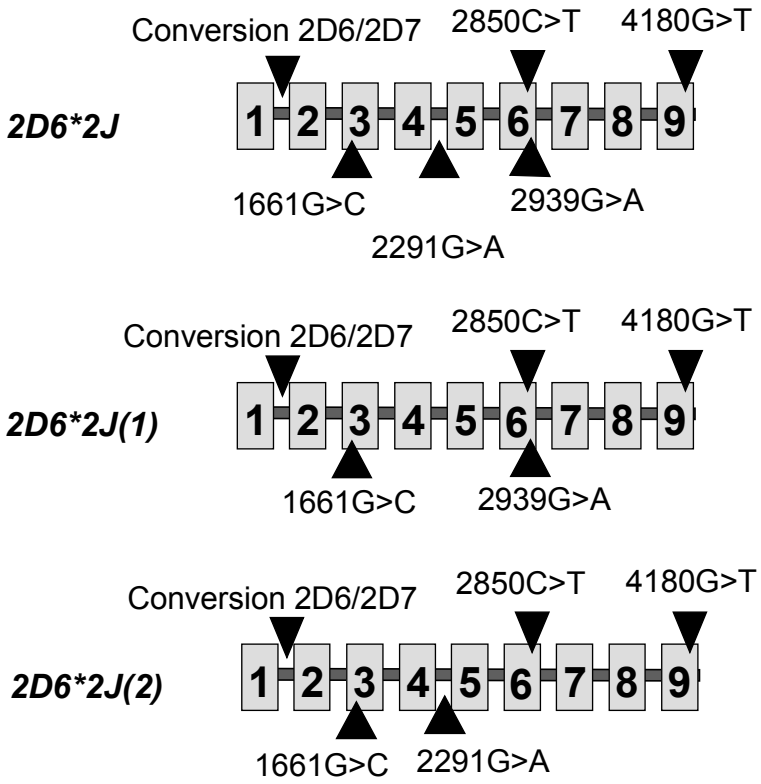

Figure 3-16 Sequence differences of alleles *CYP2D6 *2J* and constructs **2J(1)* and **2J(2).* pCMV4 expression vectors containing 4217 bp of the *CYP2D6*2J, *2J(1)* and **2J(2)* genomic sequence were constructed as described under *Material and Methods.* The 4.2 kb fragments of the **2J* construct was amplified from previously sequenced DNA sample. **2J(1)* and **2J(2)* plasmids were constructed through fragments exchanges with appropriate restriction sites. All constructs were confirmed by sequence analysis of the entire insert.

As in the similar experiments described for *CYP2D6*41* (section 3.2.4.1), quantitative immunoblotting and activity measurements using propafenone 5-hydroxylation were performed in Huh7 cells transfected with different constructs (Figure 3-17).

Quantification of protein product and propafenone 5-hydroxylase activity derived from **2* and **2J* constructs resulted in increased and decreased apoprotein content compared to wild type, respectively. Analysis of the constructs harbouring single mutations (**2J(1)*, 2939G>A and **2J(2),* 2291G>A) showed that the silent mutation 2939G>A was alone responsible for the impaired expression of **2J* (Figure 3-17). The decrease of expressed recombinant 2D6.2J of about 63 % and 78 % compared to 2D6.1 and 2D6.2, respectively, was similar to that of the **41* allele. The residual propafenone 5-hydroxylase activity of recombinant 2D6.2J was about 30 % and 15 % compared to 2D6.1 and 2D6.2, respectively.

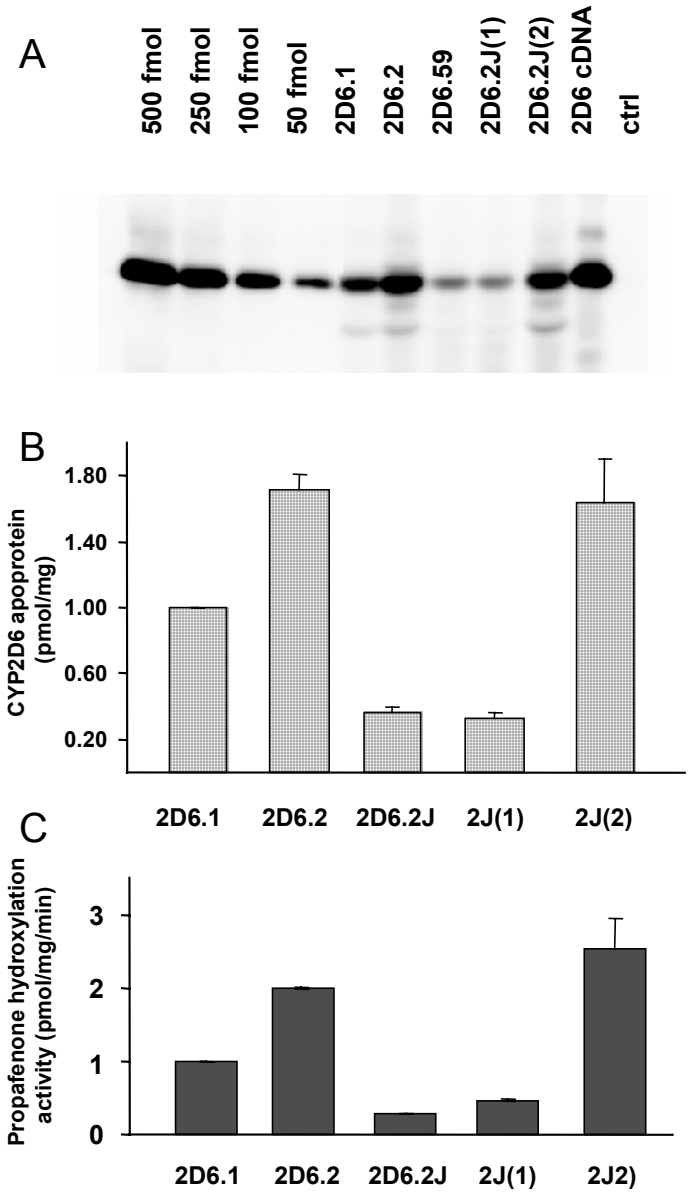

Figure 3-17 Recombinant expression analysis of genomic CYP2D6. Human Huh7 hepatoma cells were cotransfected with various pCMV-g2D6 expression vectors and with pCMV-β. After transfection cells were homogenized and analyzed for recombinant protein expression by immunoblotting using a monoclonal antibody against CYP2D6 and for transfection efficiency by β-galactosidase activity measurement. A: Western blot (20 µg protein per lane) with stably transfected lymphoblast microsomes as a standard; ctrl: protein of non-transfected cells. B and C: CYP2D6 protein (chequered bars) and propafenone hydroxylation activity (full bars), respectively, determined in transfected Huh7 cells. Quantitative β-galactosidase-normalized results are shown relative to CYP2D6.1 (wt) set at 1.0. Average ± SD of three independent transfection experiments is shown.

3.2.5.2 RT-PCR analysis of **2J, *2J(1)* and **2J(2)* constructs

To analyze the respective CYP2D6 transcripts in transfected Huh7 cells, the RT-PCR assay as for the **41* construct was performed. As shown in Figure 3-18 expression of *CYP2D6* at the mRNA level was also strongly decreased in cells transfected with clones **2J* and *2J*(1)*. A product pattern similar to the previously described samples

(Figure 3-11) was obtained with the observed fragments identified. The upper band represents the cDNA fragment between exon 5 and 7, whereas the lower band represents a mRNA splice product lacking exon 6. As for the **41* allele, only the intensity of the upper band depended on genotype, the lower band was present in all samples with similar intensity.

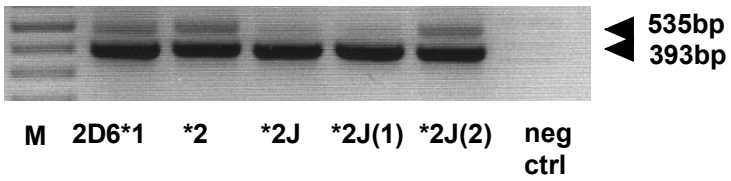

Figure 3-18 RT-PCR analysis of CYP2D6 transcripts in transfected cells. CYP2D6 transcripts were analyzed by agarose gel electrophoresis of RT-PCR products obtained from Huh7 cells following transfection with the indicated genomic expression plasmids. CYP2D6 was amplified in the region between exons 5 and 7 as described in the Method section. Neg ctrl: RNA of non-transfected cells. Results representative of several independent experiments are shown.

3.2.5.3 mRNA Mfold analysis

Previous study of the *Drosophila* genes *Adh* and *Adhr* suggests a relationship between mRNA secondary structure and gene expression (Chen et al., 1999; Parsch et al., 2000; Carlini et al., 2001). Therefore it was hypothesized that the observed effects of the synonymous mutation 2939G>A on RNA may result from changes in mRNA folding. To analyze whether the 1661G>C, 2850C>T and 2939G>A SNPs may change secondary structure of CYP2D6 mRNA, a Mfold analysis of partial CYP2D6 mRNA was performed (www.bioinfo.rpi.edu/applications/mfold). For a localized structure analysis, the sequence of exon 3 (1661G>C) and exon 6 (2850C>T and 2939G>A) was selected. Substitution of G at 1661 position with C did not change the mRNA structure at all, substitution of C at 2850 position with T changed the mRNA structure marginally, whereas the latter substitution in combination with G to A substitution at position 2939 exerted stronger predicted effects on CYP2D6 mRNA secondary structure (Figure 3-19, only the top scoring optimal structures are shown). These results indicate that single nucleotide substitution may affect the secondary structure of CYP2D6 mRNA, thus leading to increased mRNA instability.

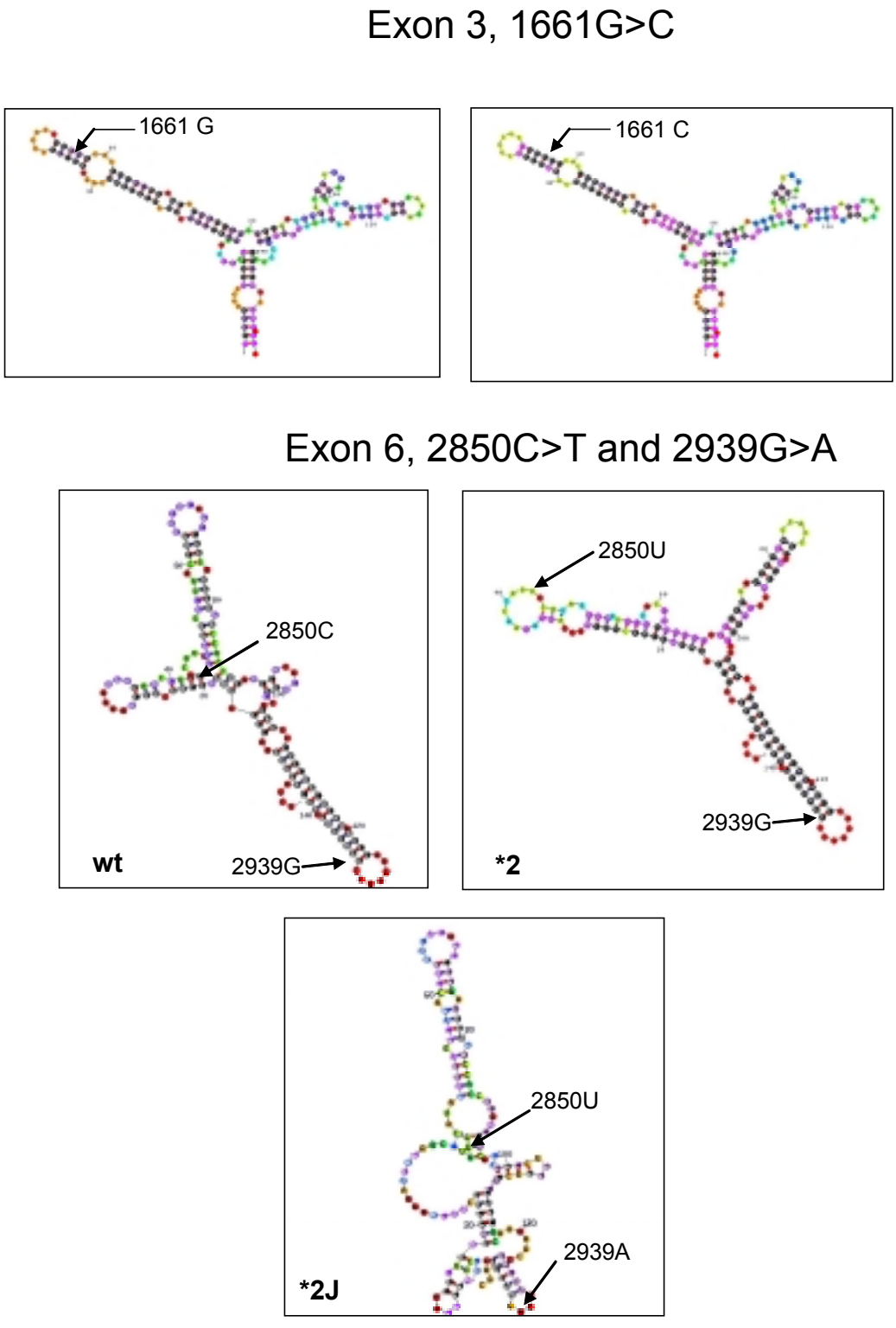

Figure 3-19 CYP2D6 mRNA secondary structure predicted by Mfold. Partial sequence of CYP2D6 mRNA, exon 3 and exon 6 was used to predict mRNA secondary structure by Mfold. Optimal structures are shown for the G to C substitution at position 1661, C to T substitution at position 2850 and G to A substitution at position 2939.

3.2.5.4 ESE analysis of the sequence surrounding exon 6

The potential impact of the 2939G>A SNPs on consensus *cis*-elements involved in splicing was analyzed using the ESE-finder program (http://rulai.cshl.edu/tools/ESE). For the analysis sequences comprising the 2939G>A 10 nt upstream and downstream of these positions were used, as for the **41* allele. The analysis of presence of 2850C>T was described in section 3.2.4.5. The 2939G>A SNP resulted in decreasing the score for SF2/ASF binding from 2.55 to -0.01 (threshold 1.95). Thus, the **2J* allele (similarly to the **41* allele) had also significantly changed scores for ESE consensus sequences in comparison to *2D6*1*, which is predicted to result in altered binding of SRp55 and SF2/ASF proteins.

3.3 Analysis of the ultrarapid metabolizer phenotype

3.3.1 *CYP2D6* analysis in human liver

The large liver bank at the IKP was collected from subjects not phenotyped in vivo with a CYP2D6 probe drug, therefore the in vivo phenotype is not available. Thus the liver samples were phenotyped in vitro using microsomal protein and propafenone as the substrate. In addition, the CYP2D6 phenotype was assessed by Western blot analysis (3.2.3.1). By a combined analysis of protein expression and enzyme activity, it was attempted to define an in vitro UM-phenotype for further analysis.

3.3.1.1 Quantitation of CYP2D6 apoprotein content by Western blot

Quantitation of CYP2D6 apoprotein was performed by Western blot of microsomes from 286 liver samples. A typical Western blot result is shown in Figure 3-5A. The normally distributed 2D6 protein values varied between 0 and 121 pmol/mg microsomal protein. The mean ± SD expression in all livers was 33.5 ± 22.7 pmol/mg microsomal protein. No significant difference between females and males in 2D6 protein expression level was observed (mean 35.43 vs. 31.84 pmol/mg, respectively; p=0.19, *t*-test). There was no significant correlation between age and 2D6 protein expression (r_s= -0.04, p= 0.44). An arbitrary threshold was set at 59 pmol/mg (dotted line) based on probit plot analysis (Figure 3-20) to define an in-vitro subgroup of 2D6 high expressors.

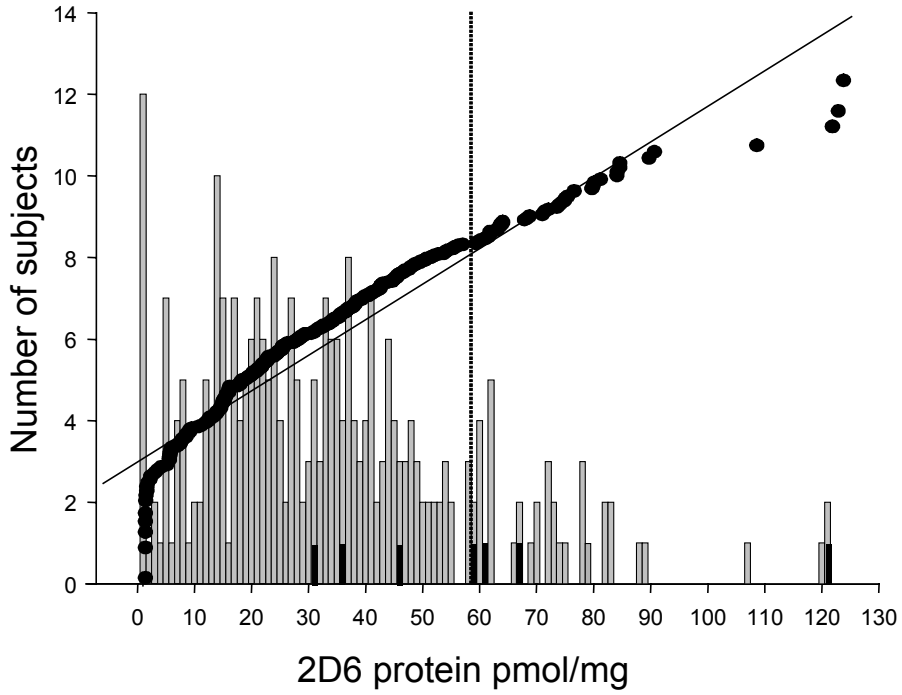

Figure 3-20 Distribution of the quantified microsomal CYP2D6 protein content among the liver bank. Histogram and probit plot analysis of 2D6 apoprotein amount in 286 liver samples.

With this threshold, a total of 34 individuals (11.8 %) were in the UM range. By analyzing the genotype of samples with very high protein content only four (Figure 3-20 black bars, right from the dotted line) samples carried three copies of functional 2D6 genes meaning that 88 % of duplication-negative samples had a protein amount in the same range as ultrarapid metabolizers. Then again, three samples had a functional gene dose of three (Figure 3-20 black bars, left from the dotted line) with a protein expression within the EM range.

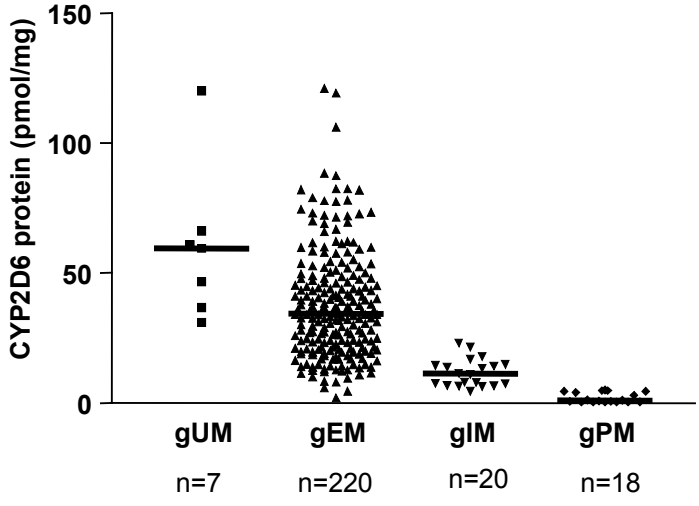

Figure 3-21 Microsomal CYP2D6 protein of four genotype groups. Immunologically quantified CYP2D6 protein of 262 livers with known genotype; g: genotype-predicted

Figure 3-21 shows the phenotype distribution in relation to predictive genotypes. The genotype-predicted UMs (gUM) are defined as carriers of three functional gene copies. The genotype-predicted EMs (gEM) are defined as carriers of at least one fully functional *2D6* copy (**1, *2* or **35*); the genotype-predicted IMs (gIM) are defined as carriers of two partially deficient genes or of one partially deficient gene in combination with a non-functional gene and the genotype-predicted PMs (gPM) are defined as carriers of two non-functional genes. There was a significant overall difference in the mean expression levels of the four genotype groups UM, EM, IM and PM ($p<0.0001$). The highest CYP2D6 content was found in the gUM group which expressed on average 60.2 $\pm$ 29.5 pmol/mg. The individuals belonging to the genotype-predicted EM (gEM) group expressed 1.6-fold less protein than gUMs (37.8 $\pm$ 21 pmol/mg, $p<0.05$, *t*-test). The average expression in the gIM group was 3-fold lower compared to the EM group (11.7 $\pm$ 5.3 pmol/mg, $p<0.0001$, *t*-test) which is in very good agreement with the recombinant expression in section 3.2.4.1. The lowest CYP2D6 amount was found in individuals belonging to the gPM group with no detectable protein expression.

3.3.1.2 CYP2D6 expression in relation to enzyme activity

Another important *in vitro* phenotyping method is the measurement of enzyme activity. As for the CYP2D6 protein expression, the propafenone hydroxylation activity was highly variable. Among 125 liver samples measured, activity varied 237-fold with values between 1.44 and 341.3 pmol 5-OH-propafenone /(mg protein x min). The normally distributed propafenone hydroxylase activity was significantly correlated to microsomal CYP2D6 content ($r=0.77$, $p< 0.0001$) (Figure 3-22). Genotype-phenotype analysis shows the discrepancy between genotype and high protein expression and enzyme activity, as most of the high expressors do not carry a predictive genotype (Figure 3-22 upper right corner). These data confirmed that the predictive value of gene duplication is limited to about 20-25 % of the individuals with high 2D6 expression and function.

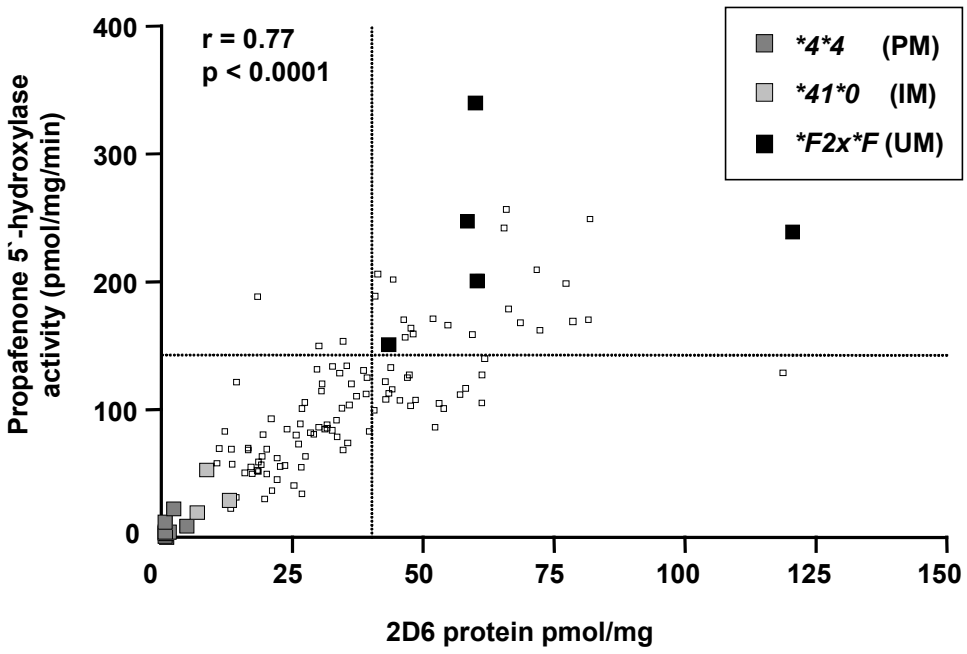

Figure 3-22 Correlation between 2D6 apoprotein expression and propafenone hydroxylation activity in human liver samples. Analysis of 125 liver samples, some of the genotypes (PM, IM, UM) are indicated (shaded boxes). Pearson correlation coefficient: r= 0.77, p<0.0001.

3.3.2 Genotyping *CYP2D7* SNP del138T by TaqMan

One hypothesis for the presence of 2D6 duplication-negative UM could be the existence of a functional pseudogene. *CYP2D7* has an insertion of a single T at position 138 in the first exon, leading to a disrupted reading frame, which classifies it as psedudogene (Kimura et al., 1989). In light of many gene-conversions and cross-over events that probably have occurred in the *CYP2D* locus, it is conceivable that the *CYP2D7* exon 1 region could have converted back to the original *CYP2D6* sequence, thereby giving rise to a full length *CYP2D7* (CYP2D6-like) protein. Pai et al. described the identification of a functional *CYP2D7* splice variant in human brain of Indian individuals, all lacking the 138T insertion. Genotyping for this SNP suggested a 50 % frequency in the Indian population (Pai et al., 2004). To test the possibility for the presence of a functional pseudogene in the Caucasian population, a TaqMan assay using *CYP2D7* specific primers and probes was developed. Positive and negative controls were generated using the artificial template system (section 2.2.1.15.4). Analysis of 287 human liver samples revealed that all were homozygous for the T insertion in position 138, causing a frame shift and a subsequent stop codon in the mRNA.

3.3.3 Relationship between HNF4 and COUPTFI mRNA expression and CYP2D6 protein expression

In the course of functional analysis of the CYP2D6 promoter, Cairns and colleagues found that the CYP2D6 promoter possesses binding sites for HNF4 and COUPTFI (Cairns et al., 1996). The nuclear receptors HNF4 and COUPTFI are positively and negatively acting transcription factors, respectively, known to regulate the transcription of many genes. Accordingly, it was hypothesized that a possible imbalance in the expression of these two transcription factors may result in the enhancement of the CYP2D6 promoter activity explaining the presence of duplication-negative UMs.

3.3.3.1 Quantitation of HNF4 and COUPTFI mRNA in human liver

In a panel of 87 RNA sample from the liverbank, HNF4 and COUPTFI mRNA expression was measured by quantitative real-time PCR. For normalization, β-actin was used as normalization gene to account for differences in RNA quality and cDNA synthesis, and the lowest value was arbitrarily set at 1. Mean HNF4 mRNA expression was 17.48 a.u. (arbitrary units) with a range between 1 and 77 a.u. whereas mean COUPTFI mRNA expression was 9.9 a.u. with a range between 0.45 and 87.57 a.u. Mean ratio of HNF4/COUPTFI mRNA expression was 4.1 a.u. with a range between 0.02 and 32.8 a.u. (Figure 3-23A). No significant influence of gender on HNF4 and COUPTFI mRNA expression level was observed (data not shown).

3.3.3.2 Analysis of HNF4, COUPTFI mRNA and CYP2D6 protein expression

Individuals having high 2D6 protein levels (>59 pmol/mg) had a mean HNF4 mRNA expression of 10.6 a.u., a mean COUPTFI mRNA expression of 13.7 a.u. and mean ratio of HNF4/COUPTFI mRNA expression of 1.2 a.u. (Figure 3-23B). Individuals having a low 2D6 protein expression (<15 pmol/mg) had a mean HNF4 mRNA expression of 19 a.u., a mean COUPTFI mRNA expression of 9.3 a.u. and mean ratio of HNF4/COUPTFI mRNA expression of 5 a.u. (Figure 3-23C).

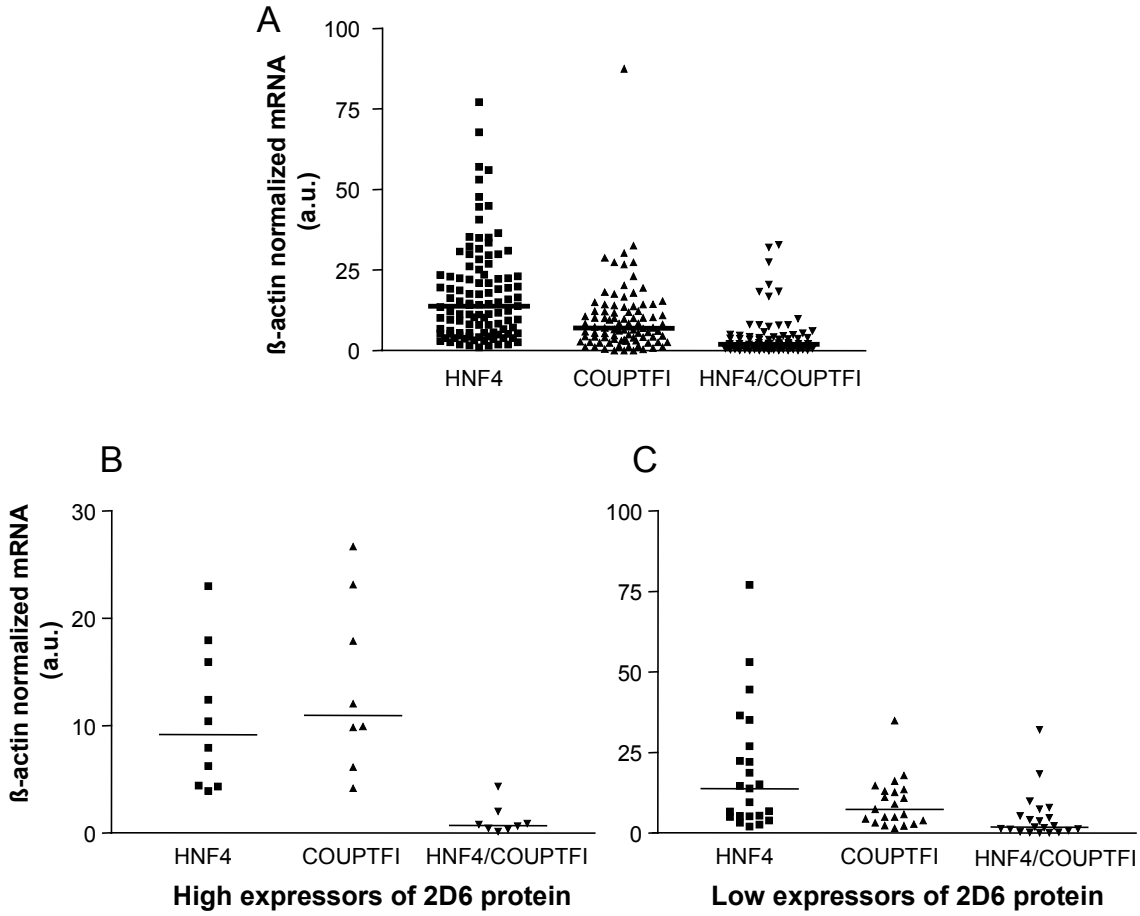

Figure 3-23 HNF4 and COUPTFI mRNA expression in human liver. A, mRNA expression of HNF4, COUPTFI, and HNF4/COUPTFI ratio in all liver samples analyzed (n=87). B, Analysis of the mRNA expression level of HNF4, COUPTFI, and HNF4/COUPTFI ratio in individuals having 2D6 protein expression >59 pmol/mg, n=8-10; C, Analysis as in B in individuals having 2D6 protein expression <15 pmol/mg, n=23.

There was no correlation between HNF4 and COUPTFI expression (data not shown), nor between HNF4 mRNA and 2D6 protein expression (Figure 3-24A), nor between COUPTFI mRNA and 2D6 protein expression (Figure 3-24B). According to the hypothesis the ratio between HNF4 and COUPTFI should affect CYP2D6 transcription. However, also no correlation between the mRNA of the two transcription factors and CYP2D6 protein was observed (Figure 3-24C).

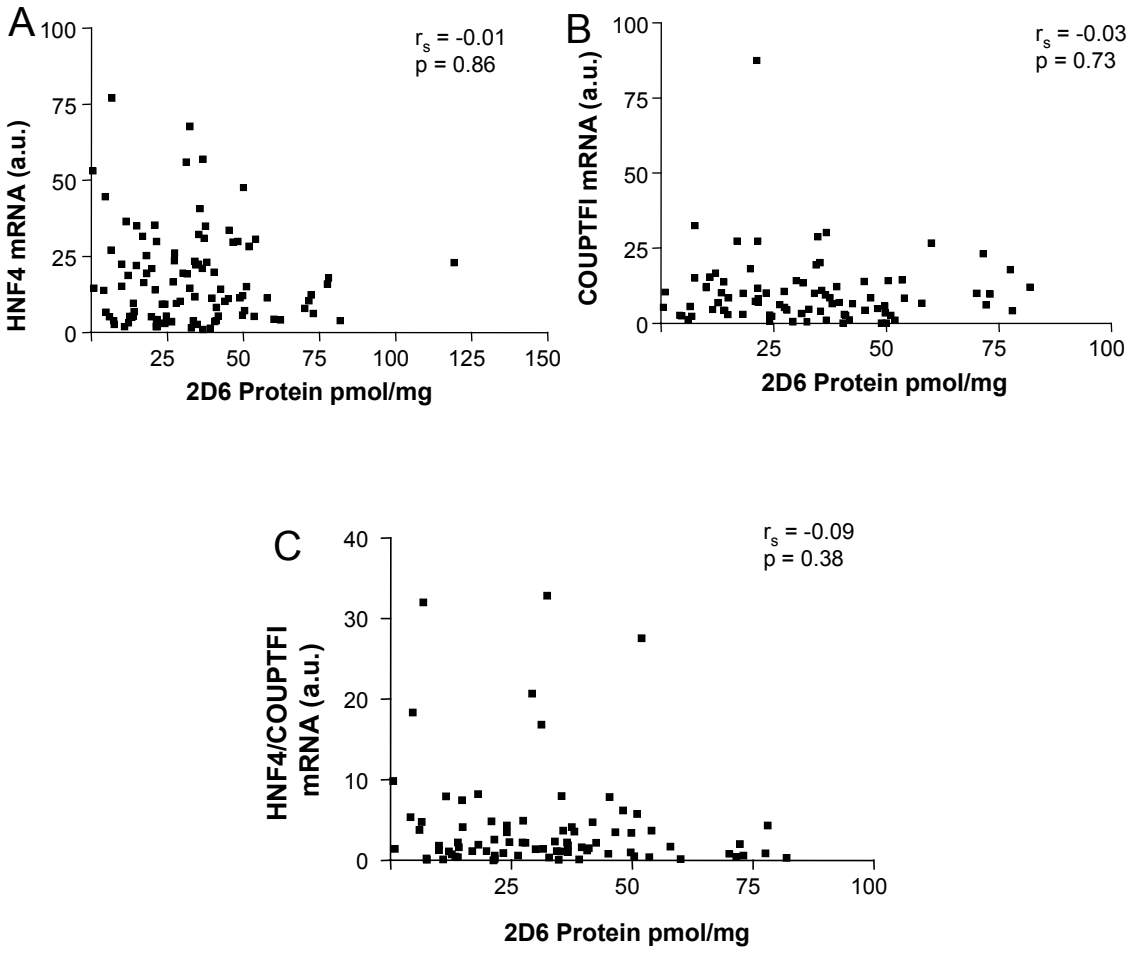

Figure 3-24 Lack of relationship between HNF4, COUPTFI and CYP2D6 protein expression. Analysis of 87 human liver samples, Spearman correlation coefficient is given.

In regard to the ultrarapid metabolizer phenotype, samples with high protein content (> 59 pmol/mg) were analyzed separately. As for the overall analysis there was no significant correlation between CYP2D6 protein expression and HNF4 mRNA expression. Although there was a tendency to the right direction, the correlations between COUPTFI mRNA and 2D6 protein expression, and between the ratio of HNF4/ COUPTFI and 2D6 protein expression, were not statistically significant (Figure 3-25).

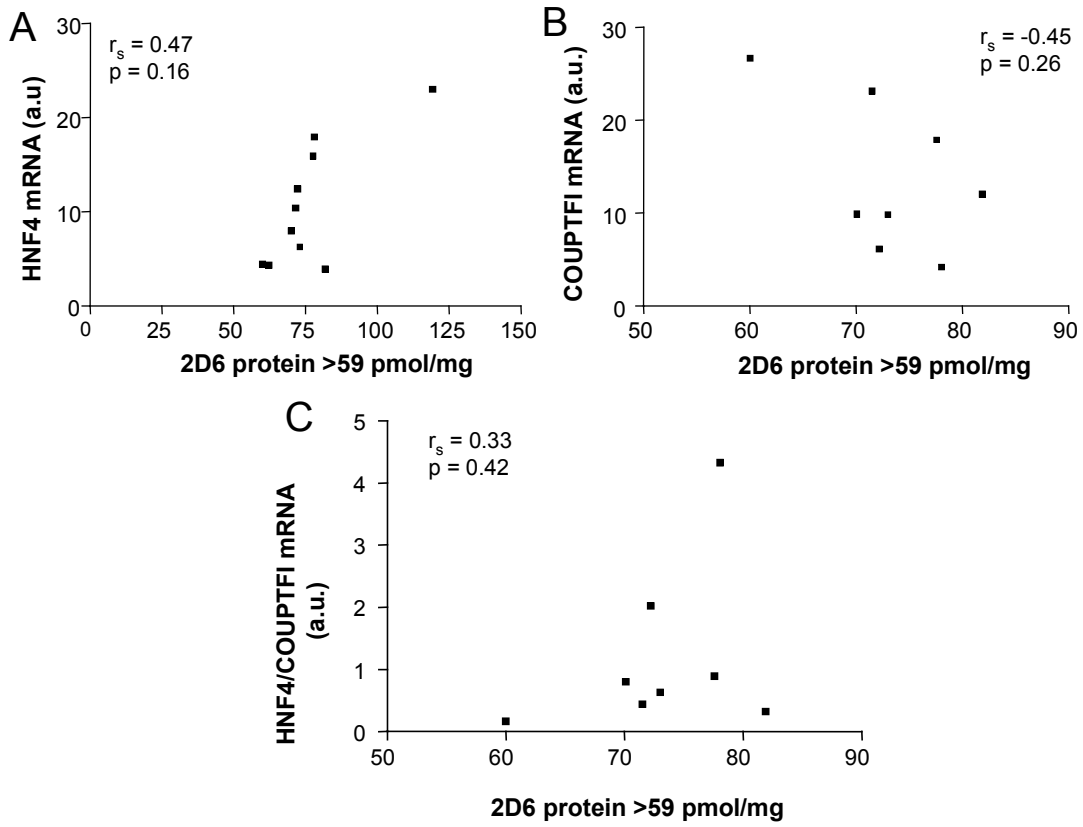

Figure 3-25 Lack of relationship between HNF4, COUPTFI and CYP2D6 high expressors. Analysis of n=8-10 samples; Spearman correlation coefficient is given.

In order to exclude a genotype-dependent HNF4 and COUPTFI mRNA expression, the liver samples were analyzed by their genotype. As expected, there was no statistically significant difference in the HNF4 (Figure 3-26A) and COUPTFI mRNA (Figure 3-26B) expression throughout the genotypes.

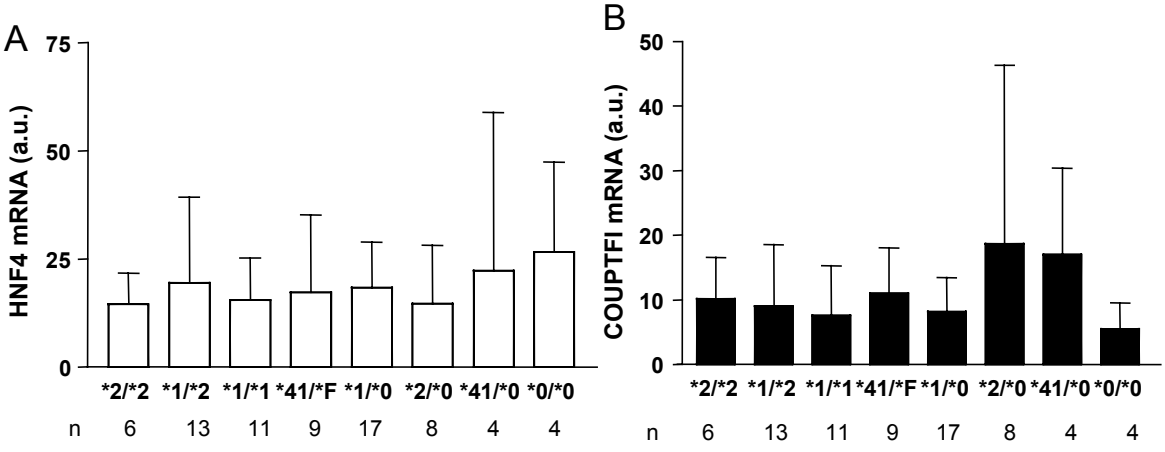

Figure 3-26 HNF4 and COUPTFI mRNA expression in relation to genotype. One-way ANOVA analysis followed by Dunnett's multiple comparisons test, p> 0.05. The nonfunctional alleles **3, *4, *5,* and **6* were collectively termed **0*. For some functional genotypes, alleles **1* and **2* were also grouped and termed **F*.

4 Discussion

4.1 Elucidation of the molecular mechanism of the IM phenotype

4.1.1 *CYP2D6*41* allele: sequence and in vivo analysis

A part of this work is devoted to the clarification of the molecular mechanism that leads to the functional impairment of the deficient **41* allele. This includes also the investigation of its relationship to other alleles, in particular to the closely related fully functional **2* allele, and its predictive value for CYP2D6 drug oxidation capacity.

Initially the **41* allele was characterized by lack of the -1584C>G change on the genetic background of the **2* allele (Raimundo et al., 2000). A practical disadvantage of this situation was that two genotyping assays had to be performed to allow identification of **41*. One assay is needed to identify **2*, which can be achieved by testing for the *CYP2D7* conversion in intron 1 or for 2850C>T (Johansson et al., 1993). A second assay has to be performed to test for the -1584 SNP, to differentiate between **2*[-1584G] and **41*[-1584C]. The molecular characterization of allele **41* in this work included the completion of the total sequence analysis of the 5' upstream region, the coding and the intronic region in comparison to the reference sequence **1* and the related allele **2*. This analysis revealed a total of nine novel intronic sequence changes. A single one of these, the intron 6 SNP 2988G>A, was proved to be specifically linked to **41* (Table 3-2). Thus, 2988G>A appeared to be the only sequence difference that directly identifies the **41* allele within the entire genomic region from about -4.1 kb to the 3' untranslated region of *CYP2D6*.

As shown by detailed genotype-phenotype correlation analysis, the 2988G>A SNP indeed identifies a functionally impaired form of the **2* allele family with high specificity and sensitivity. As most convincingly evident from Figure 3-4, 2988G>A exactly marks the transition between EM and IM phenotype. The existence of three cases (marked by X in Figure 3-4) where 2988G>A genotyping results in correct

phenotype prediction, strongly argues in favor of this polymorphism as the better marker for **41*. The results of the German population study confirm the previous hypothesis, that there exists a common genetic variant within the **2* allele family which codes for the same protein product CYP2D6.2 (R296C, S486T) but which has a profoundly reduced expression leading to low function in vivo (Raimundo et al., 2000; Zanger et al., 2001). Identification of a novel marker SNP for the **41* allele subsequently allowed to improve and simplify *CYP2D6* genotyping and phenotype prediction (Raimundo et al., 2004).

Genotype-phenotype analysis of a Ghanaian and Australian Aborigines population with our new developed TaqMan assay using the 2988G>A SNP emphasizes the previously mentioned conclusion. The existence of three discrepant cases in the Ghanaian population (Table 3-4) in which 2988G>A resulted in better phenotype prediction also confirms that this polymorphism is the better marker for **41*. The low frequency of this allele in the Australian Aborigines (1.1 %) and Ghanaian (0 %) population suggests that the **41* allele (2988A) is strongly associated with the Caucasian population (8%(Raimundo et al., 2004). As the IM phenotype in Asian and African populations is primarily due to alleles **10* and **17*, respectively, the intronic 2988G>A SNP may not play a comparable role in these populations.

4.1.2 *CYP2D6*41* allele: Recombinant expression

The primary cause for the low expression phenotype associated with the *CYP2D6*41* allele was then investigated and the genetic and functional relationships between the three major functional alleles, *2D6*1, 2D6*2*, and *2D6*41* was clarified. As already mentioned, the *CYP2D6*41* was initially identified as a low-activity variant of the common *2D6*2* allele, but the basis for the *2D6*41*-associated low expression phenotype remained however unclear because of the complex genetic and functional relationships between *2D6*1, 2D6*2,* and *2D6*41*. Somewhat surprisingly, the overall functional correlate of *2D6*2* is much more similar to *2D6*1* than to *2D6*41*, although at least 28 nucleotide changes (including the two nonsynonymous changes R296C and S486T, one silent, 11 upstream and 14 intronic SNPs) exist within a total of ~8.4 kb of contiguous sequence between *2D6**2 and *2D6*1* (Raimundo et al., 2004). Based on studies with recombinantly expressed protein variants, it was proposed that 2D6.2 is intrinsically less active than 2D6.1 (Zanger et al., 2001; Yu et al., 2002), although not all studies came to this conclusion (Marcucci et al., 2002). On the other

hand, studies in human liver microsomes revealed higher expression of 2D6.2 versus 2D6.1 in subjects with comparable genotype at the protein level (Zanger et al., 2001). Yet *2D6*1* and *2D6*2* alleles are functionally very similar in liver microsomes and *in vivo* when the related *2D6*41* is analyzed separately from *2D6*2* (Gaedigk et al., 2002; Chou et al., 2003; Raimundo et al., 2004). The initial hypothesis was therefore that -1584C>G may enhance transcription of *2D6*2*, thus effectively counterbalancing the intrinsic activity impairment of 2D6.2 protein. Lack of -1584C>G in *2D6*41* would leave the transcription of this allele at a similar rate to that of *2D6*1* but the resulting overall functional correlate would be lower due to the lower activity of 2D6.41 (or 2D6.2) protein (Zanger et al., 2001).

However, the results of this study establish a different mechanism. Causative for the low expression phenotype associated with *2D6*41* is the intronic SNP 2988G>A, as unequivocally demonstrated by heterologous expression of genomic gene fragments of all three alleles studied that lacked the entire upstream regions. P450 apoprotein, propafenone 5-hydroxylase activity and transcript levels of transiently transfected *2D6*41* amounted to about 20 to 35 % compared to *2D6*2* (Figure 3-10) in very good agreement with the differences observed in human liver here and in the previous study (Zanger et al., 2001). Thus, the 2988G>A SNP sufficiently explains the low expression phenotype and must be regarded as the key mutation of *2D6*41*, in concordance with previous analysis of contribution of the -1584C>G polymorphisms to the impaired activity of the **41* allele using reporter gene assays which lead to the conclusion the -1584C>G polymorphisms is not functionally relevant (Raimundo, 2001).

With respect to the *2D6*2* allele, the data essentially confirm higher expression compared to *2D6*1* in human liver. Whether this is due to transcriptional or posttranscriptional events remains unclear because higher expression and activity by recombinant expression in Huh7 but not in COS-1 cells was observed. It is possible, that the intracellular stability of 2D6.2 versus 2D6.1 depends on celltype-specific factors (e.g. heme supply), which could also explain why propafenone hydroxylase activity of the 2D6.2 variant was significantly increased in Huh7 but not in COS-1 cells (Figure 3-10C).

4.1.3 Elucidation of the mechanism behind 2988G>A SNP

RNA stability

The quantitative analysis of transcripts in liver had suggested an involvement of splicing in determining the phenotype of samples carrying the 2988G>A mutation (3.2.3.2). However, the recombinant system was not suitable to further investigate the splicing mechanism because the splice variant was expressed at high levels and apparently not dependent on genotype.

In order to strengthen the hypothesis of an involvement of alternative splicing it should be excluded that the observed decreased transcriptional level of the **41* allele could have accounted from altered mRNA stability and turnover. Posttranscriptional mRNA turnover represents a potentially important cause of genetic variability arising from *cis*-polymorphisms. mRNA stability can fluctuate through modulation of a number of pathways and changes in RNA structure and protein binding sites. For example, destabilizing adenylate-uridylate-rich sequence elements (ARE) are found in 3' untranslated regions (Tebo et al., 2003) of 5-8 % of human genes and mutations in these elements are linked to disease pathology in human insulin resistance (Di et al., 2002). Virtually all mRNAs have poly(A) tails, which are also important determinants of transcript stability. An interesting example for the involvement of a mutation in enhanced mRNA turnover is provided by Duan et al. describing a synonymous SNP, 957C>T, responsible for the decreased mRNA stability in the D2 dopamine receptor (Duan et al., 2003).

However, analysis of mRNA decay after treatment with ActD failed to reveal any significant difference in turnover between the **41* construct and **1* and **2* constructs. Therefore, mRNA stability does not appear to cause differential mRNA expression.

Reporter gene analysis

An intriguing hypothesis was the possibility that the region around 2988G>A mutation (intron 6) may function also as a transcriptional enhancer or silencer element. In eukaryotes, motifs such as silencers or enhancers can function at considerable distances from the promoter and are active upstream, within, or downstream of the gene, regardless of orientation with respect to the promoter (Maniatis et al., 1987). The 5' flanking regions upstream of genes are known to harbour transcriptional control elements and are thus routinely screened for sequence variants that may help to define a given clinical phenotype. By contrast, the fact that DNA sequences within

the gene (typically 5' and 3' UTR and introns) can often contribute to the control of gene expression, has been only lately appreciated. Although many of the described regulatory elements are located within intron 1, still in proximity of the transcriptional start site, as in the case of *PROC* (human protein C) gene in the liver or *DAT1* (dopamine transporter) gene in the central nervous system, the presence of transcriptional regulatory elements are also described within intron 14 of the same *DAT1* gene, many kilobases downstream of promoter region (Shamsher et al., 2000; Greenwood and Kelsoe, 2003). Another example is given by DeLong and Smith which found a highly conserved element in intron 8 capable to regulate the cyclooxygenase-1 gene expression (DeLong and Smith, 2005).

In silico analysis with the Alibaba 2.1 program of the **1* and **41* sequence surrounding intron 6 predicted a loss of binding of the YY1 (Ying Yang 1) protein for the **41* sequence. YY1 is an ubiquitously expressed zinc finger protein, involved in the regulation of many cellular genes, which functions as a transcriptional repressor and activator (Yao et al., 1998), providing a hint that the 2988G>A SNP may alter the binding of a trans-acting factor. However, the decrease at the transcript level is unlikely due to a functional role of the exon/intron 6 in influencing the rate of transcription, based on the data with reporter gene constructs containing the exon/intron 6 region fused to the tymidine kinase promoter (Figure 3-14). There was no difference in the transcriptional activity between the wild type and the **41* construct, nor between the wild type and empty control vector pGL3 TK(-105). Considering the similar result achieved by analyzing the transcriptional activity of -1584C>G polymorphism with transiently transfected HepG2 and Huh7 cells (Raimundo, 2001) it can be concluded that the functional impairment of *CYP2D6*41* allele seems not to be due to reduced transcriptional activity by any of the analyzed polymorphisms.

Alternative splicing

The splice variant lacking exon 6 resulting in a non-functional protein was first described by Kaminsky and colleagues (1997) and was found in breast tumor tissue, HepG2 and MCF7 cells (Huang et al., 1997a). The same authors analyzed CYP2D6 expression also in human lung and lung tumor tissue and didn't observe any difference in the expression pattern of this splice variant in both tissues (Huang et al., 1997b). Furthermore, this splice variant was also found in human brain tissue (Woo

et al., 1999), but none of this studies analyzed the relationship between this variant and genotype.

In this work, by both experimental approaches, i.e. in transfected cells as well as in human liver samples, substantially decreased levels of the functional transcript in parallel to the decrease in CYP2D6 apoprotein was observed predominantly with the **41* construct or in carriers of 2988G>A SNP. The assumption is that 2988G>A shifts the balance between the two alternative splice products towards the variant that lacks exon 6. This assumption is based on the observation in human liver where the amount of variant transcript in *2D6*41/null* carriers was more than 7-fold higher than in *2D6*1/null* genotypes (Figure 3-8). A significant increase in the alternative splice variant for *CYP2D6*2* compared to *2D6*1* was also noted. Although the difference is in part due to generally increased transcript levels of the *2D6*2* allele as discussed above, this suggests that not only 2988G>A but also 2850C>T can modulate splicing events around exon 6. In another recent study a further splice variant with intron 6 retention was shown to be also correlated to the 2850C>T SNP but not to the 2988G>A SNP (Denson et al., 2005). These authors did however not analyze the variant lacking exon 6. It should be pointed out in this context that according to a recent information analysis of splice sites in human CYP genes, both the splice acceptor and donor sites for exon 6 of CYP2D6 were shown to be among the weakest of the entire gene, indicating that various factors including mutations may easily influence the outcome (Rogan et al., 2003). A further observation to support the notion of labile splicing events around exon 6 is that the balance of splice variant versus functional product was extensively shifted towards the variant in transfected cells, probably due to changes in the relative amounts of certain splice factors in cell lines compared to liver (Figure 3-11). Unfortunately, this high constitutive presence of the splice variant masked any allele-dependent differences, so that the recombinant model to further investigate the splicing process may not be used.

However, to get further insight into possible mechanisms the sequences surrounding 2988G>A and 2850C>T were analyzed with the ESE-finder program, which predicts the location of putative exonic splicing enhancers (Cartegni et al., 2003). Exonic enhancers are thought to serve as binding sites for specific serine / arginine (SR) proteins. These proteins are part of a growing family of structurally related and highly conserved splicing factors that are characterized by the presence of one or two RNA recognition motives (RRM) and by a distinctive carboxy-terminal domain that is highly

enriched in Arg/Ser dipeptides (RS domain). The RRMs mediate sequence-specific binding to the RNA, and so determine substrate specifity, whereas the RS domain seems to be involved mainly in protein-protein interactions. SR proteins that are bound to ESEs can promote exon definition by directly recruiting the splicing machinery through their RS domain and/or by antagonizing the action of nearby silencer elements (Cartegni et al., 2002).

The presence of 2850C>T and 2988G>A on *2D6*41* is indeed predicted to change the scores for binding of certain splice factors to ESE consensus sequences, as illustrated in Figure 3-15. Interestingly, at each polymorphic position the mutations are predicted to result in the exchange of one splicing factor for another. However, involvement of these proteins in determining alternative splicing of CYP2D6 remains speculative, as their precise functions can not yet be predicted.

In conclusion, after pursuing different approaches the most likely mechanism by which the intron 6 SNP leads to lower CYP2D6 expression is via quantitative modulation of splicing events around exon/intron 6.

4.1.4 *CYP2D6*2J* allele

During the genotype-phenotype study of the German population, two individuals were shown to carry the **2J* allele. The base change 2939G>A was first reported by others (designated as variant M18, 3027G>A) but no phenotype correlation was reported (Marez et al., 1997). Complete genomic sequence analysis of these two samples throughout all exons and introns showed the presence of the silent mutation 2939G>A in exon 6 and the novel mutation 2291G>A in intron 4 (Figure 3-16). Both mutations were the only ones specifically associated with the two index cases. The metabolic ratio for sparteine oxidation of the two index subjects was 7.1 and 9.7, which is close to the antimode at 20 but reflects a low amount of residual enzyme activity. In agreement with the CYPallele nomenclature committee the *CYP2D6*2J* allele was therefore renamed *CYP2D6*59* (http://www.imm.ki.se/cypalleles/). The 2939G>A SNP in exon 6 was present heterozygously in 2 individuals out of 308 (0.65%), corresponding to an allele frequency of 0.3 %.

Using the recombinant expression system it was unequivocally demonstrated that the silent mutation 2939G>A in exon 6 was causative for the low expression phenotype associated with *2D6*59* allele, when analyzing constructs harbouring single mutations (**2J(1)*, 2939G>A and **2J(2),* 2291G>A). P450 apoprotein, propafenone 5-

hydroxylase activity and transcript levels of transiently transfected Huh7 cells with **2J* (*2D6*59)* and **2J(1)* amounted to about 15 to 30 % compared to *2D6*2* (Figure 3-17), in very good agreement with the *in vivo* data of the previous study (Raimundo et al., 2004). Thus, the 2939G>A SNP sufficiently explains the low expression phenotype and must be regarded as the key mutation of *2D6*59* allele. The *2D6*2J(2)* variant has, compared to *2D6*2*, only the additional intron 4 mutation, which seems not to have any functional consequence. As expected, the expression level of *2D6*2J(2)* is very similar to the **2* allele, therefore this construct essentially confirms independently from the **41* approach, the higher expression of *2D6*2* compared to *2D6*1* as observed in human liver.

Modulation of alternative splicing

The expression of *CYP2D6* at the mRNA level was also strongly decreased in cells transfected with clones **2J* (**59)* and **2J(1)*, when considering the correctly spliced product (Figure 3-18). However, the presence of an alternative splice product with invariant intensity throughout the different allelic variants, as previously observed, emphasizes the occurrence of labile splicing events around exon 6. The presence of 2850C>T and 2939G>A on *2D6*59* is indeed predicted to change the scores for binding of certain splice factors to ESE consensus sequences therefore it is possible that the 2939G>A mutation influences splicing around exon 6. Unfortunately no liver samples were available of *2D6*59* allele carriers for analysis of authentic mRNA transcripts. Therefore a possible involvement of the 2939G>A mutation in alternative splicing may not be excluded.

***CYP2D6*59* allele affecting mRNA stability?**

In this work it was shown that the naturally occurring synonymous SNP 2939G>A, exon 6, can markedly affect the in vitro expression of CYP2D6 gene while the 1661G>C SNP in exon 3 was shown to be silent. It is conceivable that the 2939G>A SNP may affect mRNA stability consistent with the changes of predicted mRNA secondary structure (Figure 3-19), suggesting that mRNA secondary structure associated with the synonymous mutation 2939A may play an important role in the regulation of CYP2D6 gene expression. However, because of the limitation of structure prediction of Mfold, other RNA secondary structure prediction methods and mRNA stability assays may be needed to perform.

Unless the *CYP2D6*59* is a rare allele (0.3 % frequency), efforts in further investigations about the mechanism behind the silent SNP 2939G>A must be weigh up. From the pharmacogenetic point of view the most important concern was to find the mutation causally responsible for impaired drug oxidation phenotype. In this respect, after identification of the causative mutation it was also shown that the mechanism leading to decreased *in vivo* function involves decreased formation of the mRNA species coding for functional 2D6 enzyme.

Summarizing this part of the work concerned with the intermediate metabolizer phenotype, the molecular characterization of two alleles strongly associated with this phenotype contributes to a better prediction of CYP2D6 expression *in vivo*. These data help to understand genotype-phenotype relationships of CYP2D6 and to improve predictive power and reliability of pharmacogenetic diagnostics.

4.2 Analysis of the UM phenotype

4.2.1 In vivo analysis

The ultrarapid metabolizer phenotype still represents a challenging phenotype, as confirmed also by the present CYP2D6 genotype-phenotype analysis in human liver. Individuals with UM phenotype express higher levels of CYP2D6 protein, but the UM phenotype prediction by genotype remains unsatisfactory. The liver bank analysis shows that in case of lack of *in vivo* data, 2D6 protein and propafenone hydroxylation activity represent a satisfactory surrogate for *in vivo* phenotype. In the German population study phenotyped with sparteine, the presence of three functional genes always correctly predicts the UM phenotype (Figure 3-3), even though representing only 28.5 % of all UMs. Contrary to the German population analysis the presence of three functional genes was not always predictive for the UM phenotype in the liver bank analysis, further reducing the predictive power of functional gene duplication from 20.5 to 11.7 %. However, it should be mentioned that the *in vitro* phenotyping methods are not specific and accurate as in vivo phenotyping. In attempt to gain more insights about the possible mechanism for the presence of duplication-negative UMs two hypotheses were tested.

4.2.2 Expression of the pseudogene *CYP2D7*

Pseudogenes are complete or partial copies of genes that are unable to code for functional polypeptides, and in the human genome, already 20,000 pseudogenes have been identified (Torrents et al., 2003). While *CYP2D8* is definitively a pseudogene, containing several frame disrupting mutations, *CYP2D7* has only a single T insertion at position 138 in the first exon that leads to a disrupted reading frame (Kimura et al., 1989). Specific mRNA derived from *CYP2D7* was initially found in human breast tissue (Huang et al., 1997a). By using TaqMan real-time quantitative PCR, it was also shown that comparable levels of *CYP2D6* and *CYP2D7/8* transcripts are expressed in human liver (Endrizzi et al., 2002). Besides, in the same study it was shown that *CYP2D6* but not the pseudogene mRNA levels were influenced by *CYP2D6* genotype. The question then arised whether *CYP2D7* may be expressed as a functional protein occasionally. Given the variety of gene-conversions and cross-over events reported in the *CYP2D* locus (Steen et al., 1995; Daly et al., 1996b; Lundqvist et al., 1999), there is a possibility that the *CYP2D7* exon 1 region could have converted back to the original *CYP2D6* sequence, resulting in a full-length CYD2D7 protein. In fact, Sachse et al. described an 'inverse' variant of such a gene-conversion. They detected a rare allele having a T insertion in position 138 in the CYP2D6 exon 1, and after analysis of the surrounding region hypothesized that this mutation most likely was caused by gene-conversion event with the *CYP2D7* pseudogene (Sachse et al., 1996). The initial hypothesis was therefore that expression of active enzyme from *CYP2D7* could have a similar effect as CYP2D6 duplication.

No indication was found when *CYP2D7* was first analyzed in genomic DNA of 17 Caucasian individuals (Lovlie et al., 2001). However, a recent report described a novel protein that is translated from *CYP2D7* splice variant metabolizing codeine at even greater extent than CYP2D6 in human brain. This variant is characterized by retention of 57 bp of intron 6 and the SNP 138delT that reverted the frame shift and allowed translation into a protein that harboured an additional 19 amino acids (Pai et al., 2004). This Indian research group reported also six homozygous DNAs for the 138delT variant among 12 samples, suggesting an allele frequency of ~50 % in the Indian population. In this work, a *CYP2D7*-specific genotyping assay was developed but none of 285 analyzed Caucasian liver DNAs carried the *CYP2D7* 138delT, in agreement with another recent study unable to identify a single subject with the

CYP2D7 138delT, among 285 genomic DNAs from different ethnic origin (Gaedigk et al., 2005a).

The absence of *CYP2D7* 138delT indicate that functional CYP2D7 or CYP2D7-like protein is absent or a rare event in the Caucasian population and cannot explain the ultrarapid metabolizer phenotype in *CYP2D6* duplication-negative individuals.

4.2.3 Transcriptional regulation of *CYP2D6*

During the characterization of the *CYP2D6* promoter Cairns et al. found a potential role for antagonistic interactions between positively and negatively regulatory elements. They found that HNF4 could activate *CYP2D6* promoter, whereas COUPTFI could inhibit HNF4 stimulation *in vitro* and that both transcription factors competed for the same binding site (DR1, direct repeat 1) on the *CYP2D6* promoter. They concluded that the contribution of DR1 element in controlling the transcription of the *CYP2D6* gene depends on the balance between a positively and negatively acting transcription factor (Cairns et al., 1996). The hepatocyte nuclear factor 4 (HNF4) is a prominent member of the family of liver-enriched transcription factors, playing a role in the expression of a large number of liver-specific genes, such as those encoding apolipoproteins, coagulation factors and P450s (Sladek, 1994). The chicken ovoalbumin upstream-promoter transcription factor (COUPTF) is an orphan member of nuclear receptor super family that was originally identified by binding to and activation of the chicken ovoalbumin gene (Pastorcic et al., 1986). Although COUPTFI can stimulate the expression of a few genes, it has mainly been identified as a negative regulator and it is known to inhibit ligand-induced transactivation by nuclear receptors like HNF4 (Kimura et al., 1993). Using a collection of 87 human liver samples, an impact of the HNF4 and COUPTFI mRNA expression on CYP2D6 protein expression could not be demonstrated. Even if there was a *2D6* genotype-independent expression of HNF4 and COUPTFI mRNA, there was no correlation between HNF4 and COUPTFI mRNA and CYP2D6 protein expression, therefore it seems unlikely that a possible imbalance of these two transcription factors are responsible for increased *2D6* expression in 2D6 duplication-negative UMs. However, it should be emphasized that only the mRNA expression of these two transcription factors was measured. It can not be excluded that HNF4 and COUPTFI may regulate/influence CYP2D6 expression at the protein level. A previous report suggested that the posttranscriptional modification of HNF4 is important for its DNA-

binding activity and consequently for its transactivational potential *in vitro* (Ktistaki et al., 1995). It would be conceivable that the 2D6 transcriptional regulation may be dependent on the phosphorylation status of HNF4. This is an interesting issue that may be pursued, as well as the sequencing of 2D6 duplication-negative samples with high protein and enzyme activity. The genetic and/or biochemical basis for the UM individuals lacking allele duplication remains therefore so far unexplained even after testing two plausible hypotheses. However, a systematical analysis of nearly 300 liver samples allowed the further characterization of the CYP2D6 enzyme and its genetic polymorphisms, emphasizing the importance of a valuable tool such as the large liver bank equipped with many data.

References

Agundez JA, Ledesma M C, Ladero J M and Benitez J (1995) Prevalence of CYP2D6 Gene Duplication and Its Repercussion on the Oxidative Phenotype in a White Population. *Clin Pharmacol Ther* **57**:265-269.

Aklillu E, Persson I, Bertilsson L, Johansson I, Rodrigues F and Ingelman-Sundberg M (1996) Frequent Distribution of Ultrarapid Metabolizers of Debrisoquine in an Ethiopian Population Carrying Duplicated and Multiduplicated Functional CYP2D6 Alleles. *J Pharmacol Exp Ther* **278**:441-446.

Allorge D, Harlow J, Boulet O, Hayhurst G P, Chowdry J, Roth E, Crewe K, Lo-Guidice J M, Lhermitte M, Broly F, Tucker G T and Ellis S W (2001) In-Vitro Analysis of the Contribution of CYP2D6.35 to Ultra-Rapid Metabolism. *Pharmacogenetics* **11**:739-741.

Armstrong M, Idle J R and Daly A K (1993) A Polymorphic CfoI Site in Exon 6 of the Human Cytochrome P450 CYP2D6 Gene Detected by the Polymerase Chain Reaction. *Hum Genet* **91**:616-617.

Barclay ML, Sawyers S M, Begg E J, Zhang M, Roberts R L, Kennedy M A and Elliott J M (2003) Correlation of CYP2D6 Genotype With Perhexiline Phenotypic Metabolizer Status. *Pharmacogenetics* **13**:627-632.

Bathum L, Johansson I, Ingelman-Sundberg M, Horder M and Brosen K (1998) Ultrarapid Metabolism of Sparteine: Frequency of Alleles With Duplicated CYP2D6 Genes in a Danish Population As Determined by Restriction Fragment Length Polymorphism and Long Polymerase Chain Reaction. *Pharmacogenetics* **8**:119-123.

Bertilsson L, Dahl M L, Sjoqvist F, berg-Wistedt A, Humble M, Johansson I, Lundqvist E and Ingelman-Sundberg M (1993) Molecular Basis for Rational Megaprescribing in Ultrarapid Hydroxylators of Debrisoquine. *Lancet* **341**:63.

Blievernicht, J. Untersuchungen zur Häufigkeit von Enzympolymorphismen des Arzneimittelmetabolismus- ein methodischer Vergleich zwischen MicroArray und alternative Methoden. 2004.
Ref Type: Thesis/Dissertation

Bock KW, Schrenk D, Forster A, Griese E U, Morike K, Brockmeier D and Eichelbaum M (1994) The Influence of Environmental and Genetic Factors on CYP2D6, CYP1A2 and UDP-Glucuronosyltransferases in Man Using Sparteine, Caffeine, and Paracetamol As Probes. *Pharmacogenetics* **4**:209-218.

Broly F and Meyer U A (1993) Debrisoquine Oxidation Polymorphism: Phenotypic Consequences of a 3-Base-Pair Deletion in Exon 5 of the CYP2D6 Gene. *Pharmacogenetics* **3**:123-130.

Brosen K and Gram L F (1989) Clinical Significance of the Sparteine/Debrisoquine Oxidation Polymorphism. *Eur J Clin Pharmacol* **36**:537-547.

Cairns W, Smith C A, McLaren A W and Wolf C R (1996) Characterization of the Human Cytochrome P4502D6 Promoter. A Potential Role for Antagonistic Interactions Between Members of the Nuclear Receptor Family. *J Biol Chem* **271**:25269-25276.

Carlini DB, Chen Y and Stephan W (2001) The Relationship Between Third-Codon Position Nucleotide Content, Codon Bias, MRNA Secondary Structure and Gene Expression in the Drosophilid Alcohol Dehydrogenase Genes Adh and Adhr. *Genetics* **159**:623-633.

Cartegni L, Chew S L and Krainer A R (2002) Listening to Silence and Understanding Nonsense: Exonic Mutations That Affect Splicing. *Nat Rev Genet* **3**:285-298.

Cartegni L, Wang J, Zhu Z, Zhang M Q and Krainer A R (2003) ESEfinder: A Web Resource to Identify Exonic Splicing Enhancers. *Nucleic Acids Res* **31**:3568-3571.

Chen Y, Carlini D B, Baines J F, Parsch J, Braverman J M, Tanda S and Stephan W (1999) RNA Secondary Structure and Compensatory Evolution. *Genes Genet Syst* **74**:271-286.

Chen ZR, Somogyi A A and Bochner F (1988) Polymorphic O-Demethylation of Codeine. *Lancet* **2**:914-915.

Chen ZR, Somogyi A A, Reynolds G and Bochner F (1991) Disposition and Metabolism of Codeine After Single and Chronic Doses in One Poor and Seven Extensive Metabolisers. *Br J Clin Pharmacol* **31**:381-390.

Cholerton S, Daly A K and Idle J R (1992) The Role of Individual Human Cytochromes P450 in Drug Metabolism and Clinical Response. *Trends Pharmacol Sci* **13**:434-439.

Chou WH, Yan F X, Robbins-Weilert D K, Ryder T B, Liu W W, Perbost C, Fairchild M, de L J, Koch W H and Wedlund P J (2003) Comparison of Two CYP2D6 Genotyping Methods and Assessment of Genotype-Phenotype Relationships. *Clin Chem* **49**:542-551.

Clarke SE and Jones B C (2002) Human Cytochromes P450 and their role in metabolism-based drug-drug interactions, in *Drug-Drug Interactions* p 55, Marcel Dekker, Inc., New York.

Dahl ML, Johansson I, Bertilsson L, Ingelman-Sundberg M and Sjoqvist F (1995) Ultrarapid Hydroxylation of Debrisoquine in a Swedish Population. Analysis of the Molecular Genetic Basis. *J Pharmacol Exp Ther* **274**:516-520.

Dalen P, Dahl M L, Ruiz M L, Nordin J and Bertilsson L (1998) 10-Hydroxylation of Nortriptyline in White Persons With 0, 1, 2, 3, and 13 Functional CYP2D6 Genes. *Clin Pharmacol Ther* **63**:444-452.

Daly AK, Brockmoller J, Broly F, Eichelbaum M, Evans W E, Gonzalez F J, Huang J D, Idle J R, Ingelman-Sundberg M, Ishizaki T, Jacqz-Aigrain E, Meyer U A, Nebert D W, Steen V M, Wolf C R and Zanger U M (1996a) Nomenclature for Human CYP2D6 Alleles. *Pharmacogenetics* **6**:193-201.

Daly AK, Fairbrother K S, Andreassen O A, London S J, Idle J R and Steen V M (1996b) Characterization and PCR-Based Detection of Two Different Hybrid CYP2D7P/CYP2D6 Alleles Associated With the Poor Metabolizer Phenotype. *Pharmacogenetics* **6**:319-328.

DeLong CJ and Smith W L (2005) An Intronic Enhancer Regulates Cyclooxygenase-1 Gene Expression. *Biochem Biophys Res Commun* **338**:53-61.

Denson J, Wu Y, Yang W and Zhang J (2005) Inter-Individual Variation of Several Cytochrome P450 2D6 Splice Variants in Human Liver. *Biochem Biophys Res Commun* **330**:498-504.

Di PR, Frittitta L, Miscio G, Bozzali M, Baratta R, Centra M, Spampinato D, Santagati M G, Ercolino T, Cisternino C, Soccio T, Mastroianno S, Tassi V, Almgren P, Pizzuti A, Vigneri R and Trischitta V (2002) A Variation in 3' UTR of HPTP1B Increases Specific Gene Expression and Associates With Insulin Resistance. *Am J Hum Genet* **70**:806-812.

Duan J, Wainwright M S, Comeron J M, Saitou N, Sanders A R, Gelernter J and Gejman P V (2003) Synonymous Mutations in the Human Dopamine Receptor D2 (DRD2) Affect MRNA Stability and Synthesis of the Receptor. *Hum Mol Genet* **12**:205-216.

Eichelbaum M, Mineshita S, Ohnhaus E E and Zekorn C (1986) The Influence of Enzyme Induction on Polymorphic Sparteine Oxidation. *Br J Clin Pharmacol* **22**:49-53.

Eichelbaum M, Spannbrucker N, Steincke B and Dengler H J (1979) Defective N-Oxidation of Sparteine in Man: a New Pharmacogenetic Defect. *Eur J Clin Pharmacol* **16**:183-187.

Endrizzi K, Fischer J, Klein K, Schwab M, Nussler A, Neuhaus P, Eichelbaum M and Zanger U M (2002) Discriminative Quantification of Cytochrome P4502D6 and 2D7/8 Pseudogene Expression by TaqMan Real-Time Reverse Transcriptase Polymerase Chain Reaction. *Anal Biochem* **300**:121-131.

Evans DA, Mahgoub A, Sloan T P, Idle J R and Smith R L (1980) A Family and Population Study of the Genetic Polymorphism of Debrisoquine Oxidation in a White British Population. *J Med Genet* **17**:102-105.

Evans WE and McLeod H L (2003) Pharmacogenomics--Drug Disposition, Drug Targets, and Side Effects. *N Engl J Med* **348**:538-549.

Evert B, Eichelbaum M, Haubruck H and Zanger U M (1997) Functional Properties of CYP2D6 1 (Wild-Type) and CYP2D6 7 (His324Pro) Expressed by Recombinant Baculovirus in Insect Cells. *Naunyn Schmiedebergs Arch Pharmacol* **355**:309-318.

Gaedigk A, Blum M, Gaedigk R, Eichelbaum M and Meyer U A (1991) Deletion of the Entire Cytochrome P450 CYP2D6 Gene As a Cause of Impaired Drug Metabolism in Poor Metabolizers of the Debrisoquine/Sparteine Polymorphism. *Am J Hum Genet* **48**:943-950.

Gaedigk A, Bradford L D, Marcucci K A and Leeder J S (2002) Unique CYP2D6 Activity Distribution and Genotype-Phenotype Discordance in Black Americans. *Clin Pharmacol Ther* **72**:76-89.

Gaedigk A, Gaedigk R and Leeder J S (2005a) CYP2D7 Splice Variants in Human Liver and Brain: Does CYP2D7 Encode Functional Protein? *Biochem Biophys Res Commun* **336**:1241-1250.

Gaedigk A, Ndjountche L, Leeder J S and Bradford L D (2005b) Limited Association of the 2988g > a Single Nucleotide Polymorphism With CYP2D641 in Black Subjects. *Clin Pharmacol Ther* **77**:228-230.

Geick A, Eichelbaum M and Burk O (2001) Nuclear Receptor Response Elements Mediate Induction of Intestinal MDR1 by Rifampin. *J Biol Chem* **276**:14581-14587.

Gonzalez FJ, Skoda R C, Kimura S, Umeno M, Zanger U M, Nebert D W, Gelboin H V, Hardwick J P and Meyer U A (1988) Characterization of the Common Genetic Defect in Humans Deficient in Debrisoquine Metabolism. *Nature* **331**:442-446.

Gorrod A.E. and Oxon M.D. (1902) The Incidence of Alkaptonuria: a Study in Chemical Individuality. *Lancet* **1**:1616-1620.

Greenwood TA and Kelsoe J R (2003) Promoter and Intronic Variants Affect the Transcriptional Regulation of the Human Dopamine Transporter Gene. *Genomics* **82**:511-520.

Griese EU, Asante-Poku S, Ofori-Adjei D, Mikus G and Eichelbaum M (1999) Analysis of the CYP2D6 Gene Mutations and Their Consequences for Enzyme Function in a West African Population. *Pharmacogenetics* **9**:715-723.

Griese EU, Ilett K F, Kitteringham N R, Eichelbaum M, Powell H, Spargo R M, LeSouef P N, Musk A W and Minchin R F (2001) Allele and Genotype Frequencies of Polymorphic Cytochromes P4502D6, 2C19 and 2E1 in Aborigines From Western Australia. *Pharmacogenetics* **11**:69-76.

Griese EU, Zanger U M, Brudermanns U, Gaedigk A, Mikus G, Morike K, Stuven T and Eichelbaum M (1998) Assessment of the Predictive Power of Genotypes for the in-Vivo Catalytic Function of CYP2D6 in a German Population. *Pharmacogenetics* **8**:15-26.

Heim MH and Meyer U A (1992) Evolution of a Highly Polymorphic Human Cytochrome P450 Gene Cluster: CYP2D6. *Genomics* **14**:49-58.

Huang Z, Fasco M J and Kaminsky L S (1997a) Alternative Splicing of CYP2D MRNA in Human Breast Tissue. *Arch Biochem Biophys* **343**:101-108.

Huang Z, Fasco M J, Spivack S and Kaminsky L S (1997b) Comparisons of CYP2D Messenger RNA Splice Variant Profiles in Human Lung Tumors and Normal Tissues. *Cancer Res* **57**:2589-2592.

Ingelman-Sundberg M (1999) Duplication, Multiduplication, and Amplification of Genes Encoding Drug-Metabolizing Enzymes: Evolutionary, Toxicological, and Clinical Pharmacological Aspects. *Drug Metab Rev* **31**:449-459.

Ingelman-Sundberg M, Daly A K, Oscarson M and Nebert D W (2000) Human Cytochrome P450 (CYP) Genes: Recommendations for the Nomenclature of Alleles. *Pharmacogenetics* **10**:91-93.

Johansson I, Lundqvist E, Bertilsson L, Dahl M L, Sjoqvist F and Ingelman-Sundberg M (1993) Inherited Amplification of an Active Gene in the Cytochrome P450 CYP2D Locus As a Cause of Ultrarapid Metabolism of Debrisoquine. *Proc Natl Acad Sci U S A* **90**:11825-11829.

Kagimoto M, Heim M, Kagimoto K, Zeugin T and Meyer U A (1990) Multiple Mutations of the Human Cytochrome P450IID6 Gene (CYP2D6) in Poor Metabolizers of Debrisoquine. Study of the Functional Significance of Individual Mutations by Expression of Chimeric Genes. *J Biol Chem* **265**:17209-17214.

Kalow, W. Pharmacogenetics: heredity and the response to drugs. 1962. W.B. Saunders, Philadelphia.
Ref Type: Serial (Book,Monograph)

Kimura A, Nishiyori A, Murakami T, Tsukamoto T, Hata S, Osumi T, Okamura R, Mori M and Takiguchi M (1993) Chicken Ovalbumin Upstream Promoter-Transcription Factor (COUP-TF) Represses Transcription From the Promoter of the Gene for Ornithine Transcarbamylase in a Manner Antagonistic to Hepatocyte Nuclear Factor-4 (HNF-4). *J Biol Chem* **268**:11125-11133.

Kimura S, Umeno M, Skoda R C, Meyer U A and Gonzalez F J (1989) The Human Debrisoquine 4-Hydroxylase (CYP2D) Locus: Sequence and Identification of the Polymorphic CYP2D6 Gene, a Related Gene, and a Pseudogene. *Am J Hum Genet* **45**:889-904.

Klingenberg M (1958) Pigments of Rat Liver Microsomes. *Arch Biochem Biophys* **75**:376-386.

Ktistaki E, Ktistakis N T, Papadogeorgaki E and Talianidis I (1995) Recruitment of Hepatocyte Nuclear Factor 4 into Specific Intranuclear Compartments Depends on Tyrosine Phosphorylation That Affects Its DNA-Binding and Transactivation Potential. *Proc Natl Acad Sci U S A* **92**:9876-9880.

Lang T, Klein K, Fischer J, Nussler A K, Neuhaus P, Hofmann U, Eichelbaum M, Schwab M and Zanger U M (2001) Extensive Genetic Polymorphism in the Human CYP2B6 Gene With Impact on Expression and Function in Human Liver. *Pharmacogenetics* **11**:399-415.

Lazarou J, Pomeranz B H and Corey P N (1998) Incidence of Adverse Drug Reactions in Hospitalized Patients: a Meta-Analysis of Prospective Studies. *JAMA* **279**:1200-1205.

Lovlie R, Daly A K, Matre G E, Molven A and Steen V M (2001) Polymorphisms in CYP2D6 Duplication-Negative Individuals With the Ultrarapid Metabolizer Phenotype: a Role for the CYP2D6*35 Allele in Ultrarapid Metabolism? *Pharmacogenetics* **11**:45-55.

Lundqvist E, Johansson I and Ingelman-Sundberg M (1999) Genetic Mechanisms for Duplication and Multiduplication of the Human CYP2D6 Gene and Methods for Detection of Duplicated CYP2D6 Genes. *Gene* **226**:327-338.

Mahgoub A, Idle J R, Dring L G, Lancaster R and Smith R L (1977) Polymorphic Hydroxylation of Debrisoquine in Man. *Lancet* **2**:584-586.

Maniatis T, Goodbourn S and Fischer J A (1987) Regulation of Inducible and Tissue-Specific Gene Expression. *Science* **236**:1237-1245.

Marcucci KA, Pearce R E, Crespi C, Steimel D T, Leeder J S and Gaedigk A (2002) Characterization of Cytochrome P450 2D6.1 (CYP2D6.1), CYP2D6.2, and CYP2D6.17 Activities Toward Model CYP2D6 Substrates Dextromethorphan, Bufuralol, and Debrisoquine. *Drug Metab Dispos* **30**:595-601.

Marez D, Legrand M, Sabbagh N, Guidice J M, Spire C, Lafitte J J, Meyer U A and Broly F (1997) Polymorphism of the Cytochrome P450 CYP2D6 Gene in a European Population: Characterization of 48 Mutations and 53 Alleles, Their Frequencies and Evolution. *Pharmacogenetics* **7**:193-202.

McLellan RA, Oscarson M, Seidegard J, Evans D A and Ingelman-Sundberg M (1997) Frequent Occurrence of CYP2D6 Gene Duplication in Saudi Arabians. *Pharmacogenetics* **7**:187-191.

Meyer UA (1991) Genotype or Phenotype: the Definition of a Pharmacogenetic Polymorphism. *Pharmacogenetics* **1**:66-67.

MOTULSKY AG (1957) Drug Reactions Enzymes, and Biochemical Genetics. *J Am Med Assoc* **165**:835-837.

Nelson DR, Koymans L, Kamataki T, Stegeman J J, Feyereisen R, Waxman D J, Waterman M R, Gotoh O, Coon M J, Estabrook R W, Gunsalus I C and Nebert D W (1996) P450 Superfamily: Update on New Sequences, Gene Mapping, Accession Numbers and Nomenclature. *Pharmacogenetics* **6**:1-42.

Osikowska-Evers B, Dayer P, Meyer U A, Robertz G M and Eichelbaum M (1987) Evidence for Altered Catalytic Properties of the Cytochrome P-450 Involved in Sparteine Oxidation in Poor Metabolizers. *Clin Pharmacol Ther* **41**:320-325.

Pai HV, Kommaddi R P, Chinta S J, Mori T, Boyd M R and Ravindranath V (2004) A Frameshift Mutation and Alternate Splicing in Human Brain Generate a Functional Form of the Pseudogene Cytochrome P4502D7 That Demethylates Codeine to Morphine. *J Biol Chem* **279**:27383-27389.

Parsch J, Russell J A, Beerman I, Hartl D L and Stephan W (2000) Deletion of a Conserved Regulatory Element in the Drosophila Adh Gene Leads to Increased Alcohol Dehydrogenase Activity but Also Delays Development. *Genetics* **156**:219-227.

Pastorcic M, Wang H, Elbrecht A, Tsai S Y, Tsai M J and O'Malley B W (1986) Control of Transcription Initiation in Vitro Requires Binding of a Transcription Factor to the Distal Promoter of the Ovalbumin Gene. *Mol Cell Biol* **6**:2784-2791.

Raimundo, S. Molekulargenetische Untersuchungen zum Mechanismus des Intermediären Metabolisierer Phänotyps für den CYP2D6 Polymorphismus. 2001. Ref Type: Thesis/Dissertation

Raimundo S, Fischer J, Eichelbaum M, Griese E U, Schwab M and Zanger U M (2000) Elucidation of the Genetic Basis of the Common 'Intermediate Metabolizer' Phenotype for Drug Oxidation by CYP2D6. *Pharmacogenetics* **10**:577-581.

Raimundo S, Toscano C, Klein K, Fischer J, Griese E U, Eichelbaum M, Schwab M and Zanger U M (2004) A Novel Intronic Mutation, 2988G>A, With High Predictivity for Impaired Function of Cytochrome P450 2D6 in White Subjects. *Clin Pharmacol Ther* **76**:128-138.

Rau T, Heide R, Bergmann K, Wuttke H, Werner U, Feifel N and Eschenhagen T (2002) Effect of the CYP2D6 Genotype on Metoprolol Metabolism Persists During Long-Term Treatment. *Pharmacogenetics* **12**:465-472.

Rogan PK, Svojanovsky S and Leeder J S (2003) Information Theory-Based Analysis of CYP2C19, CYP2D6 and CYP3A5 Splicing Mutations. *Pharmacogenetics* **13**:207-218.

Sachse C, Brockmoller J, Bauer S, Reum T and Roots I (1996) A Rare Insertion of T226 in Exon 1 of CYP2D6 Causes a Frameshift and Is Associated With the Poor Metabolizer Phenotype: CYP2D6*15. *Pharmacogenetics* **6**:269-272.

Sachse C, Brockmoller J, Bauer S and Roots I (1997) Cytochrome P450 2D6 Variants in a Caucasian Population: Allele Frequencies and Phenotypic Consequences. *Am J Hum Genet* **60**:284-295.

Schaeffeler E, Schwab M, Eichelbaum M and Zanger U M (2003) CYP2D6 Genotyping Strategy Based on Gene Copy Number Determination by TaqMan Real-Time PCR. *Hum Mutat* **22**:476-485.

Shamsher MK, Chuzhanova N A, Friedman B, Scopes D A, Alhaq A, Millar D S, Cooper D N and Berg L P (2000) Identification of an Intronic Regulatory Element in the Human Protein C (PROC) Gene. *Hum Genet* **107**:458-465.

Sladek FM (1994) Hepatocyte nuclear factor 4 (HNF-4), in *Liver Gene Expression* (Tronche FaYM ed) pp 207-230.

Smith RL (1986) *Introduction. In: Human Genetic Variations in Oxidative Drug Metabolism*.

Snyder LH (1932) Studies on Human Inheritance.IX.The Inheritance of Taste Deficiency in Man. *Ohio J Sci* **32**:436-438.

Spear BB (2001) Pharmacogenetics and Antiepileptic Drugs. *Epilepsia* **42 Suppl 5**:31-34.

Steen VM, Molven A, Aarskog N K and Gulbrandsen A K (1995) Homologous Unequal Cross-Over Involving a 2.8 Kb Direct Repeat As a Mechanism for the Generation of Allelic Variants of Human Cytochrome P450 CYP2D6 Gene. *Hum Mol Genet* **4**:2251-2257.

Steiner E, Iselius L, Alvan G, Lindsten J and Sjoqvist F (1985) A Family Study of Genetic and Environmental Factors Determining Polymorphic Hydroxylation of Debrisoquin. *Clin Pharmacol Ther* **38**:394-401.

Tebo J, Der S, Frevel M, Khabar K S, Williams B R and Hamilton T A (2003) Heterogeneity in Control of MRNA Stability by AU-Rich Elements. *J Biol Chem* **278**:12085-12093.

Torrents D, Suyama M, Zdobnov E and Bork P (2003) A Genome-Wide Survey of Human Pseudogenes. *Genome Res* **13**:2559-2567.

Tyndale R, Aoyama T, Broly F, Matsunaga T, Inaba T, Kalow W, Gelboin H V, Meyer U A and Gonzalez F J (1991) Identification of a New Variant CYP2D6 Allele Lacking the Codon Encoding Lys-281: Possible Association With the Poor Metabolizer Phenotype. *Pharmacogenetics* **1**:26-32.

Vogel F (1959) Moderne Probleme Der Humangenetik. *Erg Inn Med Kinderheilk* **12**:52-125.

Vogel F and MOTULSKY A G (1986) *Human Genetics. Problems and Approaches*. Springer-Verlag, New York.

Wang SL, Huang J D, Lai M D, Liu B H and Lai M L (1993) Molecular Basis of Genetic Variation in Debrisoquin Hydroxylation in Chinese Subjects: Polymorphism in RFLP and DNA Sequence of CYP2D6. *Clin Pharmacol Ther* **53**:410-418.

Wolbold R, Klein K, Burk O, Nussler A K, Neuhaus P, Eichelbaum M, Schwab M and Zanger U M (2003) Sex Is a Major Determinant of CYP3A4 Expression in Human Liver. *Hepatology* **38**:978-988.

Woo SI, Hansen L A, Yu X, Mallory M and Masliah E (1999) Alternative Splicing Patterns of CYP2D Genes in Human Brain and Neurodegenerative Disorders. *Neurology* **53**:1570-1572.

Yamazaki S, Sato K, Suhara K, Sakaguchi M, Mihara K and Omura T (1993) Importance of the Proline-Rich Region Following Signal-Anchor Sequence in the Formation of Correct Conformation of Microsomal Cytochrome P-450s. *J Biochem (Tokyo)* **114**:652-657.

Yao YL, Dupont B R, Ghosh S, Fang Y, Leach R J and Seto E (1998) Cloning, Chromosomal Localization and Promoter Analysis of the Human Transcription Factor YY1. *Nucleic Acids Res* **26**:3776-3783.

Yokota H, Tamura S, Furuya H, Kimura S, Watanabe M, Kanazawa I, Kondo I and Gonzalez F J (1993) Evidence for a New Variant CYP2D6 Allele CYP2D6J in a Japanese Population Associated With Lower in Vivo Rates of Sparteine Metabolism. *Pharmacogenetics* **3**:256-263.

Yu A, Kneller B M, Rettie A E and Haining R L (2002) Expression, Purification, Biochemical Characterization, and Comparative Function of Human Cytochrome P450 2D6.1, 2D6.2, 2D6.10, and 2D6.17 Allelic Isoforms. *J Pharmacol Exp Ther* **303**:1291-1300.

Zanger UM, Fischer J, Raimundo S, Stuven T, Evert B O, Schwab M and Eichelbaum M (2001) Comprehensive Analysis of the Genetic Factors Determining Expression and Function of Hepatic CYP2D6. *Pharmacogenetics* **11**:573-585.

Zanger UM, Hauri H P, Loeper J, Homberg J C and Meyer U A (1988) Antibodies Against Human Cytochrome P-450db1 in Autoimmune Hepatitis Type II. *Proc Natl Acad Sci U S A* **85**:8256-8260.

Zanger UM, Raimundo S and Eichelbaum M (2004) Cytochrome P450 2D6: Overview and Update on Pharmacology, Genetics, Biochemistry. *Naunyn Schmiedebergs Arch Pharmacol* **369**:23-37.

Zuker M (2003) Mfold Web Server for Nucleic Acid Folding and Hybridization Prediction. *Nucleic Acids Res* **31**:3406-3415.

Lebenslauf

Persönliche Daten:

Name:	Claudia Toscano
Geburtstag:	31.12.1976
Geburtsort:	Karlsruhe
Adresse:	Saarstraße 21, 71636 Ludwigsburg
Staatsangehörigkeit:	Italienisch

Ausbildung:

11. 2002- 03. 2006	**Arbeit an der Dissertation zum Doktor der Naturwissenschaften am Dr. Margarete Fischer Bosch Institut für Klinische Pharmakologie in Stuttgart** Thema: „Molecular analysis of mechanisms leading to CYP2D6 intermediate and ultrarapid metabolizer phenotypes”
10. 1995- 04. 2002	**Studium der Biologie an der Technischen Universität in Karlsruhe** Hauptfachrichtungen: Zoologie und Genetik Nebenfachrichtungen: Toxikologie und Paläontologie Diplomarbeit am Institut der Toxikologie und Genetik im Forschungszentrum Karlsruhe zum Thema: “Produktion und Charakterisierung von monoklonalen Antikörpern, die gegen Pip92 gerichtet sind “
07. 1995	**Allgemeine Hochschulreife** An der Europäischen Schule Karlsruhe

Publikationen

Originalarbeiten

Toscano C, Klein K, Blievernicht J, Saussele T, Raimundo S, Schaeffeler E, Eichelbaum M, Schwab M, Zanger UM. Modulation of splicing by intronic SNP 2988G>A responsible for decreased CYP2D6 expression in intermediate metabolizer carrying the **41* allele (provisionally accepted). *Pharmacogenetics and Genomics.*

Toscano C, Raimundo S, Klein K, Eichelbaum M, Schwab M, Zanger UM. A Silent Mutation (2939G>A, exon 6; *CYP2D6*59*) causally responsible for impaired expression and function of CYP2D6 (in press). *Pharmacogenetics and Genomics.*

Zanger UM, Schwab M, Toscano C and Eichelbaum M (2005) Limited Association of the 2988G>A Single Nucleotide Polymorphism With CYP2D6*41 in Black Subjects: Reply to the Editor. *Clinical Pharmacology and Therapeutics* 77:230-231.

Zanger UM, Klein K, Richter T, Toscano C and Zukunft J. Impact of genetic polymorphism in relation to other factors on expression and function of human drug-metabolizing P450s. *Toxicology Mechanism and Methods* 15:121-124.

Raimundo S, Toscano C, Klein K, Fischer J, Griese EU, Eichelbaum M, Schwab M, Zanger UM A novel intronic mutation, 2988G>A, with high predictivity for impaired function of cytochrome P450 2D6 in white subjects, *Clinical Pharmacology and Therapeutics*; 76:128-138.

Zanger UM, Klein K, Mürdter T, Richter T, Schaeffeler E, Toscano C and Zukunft J. Role of genetic polymorphism, drug exposure and sex for expression of hepatic cytochromes P450, *Cytochromes P450, Biochemistry, Biophysics and Drug Metabolism* Proceedings of the 13th International Conference on Cytochromes P450, June 29 - July 3, 2003, Prague (Czech Republic) Monduzzi Editore, Bologna; pp125-131.

Poster

Toscano C, Raimundo S, Klein K, Schaeffeler E, Eichelbaum M, Schwab M, Zanger UM „Molecular analysis of the *CYP2D6*41* intermediate metabolizer allele“ beim 7th International ISSX Meeting in Vancouver, Kanada

Cesaro C, Raimundo S, Klein K, Schaeffeler E, Eichelbaum M, Schwab M, Zanger UM „CYP2D6 intermediate metabolizer phenotype as a consequence of genetically determined alternative splicing“ bei der 13. International Conference on cytochrome P450 Biochemistry, Biophysics and Drug Metabolism, Prag, Tschechien

Vorträge

Toscano C, Raimundo S, Klein K, Schaeffeler E, Eichelbaum M, Schwab M, Zanger UM. „Investigation of the CYP2D6 intermediate and ultrarapid metabolizer phenotype in human liver“ bei der 3rd International Pharmacogenomics Conference in Hinxton, UK